

Chapter 3

Table of Contents

3.0	THERMAL EVALUATION.....	3.1-1
3.1	Discussion	3.1-1
3.2	Summary of Thermal Properties of Materials.....	3.2-1
3.2.1	Conductive Properties	3.2-1
3.2.2	Radiative Properties	3.2-1
3.2.2.1	Governing Radiation Principle	3.2-1
3.2.2.2	Radiation from Cask Surface	3.2-2
3.2.2.3	Radiation Across Gaps Within the Cask.....	3.2-3
3.2.2.4	Radiation from the Top of the Canister	3.2-4
3.2.3	Convective Properties	3.2-4
3.3	Technical Specifications for Components	3.3-1
3.3.1	Radiation Protection Components	3.3-1
3.3.2	Safe Operating Ranges.....	3.3-1
3.4	Thermal Evaluation for Normal Conditions of Transport	3.4-1
3.4.1	Thermal Models	3.4-2
3.4.1.1	Analytical Models: Cask with PWR Fuel Canister.....	3.4-4
3.4.1.2	Analytical Models: Cask with BWR Fuel Canister	3.4-13
3.4.1.3	Cask Impact Limiter Thermal Model.....	3.4-19
3.4.1.4	Personnel Barrier Thermal Model.....	3.4-20
3.4.1.5	Test Model	3.4-21
3.4.2	Maximum Temperatures.....	3.4-22
3.4.2.1	Preferential Loading.....	3.4-22
3.4.3	Minimum Temperatures.....	3.4-24
3.4.4	Maximum Internal Pressures	3.4-24
3.4.4.1	Maximum Internal Pressure for PWR Fuel Canister and Transport Cask	3.4-25
3.4.4.2	Maximum Internal Pressure for BWR Fuel Canister and Transport Cask	3.4-27
3.4.5	Maximum Thermal Stresses	3.4-28


Table of Contents (Continued)

3.4.6	Maximum Allowable Cladding Temperature and Canister Heat Load	3.4-28
3.4.6.1	Maximum Allowable Cladding Temperature	3.4-29
3.4.7	Evaluation of Package Performance for Normal Conditions of Transport	3.4-33
3.5	Thermal Evaluation for Hypothetical Accident Conditions.....	3.5-1
3.5.1	Thermal Models	3.5-1
3.5.1.1	Analytical Models	3.5-1
3.5.1.2	Test Model	3.5-3
3.5.2	Package Conditions and Environment	3.5-4
3.5.3	Package Temperatures	3.5-4
3.5.4	Maximum Internal Pressures	3.5-5
3.5.5	Maximum Thermal Stresses	3.5-5
3.5.6	Evaluation of Package Performance for Hypothetical Accident Conditions	3.5-6
3.6	Thermal Evaluation for Site Specific Contents	3.6-1
3.6.1	Maine Yankee Site Specific Contents.....	3.6-1
3.6.1.1	Spent Fuel	3.6-1
3.6.1.2	Maine Yankee Greater Than Class C Waste	3.6-13
3.7	References	3.7-1

List of Figures

Figure 3.1-1	Definition of the Gap Between Basket, Canister, and Inner Shell for Horizontal Position of Universal Transport Cask Containing PWR Fuel.....	3.1-4
Figure 3.1-2	Definition of the Gap Between Basket Canister, and Inner Shell for Horizontal Position of Universal Transport Cask Containing BWR Fuel	3.1-5
Figure 3.4-1	Three-Dimensional PWR Cask Finite Element Model.....	3.4- 54
Figure 3.4-2	Design Basis PWR Fuel Assembly Axial Power Distribution	3.4- 55
Figure 3.4-3	PWR 14x14 Fuel Assembly Two-Dimensional Finite Element Model....	3.4- 56
Figure 3.4-4	Two-Dimensional PWR Fuel Tube Model	3.4- 57
Figure 3.4-5	Three-Dimensional BWR Cask Finite Element Model	3.4- 58
Figure 3.4-6	Design Basis BWR Fuel Assembly Axial Power Distribution	3.4- 59
Figure 3.4-7	BWR 9x9 Fuel Assembly Two-Dimensional Finite Element Model	3.4- 40
Figure 3.4-8	Two-Dimensional BWR Fuel Tube (with BORAL) Model	3.4- 41
Figure 3.4-9	Two-Dimensional BWR Fuel Tube (without BORAL) Model	3.4- 42
Figure 3.4-10	Cask Impact Limiter Thermal Model.....	3.4- 43
Figure 3.4-11	Personnel Barrier Thermal Model	3.4- 44
Figure 3.4-12	Temperature Results at Key Points of the Personnel Barrier	3.4- 45
Figure 3.4-13	PWR Fuel Dry Storage Temperature versus Cladding Stress	3.4- 46

List of Figures (Continued)

Figure 3.4-14	BWR Fuel Dry Storage Temperature versus Cladding Stress	3.4- 46
Figure 3.4-15	PWR Fuel Cladding Dry Storage Temperature versus Basket Heat Load	3.4- 47
		
Figure 3.5-1	Two-Dimensional Axis-Symmetric Finite Element Cask Model (PWR and BWR)	3.5- 7
Figure 3.5-2	Upper Region of Two-Dimensional Axis-Symmetric Cask Finite Element Model (PWR and BWR)	3.5- 8
Figure 3.5-3	Lower Region of Two-Dimensional Axis-Symmetric Cask Finite Element Model (PWR and BWR)	3.5- 9
Figure 3.5-4	Hypothetical Accident Conditions Maximum Lead Temperature History (PWR)	3.5- 10
Figure 3.5-5	Hypothetical Accident Conditions Maximum Neutron Shield Exterior Temperature History (PWR)	3.5- 11
Figure 3.5-6	Hypothetical Accident Conditions Maximum Cask Inner Shell Temperature History (PWR)	3.5- 12
Figure 3.5-7	Hypothetical Accident Conditions Maximum Cask Outer Shell Temperature History (PWR)	3.5- 13
Figure 3.5-8	Hypothetical Accident Conditions Maximum Lower Neutron Shield Temperature History (PWR)	3.5- 14

List of Tables

Table 3.1-1	Thermal Analysis Bounding Conditions - Normal Conditions of Transport....	3.1-6
Table 3.2-1	Thermal Properties of Solid Neutron Shield (NS-4-FR)	3.2-6
Table 3.2-2	Thermal Properties of Stainless Steel	3.2-7
Table 3.2-3	Thermal Properties of Carbon Steel.....	3.2-8
Table 3.2-4	Thermal Properties of Chemical Copper Lead.....	3.2-9
Table 3.2-5	Thermal Properties of Type 6061 T651 Aluminum Alloy	3.2-10
Table 3.2-6	Thermal Properties of Helium	3.2-11
Table 3.2-7	Thermal Properties of Dry Air.....	3.2-12
Table 3.2-8	Thermal Properties of Copper.....	3.2-13
Table 3.2-9	Thermal Properties of Zircaloy and Zircaloy-4 Cladding.....	3.2-14
Table 3.2-10	Thermal Properties of Fuel (UO ₂).....	3.2-15
Table 3.2-11	Thermal Properties of BORAL Composite Sheet.....	3.2-16
Table 3.2-12	Thermal Properties of Redwood (Air Dry).....	3.2-17
Table 3.2-13	Thermal Properties of Fiberfrax Ceramic Fiber Paper	3.2-18
Table 3.2-14	Gaps Within the Universal Transport Cask	3.2-19
Table 3.4-1	Maximum Component Temperatures - Normal Conditions of Transport, Maximum Decay Heat, Maximum Ambient Temperature	3.4- 48
Table 3.4-2	Maximum Component Temperatures - Normal Conditions of Transport, Maximum Decay Heat, Minimum Ambient Temperature.....	3.4- 49
Table 3.4-3	Universal Transport Cask Thermal Performance Summary For Component Operating Temperature	3.4- 50

List of Tables (Continued)

Table 3.4-4	Maximum Internal Pressures for Transport	3.4-51
Table 3.4-5	PWR Per Assembly Fuel Generated Gas Inventory	3.4-52
Table 3.4-6	PWR Canister Free Volume (No Fuel or Inserts)	3.4-52
Table 3.4-7	PWR Maximum Normal Condition Pressure Summary	3.4-52
Table 3.4-8	BWR Per Assembly Fuel Generated Gas Inventory	3.4-53
Table 3.4-9	BWR Canister Free Volume (No Fuel or Inserts)	3.4-53
Table 3.4-10	BWR Maximum Normal Condition Pressure Summary	3.4-53
Table 3.4-11	PWR Cladding Stress Level Comparison Chart	3.4-54
Table 3.4-12	BWR Cladding Stress Level Comparison Chart	3.4-55
Table 3.4-13	Cladding Stress as a Function of Fuel Assembly Average Burnup and Temperature	3.4-56
Table 3.4-14	Maximum Allowable Initial Storage Temperature (°C) as a Function of Initial Cladding Stress and Initial Cool Time	3.4-56
Table 3.4-15	Maximum Allowable Cladding Temperature for PWR and BWR Fuel ...	3.4-57
Table 3.4-16	Maximum Allowable Decay Heat for PWR and BWR Systems	3.4-57
Table 3.4-17	Temperature Bias Applied to Maximum Allowable Decay Heats	3.4-58
Table 3.5-1	Maximum Component Temperatures - Hypothetical Accident Condition Fire Transient (PWR Cask)	3.5-26
Table 3.5-2	Maximum Component Temperatures - Hypothetical Accident Condition Fire Transient (BWR Cask)	3.5-27
Table 3.5-3	Maximum Internal Pressures for Hypothetical Accident Conditions	3.5-28

3.0 THERMAL EVALUATION

This chapter presents the thermal design and analyses of the Universal Transport Cask for the 10 CFR 71 normal conditions of transport and hypothetical accident conditions. The analyses include consideration of design basis PWR and BWR fuel. Results of the analyses demonstrate that with the design basis payloads, the Universal Transport Cask meets the thermal performance requirements of 10 CFR 71 [1] and IAEA Safety Series No. 6 [2].

3.1 Discussion

The Universal Transport Cask is designed to transport one of three classes of PWR fuel or one of two classes of BWR fuel, which are already sealed in a Transportable Storage Canister (canister). Only the bounding evaluation for the PWR and BWR classes of fuel is reported herein. The bounding case is represented by a configuration consisting of the shortest canister, shortest fuel tube, and shortest fuel assemblies with the lowest effective thermal conductivity. The fuel assemblies are confined within the fuel basket. The shortest fuel basket contains the fewest support disks and longest space in the bottom of the cask cavity. The result is greater concentration of heat and maximized thermal resistance for rejection of heat through the cavity top and bottom. The shorter fuel tube results in reduced axial conductance.

■ The design basis heat loads are 20 kW for up to 24 PWR assemblies and 16 kW for up to 56 BWR fuel assemblies. The individual PWR assembly decay heat is limited to 0.83 kW and the individual BWR assembly decay heat load is limited to 0.29 kW. As shown in Section 3.4.6, the thermal analysis considers a range of fuel assembly burnup and cool times for both fuel types to establish the allowable cladding temperatures. These limits are used to establish the allowable decay heat loads for fuel having cooling times of 5 years or more

The thermal analyses presented in the following sections use helium as the cover gas in the cask cavity and in the canister. ■

Heat transfer from the Universal Transport Cask to the environment is by passive means only. No forced cooling is necessary. Conduction and radiation are the means by which heat is transferred from the fuel assemblies to the fuel tubes and through the tubes to the support disks and heat transfer disks. Heat is transferred through the support disks and heat transfer disks by conduction and radiation. Radiation and conduction are the means by which heat is transferred from the support disks and heat transfer disks to the canister wall and then to the cask cavity inner wall. From the Universal Transport cask cavity inner shell surface, heat is conducted through the lead (gamma shield) and then through the cask outer shell.

The neutron shield region surrounding the outer shell along most of the cask's length conducts heat to the neutron shield shell, primarily through the Cu/SS fins located within the NS-4-FR radial neutron shield material. The stainless steel shell that encloses the radial neutron shield is exposed to the environmental ambient temperature. Heat is removed from the surface of the neutron shield shell by convection and radiation. Heat transfer through the cask lid at the top of the cask and through the bottom forging and enclosed neutron shield material at the bottom of the cask is by conduction. Because of the insulating characteristics of the impact limiters, essentially no heat is removed from the ends of the cask. The bounding thermal conditions for the analysis required by 10 CFR 71 and IAEA Safety Series No. 6 under normal conditions of transport are presented in Table 3.1-1.

During normal conditions of transport and hypothetical accident conditions, the cask must reject the fuel decay heat to the environment without exceeding the operational temperature ranges of the cask seals or other components important to safety. In addition, to maintain fuel rod integrity for normal conditions of transport, the fuel must be maintained at a sufficiently low temperature in an inert atmosphere such that thermally induced fuel rod cladding deterioration is precluded. To preclude fuel degradation, maximum allowable temperatures corresponding to different burnup and cooling times have been established as shown in Table 3.4-15 for normal conditions of transport for the PWR and BWR fuel. Finally, the thermally induced stresses, in combination with pressure and mechanical load stresses, must be below allowable stress levels.

The temperatures for the various components of the fuel, canister, basket, and cask during normal conditions of transport and hypothetical accident condition fire are calculated by using finite element methods. For both normal conditions and the hypothetical accident conditions, the cask

loaded with PWR fuel and the cask loaded with BWR fuel are analyzed by using separate finite element models. For each fuel configuration, the thermal analyses of the cask for normal conditions of transport are performed by using three-dimensional finite element models of the loaded cask. The cask is transported in a horizontal orientation. Figures 3.1-1 and 3.1-2 show the gaps in the cask for PWR and BWR configurations, respectively. These models are described in Section 3.4.1.1 and 3.4.1.2. The thermal analyses of the cask for the hypothetical accident fire condition are performed by using two-dimensional models of the cask. These models are described in Section 3.5.1.1.

Results of thermal analysis of the package are presented in Sections 3.4.7 and 3.5.6. The results demonstrate that the maximum fuel rod cladding temperatures remain below the allowable temperatures for normal conditions of transport (Table 3.4-15) and hypothetical accident conditions (1,058°F). The thermally induced stresses, combined with pressure and mechanical load stresses, are within the allowable levels, as demonstrated in Chapter 2.0. Therefore, the cask design and operation are in conformance with temperature and thermal stress criteria.

The thermal results presented in this chapter, and other properties evaluated herein, are used in other analyses included in this Safety Analysis Report. The material properties and allowable stresses at the corresponding temperatures are used in the structural calculations presented in Chapter 2.0. The structural evaluation of components also incorporates stresses resulting from differential thermal expansion and temperature effects on the cask internal pressure as applicable.

Figure 3.1-1 Definition of Gap Between Basket, Canister, and Inner Shell for Horizontal Position of the Universal Transport Cask Containing PWR Fuel

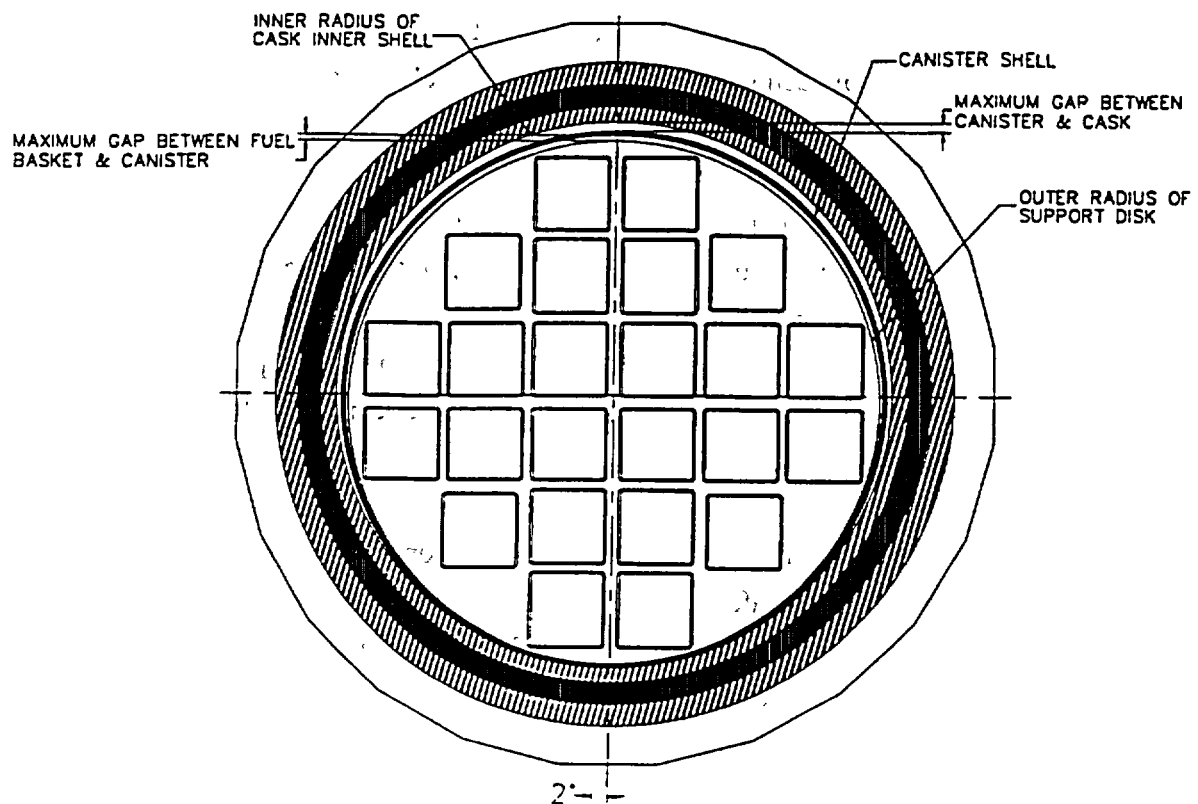


Table 3.2-12 Thermal Properties of Redwood (Air Dry)

Property (units)	Value
Conductivity (Btu/hr-in-°F):	
Parallel to Grain [23]	0.012
Transverse to Grain [23]	0.005
Density (lbm/in ³) [23]	0.014

Table 3.2-13 Thermal Properties of **Fiberfrax Ceramic Fiber Paper**

Property (units) ¹	Temperature		
	500°F	1000°F	2000°F
Conductivity ² (Btu/hr-in-°F) [21]	0.0028	0.0055	0.0090
Density ³ (lbm/in ³) [21]	0.0058		

1. Grades 550, 880, and 970

2. Highest thermal conductivity among Grades 550, 880, and 970

3. Lowest density among Grades 550, 880, and 970.

3.4 Thermal Evaluation for Normal Conditions of Transport

The finite element method is used to evaluate the thermal performance of the Universal Transport Cask for normal conditions of transport as specified in 10 CFR 71. The general-purpose finite element analysis program ANSYS Revision ~~5.5~~ [5] is used to perform the finite element evaluations.

The normal conditions of transport used in the thermal evaluation of the cask are as follows:

1. Hot Conditions: maximum decay heat generation, ambient temperature = 100°F, solar insolation (solar insolation applied according to Table 3.1-1)
2. Cold Conditions: maximum decay heat generation, ambient temperature = -40°F, no solar insolation
3. Minimum Temperature Conditions: no decay heat generation, ambient temperature = -40°F, no solar insolation (no analysis is performed for this condition because all component temperatures will be -40°F for steady state conditions).

The objectives of the cask thermal analyses under normal conditions of transport are as follows:

1. Demonstrate that the cask can safely maintain the design basis temperatures required for fuel cladding integrity under the range of thermal conditions expected during normal conditions
2. Demonstrate that cask components important to safety are maintained within their safe operating temperature ranges
3. Provide thermal input to the structural analyses.

The first objective is met by demonstrating that the cask maintains maximum fuel rod cladding temperatures below the allowable temperatures during normal conditions.

The second objective is met by comparing the results of the analyses with the safe operating ranges established in Section 3.3.

The third objective is met by using the results of the thermal analyses (as direct import of ANSYS temperature data, as maximum and minimum component temperatures, or as allowable look-up temperatures) as input to the structural analyses, which demonstrate that the combined load stresses are within allowable limits.

3.4.1 Thermal Models

The finite element method is used to evaluate the Universal Transport Cask for exposure to normal conditions of transport as specified in 10 CFR 71. This section describes the finite element models used in the thermal evaluation of the cask under normal conditions of transport. Separate three-dimensional finite element models are used to evaluate the cask loaded with PWR fuel and the cask loaded with BWR fuel. In addition, a separate model is used to determine the volumetric average temperature of the cask impact limiter for normal conditions. The analyses for normal conditions of transport consider the transport cask oriented horizontally.

For each fuel-loading configuration, the cask is evaluated for normal conditions of transport using a three-dimensional half-symmetry (180°) finite element model of the loaded cask including internal components. The three-dimensional finite element models of the cask/internal components both comprise five parts: basket with fuel tube and fuel assembly; canister, spacer (between canister bottom and shell bottom forging); transport cask body; and gases between components. To model the cask in a horizontal orientation, the fuel basket in each model is modeled in contact with the canister on one side which, in turn, is in contact with the inner shell of the cask on one side—thus simulating no gap on one side of the basket and canister and a maximum gap at the opposite side (see Figure 3.1-1 for the PWR fuel configuration and Figure 3.1-2 for the BWR fuel configuration).

Gaps within the models are adjusted to account for differential expansion on the basis of thermal and defined physical contact conditions. Solar insolation, natural convection and thermal radiation boundary conditions based on ambient temperature are applied to the outer surface of

the corresponding total heat is only 15.7 kW and the heat density is 88% of the 20 kW over 144 inches. The 20kW over 144 inches is considered to be controlling.

There are a number of conservative conditions in this three-dimensional cask model:

1. The fuel assembly is conservatively considered to be located at the center of the fuel tube. (The fuel assembly will be in contact with the fuel tube on its side since the cask is in the horizontal position during transport. The contact will reduce the maximum component temperature.)
2. The fuel tube is conservatively considered to be located at the center of the slots of the support disks. (The fuel tube will be in contact with the support disk since the cask is in the horizontal position during transport. The contact will reduce the maximum component temperature.)
3. Convection heat transfer is conservatively ignored in the model.
4. The gap between the lead and cask inner shell is conservatively considered to 360° around the shell. (A good portion of the lead will be in contact with the inner shell since the cask is in the horizontal position during transport. The contact will reduce the maximum component temperature.)

A sensitivity study was performed to assess the effect on maximum temperatures of fuel cladding and basket for the variations of the following parameters, which are considered to be critical in the main heat transfer path:

1. Emissivity of stainless steel (fuel tube, support disks, canister shell, cask shells) and aluminum (heat transfer disk)
2. Convection heat transfer coefficient at transport cask outer surface
3. Contact area between the disks and canister shell
4. Heat transfer disk thickness
5. Gap between the disks and canister shell
6. Gap between the canister shell and the cask inner shell
7. Cask radial neutron shield copper fin thickness
8. Emissivity of copper lead

A total of nine (8) thermal analyses were performed using the thermal model described in this section. The changes in the model and the temperature results for the eight cases are shown in the table following. The analysis results indicate that the increase in the maximum fuel cladding

and basket temperature is $\leq 8^{\circ}\text{F}$ for each of the cases. Therefore, the effect of variation of all these parameters is not significant. Additionally, an analysis is performed (Case 9) to evaluate the combined effect of Cases 1, 3, 4, 5, 7 and 8. The increase in the maximum fuel cladding and basket temperature for the combined case (no. 9) is $\leq 17^{\circ}\text{F}$. The maximum fuel cladding and basket temperatures remain below their allowable temperatures for the combined case. Based on the above discussion on the conservatism in the model and the results of the sensitivity study, it is concluded that the calculated temperatures using the thermal models are conservative and the system has an adequate margin of safety.

Case No.	Description	Maximum Temperature ($^{\circ}\text{F}$)		
		Fuel Cladding	Support Disks	Heat Transfer Disks
Base	Original analysis	673	608	605
1	10% reduction of the emissivity of stainless steel and aluminum	678	613	610
2	10% reduction of the heat transfer coefficient at cask outer surface	678	614	610
3	Reduced contact area between disks and canister shell (reduced from 2° to 1° in the half-symmetry model)	673	608	605
4	8% reduction in heat transfer disk thickness based on the plate thickness tolerance	680	616	613
5	Increased gap between disks and canister shell based on the tolerance of the diameter of disks and canister shell and the canister shell thickness	676	611	608
6	Increased gap between canister shell and cask inner shell based on the tolerance of the diameter of canister shell and the cask inner shell	675	610	607
7	6% reduction of the cask radial neutron shield copper fin thickness based on the plate thickness tolerance	674	609	606
8	10% reduction of the lead emissivity	673	608	605
9	Combined (1+3+4+5+7+8)	689	625	622

3.4.1.1.2 Two-Dimensional Fuel Assembly Model: PWR Fuel

The effective conductivity of the fuel is determined by a detailed two-dimensional finite element thermal model of the PWR 14x14 fuel assembly. Taking advantage of the symmetry of the cross-section of the fuel, the finite element model represents a one-quarter section of the fuel. The model includes the fuel pellets, cladding, gas between the fuel rods, and gas occupying the gap between the fuel pellets and cladding. Modes of heat transfer modeled include conduction and radiation between individual fuel rods for the steady-state condition. The model is shown in Figure 3.4-3. Thermal analyses of the other PWR fuel assemblies (i.e., 17x17, 16x16, and 15x15) are performed; however, because the PWR 14x14 fuel assembly results in the lowest effective thermal conductivities, only the analysis of that fuel assembly is presented in this section.

ANSYS PLANE 55 conduction elements and LINK31 radiation elements are used in the model, which includes a total of 49 fuel rods (representing a total of 196 fuel rods for the full cross-section). Each fuel rod consists of the pellet, Zircaloy cladding, and a gap between the pellet and clad. The gas in the gap between the pellet and clad, as well as the gas between the fuel rods, is modeled as helium. Radiation elements are defined between rods and from rods to the boundary of the model (inside surface of the fuel tube). Radiation across the gap between the pellet and clad is conservatively ignored. Effective emissivities are determined by using the formula shown in Section 3.4.1.1.1.

The effective conductivity for the fuel is determined by using a two-step procedure. Using the fuel assembly model, a uniform temperature is applied to the exterior of the model (see Figure 3.4-3) in conjunction with the volumetric heat generation. From this analysis, the maximum temperature located at the center of the fuel assembly is determined. This maximum temperature occurs at the corner of the model, which represents the center of the entire fuel assembly.

A Sandia National Laboratory Report [10] defines an expression for use in determining the maximum temperature of a square cross section of an isotropic homogeneous fuel with uniform volumetric heat generation. At the boundary of this square cross section, the temperature is constrained to be uniform. The expression for the maximum temperature is given by:

$$T_c = T_e + 0.29468 \frac{Q a^2}{K_{eff}}$$

where:

T_c = temperature at center of fuel (°F)

T_e = temperature applied at exterior of fuel (°F)

Q = volumetric heat generation rate (Btu/hr-in³)

a = half-length of square cross section of fuel (inch)

K_{eff} = effective thermal conductivity for isotropic homogeneous fuel material (Btu/hr-in-°F).

Using the maximum temperature, located at the center of the fuel, from the detailed fuel assembly model, the preceding expression is used to determine the K_{eff} for an isotropic homogeneous representation of the fuel assembly.

Volumetric heat generation based on the design heat load of 20 kW with a peaking factor of 1.1 is applied to the fuel pellets. The temperature at the boundary of the model is constrained to be uniform. The effective conductivity is determined on the basis of the heat generated and the temperature difference from the center of the model to its edge. The temperature-dependent effective properties are established by using different boundary temperatures. The effective conductivity in the axial direction of the fuel assembly is calculated on the basis of a weighted average of the axial cross sectional area.

3.4.1.1.3 Two-Dimensional Fuel Tube Model: PWR Fuel

The effective conductivity of the fuel tube and BORAL plate, which is used in the three-dimensional canister model, is determined by the two-dimensional fuel tube model. As shown in Figure 3.4-4, this model includes the fuel tube, the BORAL plate (including the core matrix sandwiched by aluminum claddings), gaps on both sides of the BORAL plate, and a gap between the stainless steel cladding for the BORAL plate and the support disk or heat transfer disk. The BORAL plate in the PWR fuel tube is composed of 62.34% B₄C and 37.66% aluminum.

ANSYS PLANE55 conduction elements and LINK31 radiation elements are used to construct the model, which consists of eight layers of conduction elements and six radiation elements that are defined at the gaps (two per gap). The thickness of the model (x-direction) is the distance measured from the inside dimension of the fuel tube to the inside dimension of the slot in the support disk (assuming that the fuel tube is located at the center of the disk slot). The tolerance

of the BORAL plate core thickness, 0.003 inch, is used as the gap size for both sides of the BORAL plate. The model height is defined to be the same dimension as the model thickness.

A heat flux is applied at the left side of the model and the temperature at the right boundary of the model is constrained. The heat flux is determined on the basis of design heat load of 20 kW with a peaking factor of 1.1. The maximum temperature of the model (at the left boundary where the heat flux is applied) is calculated by using ANSYS. The effective conductivity through the thickness of the tube is determined by using the following equation:

$$q = K_{\text{eff}}(A/L) \Delta T, \text{ or}$$
$$K_{\text{eff}} = qL/(A \Delta T)$$

where:

q = heat rate applied to inner surface of fuel tube (Btu/hr)

A = area (in²)

L = thickness of composite tube model (in)

ΔT = temperature difference across the model (°F)

K_{eff} = effective conductivity (Btu/hr-in-°F).

The temperature-dependent conductivity for heat conduction through the wall (K_{eff}) is determined by varying the temperature constraint at the boundary of the model and then resolving for the temperature difference. The effective conductivity for heat conduction parallel to the axis of the cask body or in the plane of the tube wall is calculated on the basis of the weighted average of the thickness and conductivity of the individual layers.

3.4.1.2 Analytical Models: Cask with BWR Fuel Canister

The finite element ANSYS models used in the thermal analysis of the cask transporting BWR fuel are similar to those used in the thermal analysis of the cask with PWR fuel canister discussed in previous sections. A three-dimensional model is employed to evaluate the cask in a horizontal position with the basket in contact with the canister, which, in turn, is in contact with the cask inner shell. The fuel regions and the fuel tubes with BORAL plates are modeled by using effective conductivities. A detailed two-dimensional thermal model of the fuel assembly is used to determine the effective conductivity of the fuel. A two-dimensional thermal model of the fuel tube is used to calculate the effective conductivities of the fuel tube wall and BORAL plate.

Another two-dimensional thermal model for the fuel tube is used to calculate the effective conductivity of the fuel tube wall with no BORAL plate present. These four ANSYS thermal models are described in the following sections.

3.4.1.2.1 Three-Dimensional Cask Model: Cask with BWR Fuel Canister

The three dimensional Universal Transport Cask model is a half-symmetry finite element model constructed by using ANSYS Revision 5.5. The model considers the fuel assemblies, fuel tubes, stainless steel support disks, aluminum heat transfer disks, canister shell, lids and bottom plate, spacers at the bottom of the canister, cask inner shell, lead, outer shell, neutron shield, and neutron shield shell. The ANSYS model is shown in Figure 3.4-5. As shown in the figure, the internal cavity of the canister contains the active fuel region: the top and bottom fittings of the fuel assemblies, fuel tubes enclosing the top and bottom fittings, and the first stainless steel support.

For the BWR configuration, the gas inside the canister and the cask cavity is modeled as helium because the cavity will be backfilled with helium prior to transport. Conduction and radiation are modeled by using ANSYS "SOLID70" and "LINK31" elements, respectively. The principal gaps applied to the model are shown in Figure 3.1-2 and are described in Section 3.2.2.3. In establishing these gaps, the differential thermal expansion between the components is considered.

Because the canister is in horizontal position during transport, the elements for the canister shell are shifted downwards to simulate contact with the inner shell of the cask. Similarly, the support disks and the heat transfer disks are shifted downward to simulate contact with the canister shell. As shown in Figure 3.1-2, a 2-degree contact is considered for the gaps between the canister shell and the cask inner shell and between the support disk and the canister shell. This contact is simulated by using appropriate conductivity (100 Btu/hr-inch-°F) for elements at the contact locations. The aluminum heat transfer disks are assumed to have only a line contact with the canister shell because the heat transfer disks are not subjected to any loads other than their own weight.

To account for differential expansion, gaps within the model are adjusted on the basis of temperature and defined physical contact conditions. Solar insolation and ambient temperature

conditions are applied to the neutron shield shell when appropriate. Insolation is used at the exterior surface of the cask and is based on the amount of insolation required by 10 CFR 71 to be applied over a 12-hr period evaluated in the steady state (applied over 24 hr simulating 12-hr period of solar exposure and 12-hr period of no solar exposure). The heat flux resulting from insolation on a curved surface is calculated as follows:

$$1475 \frac{\text{Btu}}{12 \text{ hr} \cdot \text{ft}^2} \times \frac{12 \text{ hr}}{24 \text{ hr}} \times \frac{1 \text{ ft}^2}{144 \text{ in}^2} = 0.427 \text{ Btu/hr-in}^2$$

Multiplying this value by the emissivity of the cask surface, $\epsilon = 0.36$, gives a heat flux resulting from insolation on curved surfaces of $0.154 \text{ Btu/hr-in}^2$. Using the same method and a heat flux of $2,950 \text{ Btu/12 hr-ft}^2$ ($0.853 \text{ Btu/hr-in}^2$), gives a heat flux resulting from insolation on flat surfaces of $0.307 \text{ Btu/hr-in}^2$.

The model is analyzed to determine the maximum temperatures for the basket, canister, cask shells, radial shielding, and surface conditions under normal conditions of transport. All material properties are shown in Tables 3.2-1 through 3.2-13.

The fuel regions (inside tubes) are modeled as homogeneous regions with effective conductivities determined by the two dimensional fuel model as described in Section 3.4.1.2.2. All sides of the BWR fuel tubes do not contain the BORAL plate. Therefore, two different two-dimensional BWR fuel tube models are analyzed to establish the effective conductivities used in the three dimensional analysis of the cask with BWR fuel. The models consist of the BORAL plate (where applicable), including gas gaps on both sides of the BORAL sheet (where applicable), and the gap between the stainless steel cladding for the BORAL and the support disks and heat transfer disks. These models are discussed in Section 3.4.1.2.3.


The radial neutron shield of the transport cask for the BWR configuration is identical to PWR configuration. The modeling of the radial neutron shield is described in Section 3.4.1.1.

In the model, radiation heat transfer is considered from the top of the fuel region to the bottom surface of the canister shield lid, from the bottom of the fuel region to the top surface of the canister bottom plate, and from the exterior surfaces of the fuel tubes to the inner surface of the

canister shell. This radiation is modeled by using LINK31 radiation elements. Radiation across gaps in the model is described in Sections 3.2.2.3 and 3.2.2.4.

Radiation at the neutron shield shell surface to ambient is combined with the convection effect by using the method described in Section 3.2.2.2. The convection heat transfer coefficient is calculated on the basis of the formula shown in Section 3.2.3. Effective emissivities are used for all radiation calculations, with the form factor taken to be unity. Effective emissivity is computed by using the following formula [9] based on corresponding material emissivities:

$$\epsilon_{\text{eff}} = 1 / (1/\epsilon_1 + 1/\epsilon_2 - 1)$$

Solar insolation is applied to the neutron shield shell surface for the **Hot condition** (ambient temperature = 100°F) . A value of 0.154 Btu/hr-inch² is used as the heat flux at the neutron shield shell surface on the basis of the 1,475 Btu/hr-ft² heat flux for a curved surface. Calculation of the heat flux resulting from insolation on a curved surface is discussed earlier in this section.

Volumetric heat generation (Btu/hr-inch³) is applied to the active fuel region on the basis of a total heat load of 16 kW, a shortest active fuel rod length of 144 inches, and an axial power with a peaking factor of 1.22 as shown in Figure 3.4-6.

3.4.1.2.2 Two-Dimensional Fuel Assembly Model: BWR Fuel

The effective conductivity of the fuel is determined by a detailed two-dimensional finite element thermal model of the BWR 9x9 fuel assembly. Taking advantage of the symmetry of the cross-section of the fuel, the finite element model represents a one-quarter section of the fuel. The model includes the fuel pellets, cladding, gas between the fuel rods, and gas occupying the gap between the fuel pellets and cladding. Modes of heat transfer modeled include conduction and radiation between individual fuel rods for the steady-state condition. The model is shown in Figure 3.4-7. Thermal analyses of the other BWR fuel assemblies (i.e., 7x7 and 8x8) are performed; however, because the BWR 9x9 fuel assembly results in the lowest effective thermal conductivities, only the analysis of that fuel assembly is presented in this section.

ANSYS PLANE55 conduction elements and LINK31 radiation elements are used in the model, which includes a total of 20.25 fuel rods (representing a total of 81 fuel rods for the full cross-section). Each fuel rod consists of the pellet, Zircaloy cladding, and a gap between the pellet and clad. The gas in the gap between the pellet and clad, as well as the gas between the fuel rods, is modeled as helium. Radiation elements are defined between rods and from rods to the boundary of the model (inside surface of the fuel tube). Radiation effect at the gaps between the pellet and clad is conservatively ignored. Effective emissivities are determined by using the formula shown in Section 3.4.1.1.1.

The effective conductivity for the fuel is determined by using a two-step procedure. Using the fuel assembly model, a uniform temperature is applied to the exterior of the model (see Figure 3.4-7) in conjunction with the volumetric heat generation. From this analysis, the maximum temperature located at the center of the fuel assembly is determined. This maximum temperature occurs at the corner of the model, which represents the center of the entire fuel assembly.

A Sandia National Laboratory Report [10] defines an expression for use in determining the maximum temperature of a square cross section of an isotropic homogeneous fuel with uniform volumetric heat generation. At the boundary of this square cross section, the temperature is constrained to be uniform. The expression for the maximum temperature is given by:

$$T_c = T_e + 0.29468 \frac{Q a^2}{K_{eff}}$$

where:

T_c = temperature at center of fuel (°F)

T_e = temperature applied at exterior of fuel (°F)

Q = volumetric heat generation rate (Btu/hr-in³)

a = half-length of square cross section of fuel (inch)

K_{eff} = effective thermal conductivity for isotropic homogeneous fuel material (Btu/hr-in-°F).

Using the maximum temperature, located at the center of the fuel, from the detailed fuel assembly model, the preceding expression is used to determine the K_{eff} for an isotropic homogeneous representation of the fuel assembly.

Volumetric heat generation based on the design heat load of 16 kW with a peaking factor of 1.22 is applied to the fuel pellets. The temperature at the boundary of the model is constrained to be uniform. The effective conductivity is determined on the basis of the heat generated and the temperature difference from the center of the model to its edge. The temperature-dependent effective properties are established by using different boundary temperatures. The effective conductivity in the axial direction of the fuel assembly is calculated on the basis of the material area ratio.

3.4.1.2.3 Two-Dimensional Fuel Tube Models: BWR Fuel

The fuel tubes in the BWR fuel basket differ from those in the PWR fuel basket in that not all sides of the fuel tubes contain BORAL. Therefore, two effective conductivity models are necessary—one fuel tube model with the BORAL plate (a total of 10 layers of materials) and another fuel tube model with a gas gap replacing the BORAL plate (a total of 4 layers of materials). Additionally, the BORAL plate in the BWR fuel tube is composed of 16.46% B₄C and 83.54% aluminum, whereas the BORAL plate in the PWR fuel tube is composed of a 62.34%—37.66% composition of B₄C and aluminum.

The effective conductivity of the fuel tube and BORAL plate, which is used in the three-dimensional canister model, is determined by a two-dimensional fuel tube model. As shown in Figure 3.4-8, this model includes the fuel channel, gas gaps between the fuel channel and fuel tube, the fuel tube, the BORAL plate (including the core matrix sandwiched by aluminum claddings), gas gaps on both sides of the BORAL plate, and a gas gap between the stainless steel cladding for the BORAL plate and the support disk or heat transfer disk.

Additionally, the effective conductivity of the fuel tube without the BORAL plate, which is used in the three-dimensional canister model, is determined by another two-dimensional fuel tube model. As shown in Figure 3.4-9, this model includes the fuel channel, gas gaps between the fuel channel and stainless steel fuel tube, the fuel tube, and a gas gap between the stainless steel cladding and the support disk or heat transfer disk.

ANSYS PLANE55 conduction elements and LINK31 radiation elements are used to construct the models. The model with the BORAL plate consists of 10 layers of conduction elements and 8 radiation elements that are defined at the gas gaps (two per gap). The model without the BORAL plate consists of four layers of conduction elements and four radiation elements that are

defined at the gas gaps (two per gap). The thickness of the models (x-direction) is the distance measured from the inside dimension of the fuel channel to the inside dimension of the slot in the support disk (assuming that the fuel tube is located at the center of the disk slot). In the model containing the BORAL plate, the tolerance of the BORAL plate core thickness, 0.0045 inch, is used as the gap size for both sides of the BORAL plate. The height of the models is defined to be the same dimension as the thickness of the models.

In each analysis, a heat flux is applied at the left side of the model and the temperature at the right boundary of the model is constrained. The heat flux is determined on the basis of the design heat load of 16 kW with a peaking factor of 1.22. The maximum temperature of the model (at the left boundary) and the temperature difference (ΔT) across the model are calculated by using ANSYS. The effective conductivity is determined by using the following formula:

$$q = K_{\text{eff}}(A/L) \Delta T$$

or

$$K_{\text{eff}} = qL/(A \Delta T)$$

where:

q = heat rate applied to inner surface of fuel tube (Btu/hr)

A = area (in²)

L = thickness of composite tube model (in)

ΔT = temperature difference across the model (°F)

K_{eff} = effective conductivity (Btu/hr-in-°F).

The temperature-dependent conductivity (K_{eff}) in each analysis is determined by varying the temperature constraint at the boundary of the model and then re-solving for the temperature difference. The effective conductivity for the parallel path is calculated on the basis of area ratio of material.

3.4.1.3 Cask Impact Limiter Thermal Model

As described in Sections 3.4.1.1 and 3.4.1.2, the cask impact limiters are not explicitly modeled in the 3D cask models. In these models, the cask ends enclosed by the impact limiters are modeled as being adiabatic surfaces. The cask impact limiters are evaluated thermally for normal operating conditions in this section. Specifically, the volumetric average temperature of the redwood material in the cask impact limiters is calculated using an ANSYS finite element

model. Taking advantage of the symmetrical geometry of the cask impact limiters about the major axis of the cask, the finite element model is an axisymmetric representation of one of the impact limiters with the cask oriented in a horizontal position. This represents the orientation of the impact limiters during normal transport. The cask impact limiter thermal model is shown in Figure 3.4-10.

The finite element model of the cask impact limiter is constructed of PLANE55 axisymmetric thermal elements, and radiation and conduction heat transfer across air gaps within the model are accounted for using effective thermal conductivity properties for air using the method described in Section 3.2.2.3. Air gaps are modeled between the cask and impact limiter based upon nominal dimensions. Additionally, a 0.125-in. thick layer of Fiberfrax® Ceramic Fiber Paper is modeled between the impact limiter redwood and the cask mating surface of the impact limiter. A heat flux of 0.13 Btu/h-in², which represents the package contents, is applied to the interior surface of the cask lid. This heat flux is obtained from the thermal results for the 3D cask model with the PWR canister and air as the canister cover gas (described in Section 3.4.1.1) by conservatively assuming the heat transfer rate to the cask lid is equal to the heat transfer rate to the canister shield lid.

Heat fluxes representing the normal conditions solar heat loads are applied to the cylindrical and vertical flat end surfaces of the impact limiter as shown in Figure 3.4-10. The solar heat flux applied to the vertical flat surfaces of the impact limiter 0.0769 Btu/h-in² model (which is in the normal transport orientation) are calculated in the same manner described in Section 3.4.1.1.1 using the prescribed solar heat flux value of 737 Btu/12-hr-ft². A solar heat flux of 0.154 Btu/hr-in² is applied to the cylindrical portions of the cask and impact limiter modeled.

A steady-state heat transfer analysis is performed using the ANSYS model described in this Section. The volumetric average temperature of the cask impact limiter redwood material (T_{avg}) is calculated from the results of the thermal steady state analysis.

3.4.1.4 Personnel Barrier Thermal Model

According to 10 CFR 71.43(g), a package must be designed, constructed, and prepared for transport such that in still air at 100°F and shade, no accessible surface of the package has a temperature exceeding 185°F in an exclusive use shipment. Compliance with 10 CFR 71.43(g) is demonstrated by performing a computational fluid dynamics (CFD) analysis on a finite

element model of the air between the cask surface (i.e., neutron shield shell) and the personnel barrier using ANSYS/FLOTTRAN. The finite element model is constructed of two-dimensional FLUID141 elements and is presented in Figure 3.4-11.

Because of geometrical symmetry, only one-half of the cask and the air around the cask is modeled. In addition to the natural convection of the air, thermal radiation heat transfer from the cask outer surface to the personnel barrier is considered in this model. It is conservative to only model the air between the cask surface and the personnel barrier because it results in a higher air velocity and more heat is carried to the top of the personnel barrier. Along the centerline of the model, the horizontal velocity component is specified to be zero. The nodes at the location of the personnel barrier (except the top side) are conservatively defined as wall conditions (Velocity = 0) to force all of the heat out from the top of the barrier. At the inlet (bottom side of the model), the pressure is set to atmospheric pressure with the temperature constrained to 100°F. The portion of the model corresponding to the cask surface constrains both the horizontal and vertical components of the velocity to be zero.

The cask and personnel barrier are not explicitly modeled in this analysis—only the air surrounding the cask is modeled. It is conservative that the personnel barrier is not explicitly modeled because it will not have a temperature greater than the temperature of the air in contact with it. The temperatures of nodes in the model that correspond to the air adjacent to the cask surface are constrained as boundary conditions of the model. The temperature is considered to be linearly distributed, with the bottom and top temperatures equal to 267°F and 244°F respectively.

Since the personnel barrier is not explicitly modeled, its temperature is considered to be the temperature of the air at coordinates that correspond to the location of the personnel barrier surface. The maximum temperature of the personnel barrier occurs at the top most location at the centerline of the model. The temperatures at key points from the analysis using the model described above are shown in Figure 3.4-12.

3.4.1.5 Test Model

The methods previously described have been used in previous transport cask licensing and are sufficient to show that the Universal Transport Cask meets the criteria set forth in Section 3.4. Therefore, no thermal test model is created.

3.4.2 Maximum Temperatures

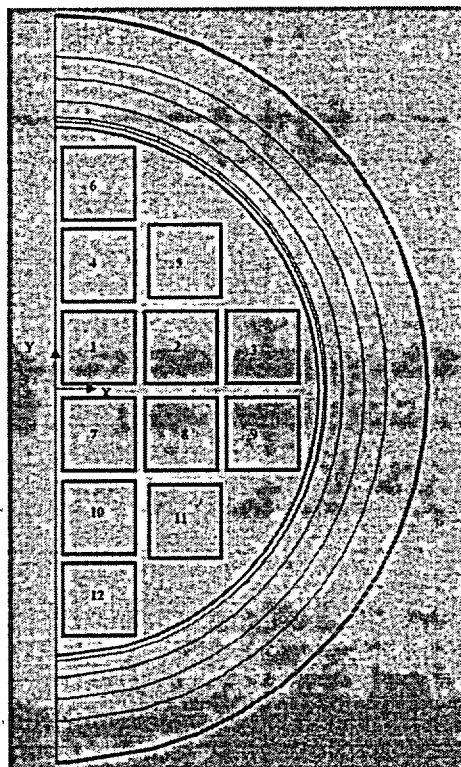
Using the thermal models described in Sections 3.4.1.1 and 3.4.1.2, temperatures for the PWR and BWR cask body, canister, basket, and fuel rod cladding are determined for three normal conditions of transport: (1) maximum decay heat, 100°F ambient temperature, and solar insolation; (2) maximum decay heat, -40°F ambient temperature, and no insolation; and (3) no decay heat, -40°F ambient temperature, and no insolation. The maximum temperatures of the principal PWR and BWR cask components, canister, basket components, and fuel rod cladding are shown in Tables 3.4-1 and 3.4-2 for the first two environmental conditions listed above. For the third environmental condition (i.e., no decay heat, -40°F ambient temperature, and no insolation), no analysis is necessary because all package temperatures will equilibrate to -40°F. The cask body maximum allowable component temperatures are shown in Section 3.3.2 and Table 3.4-3.

Using the thermal model described in Section 3.4.1.3, the volumetric average temperature of the redwood in the impact limiters is 135°F.

3.4.2.1 Preferential Loading

This section provides the evaluation of preferential fuel loading in accordance with Section B 2.1.2 of Chapter 12 of the Safety Analysis Report for the UMS® Universal Storage System, Docket Number 72-1015. As stated in Section 12B2.1.2, loading of the fuel assemblies designated for a given canister must be administratively controlled to ensure that the fuel cladding temperature limits are not exceeded for any fuel assembly, unless all of the designated fuel assemblies have a cooling time of 7 years or more. Fuel with the shortest cooling time (and, therefore, having a higher allowable cladding temperature) is placed in the center of the basket. Fuel with the longest cooling time (and, therefore, having a lower allowable cladding temperature) is placed in the periphery of the basket. Canisters containing fuel assemblies all of which have a cooling time of 7 years or more, do not require preferential loading.

For the transport conditions, three (3) thermal analyses have been performed using the three-dimensional cask model for the cask containing PWR fuel (Section 3.4.1.1.1). Note that the PWR configuration is selected since it is governing. The BWR configuration is considered to be bounded by the evaluation of the PWR configuration. The basket locations refer to those shown in the following figure.



For this analysis, heat load per assembly is based on Table 3.4-16: 5-year cooled fuel: 0.833 (20/24) kW; 6-year cooled fuel: 0.8125 (19.5/24) kW; 7-year cooled fuel: 0.742 (17.8/24) kW and 15-year cooled fuel: 0.70 (16.8/24) kW

Case 1 considers the loading pattern having 5-year cooled fuel in the center of the basket (Locations 1 and 7), 7-year cooled fuel in the periphery positions (Location 3, 5, 6, 9, 11, and 12) and 6-year cooled fuel in the intermediate positions (Locations 2, 4, 8, and 10). The heat load for each fuel assembly is determined based on the maximum allowable heat load as shown in Table 3.4-16. The allowable temperatures are obtained from Table 3.4-15, based on the burnup and cool time corresponding to the analyzed heat load. The calculated maximum temperature at each fuel position and the corresponding allowable temperature is:

Basket Location	1	2	3	4	5	6	7	8	9	10	11	12
Fuel Cool Time (Years)	5	6	7	6	5	7	5	6	7	6	7	7
T_{max} (°F)	654	613	642	628	623	621	636	694	624	625	618	685
$T_{allowable}$ (°F)	705	693	653	693	653	653	705	693	653	693	653	653

Case 2 considers the loading pattern having 5-year cooled fuel in the center of the basket (Locations 1 and 7) and 7-year cooled fuel in all other basket positions (Locations 2 to 6 and 8 to

12). The calculated maximum temperature at each position and the corresponding allowable temperature are:

Basket Location	1	2	3	4	5	6	7	8	9	10	11	12
Fuel Cool Time (Years)	7	7	7	7	7	7	7	7	7	7	7	7
T _{max} (°F)	642	595	536	609	564	562	624	576	516	557	510	478
T _{allowable} (°F)	705	653	653	653	653	653	705	653	653	653	653	653

Case 3 considers the loading pattern having 15-year cooled fuel in the center of the basket (Locations 1 and 7) and 7-year cooled fuel in all other basket positions (Locations 2 to 6 and 8 to 12). The calculated maximum temperature at each fuel position and the corresponding allowable temperature are:

Basket Location	1	2	3	4	5	6	7	8	9	10	11	12
Fuel Cool Time (Years)	15	7	7	7	7	7	15	7	7	7	7	7
T _{max} (°F)	610	583	528	596	555	553	593	564	508	546	502	471
T _{allowable} (°F)	631	653	653	653	653	653	631	653	653	653	653	653

Cases 1 and 2 bound all possible loading configurations for fuel assemblies with a cool time of 7 years or less, which require preferential loading. These results show that the maximum fuel cladding temperature for each assembly will not exceed its allowable temperature, if fuel loading is administratively controlled such that fuel with the shortest cooling time is placed in the center positions of the basket and fuel with the longest cooling time is placed in the periphery positions.

Case 3 represents a bounding configuration for canisters containing fuel assemblies, all of which have a cooling time of 7 years or more. The analysis results show that no preferential loading is required.

3.4.3 Minimum Temperatures

The minimum temperatures of the cask and components occur with no heat load and -40°F. These conditions yield a uniform -40°F temperature throughout the Universal Transport Cask package. All package components are capable.

3.4.4 Maximum Internal Pressures

In the following sections, the maximum internal operating pressures for normal conditions of transport are calculated for the PWR and BWR Transportable Storage Canisters and for the Universal Transport Cask cavity. The maximum operating pressure for the canister and cask cavity are summarized in Table 3.4-4.

3.4.4.1

Maximum Internal Pressure for PWR Fuel Canister and Transport Cask

The internal pressures within the PWR fuel canister and transport cask are a function of fuel type, fuel condition (failure fraction), burnup, canister type, and the backfill gases in the canister and cask cavity. Gases included in the pressure evaluation include rod-fill, rod fission and rod backfill gases, canister and cask backfill gases and burnable poison generated gases. Each of the fuel types expected to be loaded into the UMS® system is separately evaluated to arrive at a bounding canister pressure.

Fission gases include all fuel material generated gases including long-term actinide decay generated helium. Based on detailed SAS2H calculations of the maximum fissile material mass assemblies in each canister class, the quantity of gas generated by the fuel rods rises as burnup and cool time is increased and enrichment is decreased. To assure the maximum gas is available for release, the PWR inventories are extracted from conservatively high 60,000 MWD/MTU burnup cases at an enrichment of 1.9 wt. % ²³⁵U and a cool time of 40 years. Gases included are all krypton, iodine, and xenon isotopes in addition to helium and tritium (T₂). Molar quantities for each of the maximum fissile mass assemblies are summarized in Table 3.4-5. Fuel generated gases are scaled by fissile mass to arrive at molar contents of other UMS® fuel types.

Fuel rod backfill pressure varies significantly between the PWR fuel types. The maximum reported backfill pressure is listed for the Westinghouse 17X17 fuel assembly at 500 psig. With the exception of the B&W fuel assemblies, which are limited to 435 psig, all fuel assemblies evaluated are set to the maximum 500 psig backfill reported for the Westinghouse assembly. Backfill quantities are based on the free volume between the pellet and the clad and the plenum volume. The fuel rod backfill gas temperature is conservatively assumed to have an initial temperature of 68°F.

Burnable poison rod assemblies (BPRAs) placed within the UMS® canister may contribute additional molar gas quantities due to (n, alpha) reactions of fission generated neutrons with ¹⁰B during in-core operation. ¹⁰B forms the basis of a portion of the neutron poison population. Other neutron poisons, such as gadolinium and erbium, do not produce a significant amount of helium nuclides (alpha particles) as part of their activation chain. Primary BPRAs in existence include Westinghouse Pyrex (borosilicate glass) and WABA (wet annular burnable absorber) configurations, as well as B&W BPRAs and shim rods employed in GE cores. The GE shim rods replace standard fuel rods to form a complete assembly array. The quantity of helium available for release from the BPRAs is directly related to the initial boron content of the rods and the

release fraction of gas from the matrix material in question. Release from either of the low temperature, solid matrix materials is likely to be limited, but no release fractions were available in open literature. Therefore, a 100% release fraction is assumed based on a boron content of 0.0063 g/cm³ ¹⁰B per rod, with the maximum number of rods per assembly. The maximum number of rods is 16 for Westinghouse core 14 x 14 assemblies, 20 rods for Westinghouse and B&W 15 x 15 assemblies, and 24 rods for Westinghouse and B&W 17 x 17 assemblies. The length of the absorber is conservatively taken as the active fuel length. CE core shim rods are modeled at 0.0126 g/cm³ ¹⁰B for 16, 12, and 12 rods applied to CE manufactured 14 x 14, 15 x 15 and 16 x 16 cores, respectively.

The canister backfill gases are conservatively assumed to be at 250°F, which is below the maximum canister shell temperature of 285°F after 9 hours of vacuum drying. The initial pressure of the canister backfill gas is 1 atm (0.0 psig). The cask backfill temperature and pressure are assumed to be 68°F and 1 atm. Free volume inside each PWR canister class is listed in Table 3.4-6. Also included are the total canister and cask free volumes. The listed free volumes do not include fuel assembly components since these components vary for each assembly type and fuel insert. By subtracting the rod and guide tube volumes and all hardware component volumes from the listed free volume, the free volume of the canisters including fuel assemblies and a load of 24 BPRAs can be determined. For the Westinghouse BPRAs, the Pyrex volume is employed since it displaces more volume than the WABA rods.

The total pressure for each of the UMS[®] payloads is found by calculating the releasable molar quantity of each gas (30% of the fission gas, 100% of the rod backfill, BPRA and shim rod gases adjusted for the 3% fuel failure fraction and the canister and cask backfill gases), and summing the quantities directly. The quantity of gas is then employed in the ideal gas equation in conjunction with the average gas temperature at normal operating conditions to arrive at system pressures. The normal condition average temperature of the gas within the PWR canister and cask is considered to be 453°F. Each of the UMS[®] PWR fuel types is individually evaluated for normal condition pressure, and the maximum normal condition canister and cask pressures are determined to be 6.15 psig and 6.91 psig, respectively. A summary of the maximum pressure in the canister and in the cask for each PWR canister class is shown in Table 3.4-7. The table also includes the fuel type producing the listed maximum pressures.

The maximum normal condition cask pressure for a PWR payload (West 17 Std) is calculated as follows:

$$P = \frac{nRT}{V}$$

$$n = (0.03 \times n_{\text{rodbackfill}}) + (0.03 \times 0.30 \times n_{\text{fuelgas}}) + (0.03 \times n_{\text{BPRAs}}) + n_{\text{canisterbackfill}} + n_{\text{caskbackfill}}$$

$$n = (0.03 \times 134) + (0.03 \times 0.30 \times 965) + (0.03 \times 133) + 184 + 45 = 246 \text{ moles}$$

$$P = \frac{246 \text{ mol} \times 0.08205 \frac{\text{atm} \cdot \text{l}}{\text{mol} \cdot \text{K}} \times 510 \text{ K}}{6995 \text{ l}} = 1.47 \text{ atm} = 21.61 \text{ psia} = 6.91 \text{ psig}$$

Similar, the maximum canister pressure for a PWR payload (B&W 17x17) transportable storage canister is:

$$n = (0.03 \times n_{\text{rodbackfill}}) + (0.03 \times 0.30 \times n_{\text{fuelgas}}) + (0.03 \times n_{\text{BPRAs}}) + n_{\text{canisterbackfill}}$$

$$n = (0.03 \times 169) + (0.03 \times 0.30 \times 962) + (0.03 \times 132) + 195 = 213 \text{ moles}$$

$$P = \frac{213 \text{ mol} \times 0.08205 \frac{\text{atm} \cdot \text{l}}{\text{mol} \cdot \text{K}} \times 510 \text{ K}}{6275 \text{ l}} = 1.42 \text{ atm} = 20.8 \text{ psia} = 6.15 \text{ psig}$$

3.4.4.2 Maximum Internal Pressure for BWR Fuel Canister and Transport Cask

BWR canister and cask maximum pressures are determined in the same manner as those documented for the PWR cases. Primary differences between PWR and BWR analysis include a maximum normal condition average gas temperature of 366°F, rod backfill gas pressures of 132 psig, and pressurizing gases are limited to fission gases (including helium, actinide decay gas), rod backfill gases, and canister and cask backfill gas. The 132 psig employed in this analysis is significantly higher than the 6 atmosphere maximum pressure reported in open literature. BWR assemblies do not contain an equivalent to the PWR BPRAs and, therefore, do not require ¹⁰B helium generated gases to be added. Fissile gas inventories for the maximum fissile material assemblies in each of the three BWR lattice configurations (7 x 7, 8 x 8, and 9 x 9) are shown in Table 3.4-8. Free volumes, without fuel components, in UMS® canister classes 4 and 5 are shown in Table 3.4-9. Cask and canister maximum pressures for each canister class are listed in Table 3.4-10. The maximum normal condition pressure of 3.47 psig is based on a GE 7 x 7 assembly designed for a BWR/2-3 reactor and burned to 60,000 MWD/MTU. Cask maximum pressure for the GE 7 x 7 fuel is 3.65 psig. High burnups, greater than 45,000 MWD/MTU, are typically obtained from updated assembly designs such as the GE 9 x 9 assembly. The normal condition pressure for a UMS® canister containing the GE 9 x 9 fuel assembly with 79 fuel rods is 3.33 psig. Similar fuel masses and displaced volume account for similar system pressures.

The maximum normal condition cask pressure for a BWR payload (GE 7x7 UMS Class 4) is calculated as follows:

$$P = \frac{nRT}{V}$$

$$n = (0.03 \times n_{\text{rodbackfill}}) + (0.03 \times 0.30 \times n_{\text{fuelgas}}) + n_{\text{canisterbackfill}} + n_{\text{caskbackfill}}$$

$$n = (0.03 \times 75) + (0.03 \times 0.30 \times 940) + 194 + 9 = 214 \text{ moles}$$

$$P = \frac{214 \text{ mol} \times 460 \text{ K}}{6460 \text{ l}} \times 0.08205 \frac{\text{atm} \cdot \text{l}}{\text{mol} \cdot \text{K}} = 1.25 \text{ atm} = 18.35 \text{ psia} = 3.65 \text{ psig}$$

Similarly, the maximum canister pressure for a BWR payload (GE 7x7 UMS Class 4) transportable storage canister is:

$$n = (0.03 \times n_{\text{rodbackfill}}) + (0.03 \times 0.30 \times n_{\text{fuelgas}}) + n_{\text{canisterbackfill}}$$

$$n = (0.03 \times 75) + (0.03 \times 0.30 \times 940) + 194 = 205 \text{ moles}$$

$$P = \frac{205 \text{ mol} \times 0.08205 \frac{\text{atm} \cdot \text{l}}{\text{mol} \cdot \text{K}} \times 460 \text{ K}}{6275 \text{ l}} = 1.24 \text{ atm} = 20.8 \text{ psia} = 3.47 \text{ psig}$$

3.4.5 Maximum Thermal Stresses

The ANSYS computer code is used to obtain temperatures for use in the structural analyses of Chapter 2.0. These temperatures are presented in Tables 3.4-1 and 3.4-2. The thermal stress calculations for normal conditions of transport are performed in Sections 2.6.1 and 2.6.2.

3.4.6 Maximum Allowable Cladding Temperature and Canister Heat Load

The maximum allowable cladding temperatures are calculated for PWR and BWR systems based on fuel assembly type, maximum burnup, and minimum initial cool time. Allowable heat loads are determined by relating cladding temperature to canister heat load.

Cladding stresses are calculated for a set of representative PWR and BWR assemblies at 40,000 MWD/MTU and 380°C. The limiting highest stress assemblies, the Westinghouse 14x14 and GE 9x9 (150-inch fuel region), are then evaluated at various burnups to determine the maximum allowable fuel cladding temperature based on PNL-6364 criteria [28]. Maximum allowable cladding temperatures are generically calculated for PWR and BWR burnups ranging from 35,000 MWD/MTU to 45,000 MWD/MTU. PWR burnups are extended to 50,000 MWD/MTU.

to envelop the Maine Yankee specific inventory. After applying a bias to the maximum allowable cladding temperatures, the maximum allowable heat load is calculated as a function of burnup and minimum initial cool time.

B.4.6.1 Maximum Allowable Cladding Temperature

Based on PNL-6364, the cladding temperature limit is expressed as a function of initial dry storage temperature, initial cladding stress at the dry storage temperature, and initial storage time. For this evaluation, the transport temperatures and transport times are applied.

The initial cladding stress is a function of the rod internal pressure, temperature, diameter of the fuel rod, and fuel cladding thickness. The initial cladding stress (σ_{mhoop}) for a particular assembly is calculated as [28]:

$$\sigma_{mhoop} = \frac{(P)(D_{mid})}{2t} \times \alpha \times \frac{T_2}{T_1} \times \frac{69,684}{10,000}$$

where:

σ_{mhoop} = dry storage cladding hoop stress, MPa

P = internal gas pressure of the rod, psi

T_1 = temperature at which P was determined, K

t = cladding wall thickness, in

D_{mid} = cladding midwall diameter, in

α = a factor, 0.95 for PWR rods or 0.90 for BWR rods

T_2 = allowable storage temperature for σ_{mhoop} , K

To account for cladding oxidation during in-core fuel assembly operation and storage of the fuel in the spent fuel pool, the nominal cladding thickness is reduced by 0.06 mm and 0.125 mm for PWR and BWR fuel rods, respectively [3]. For higher burnup PWR fuels (i.e., rod peak burnup up to 50,000 MWD/MTU), Maine Yankee experience is that the maximum oxide layer thickness on the fuel cladding is 120 microns [30]. The allowable cladding temperature calculations at 50,000 MWD/MTU therefore employ an oxide layer thickness of 0.012 cm.

The pressure in the fuel assembly rods is produced by the combination of fill gas and fission gas. For a given fuel assembly design, the fill gas quantity is fixed and does not vary with discharge burnup. Based on the initial pressure and temperature of the fill gas, the number of moles of gas are calculated using the ideal gas law:

$$PV = NRT$$

where:

P = Pressure

V = Volume (free volume inside fuel rod)

N = Number of moles of gas

R = Universal gas constant

T = Temperature of the gas

The number of moles of fill gas are added to the fission gas quantity and converted to a cladding internal pressure at storage conditions.

The fission gas quantity pressurizing the fuel cladding is calculated on the basis of the burnup and a fission gas release fraction. While the amount of fission gas produced is a predictable quantity (directly correlated to the number of fissions required to produce the desired burnup), the release fraction of the gas from the pellet into the pellet-cladding void depends on fill gas pressure and reactor operating conditions.

The number of fissions (Z) is related to the burnup by:

$$Z = X \text{ Burnup} \frac{\text{MWd}}{\text{MTU}} \times 1.0 \times 10^6 \frac{\text{W}}{\text{MW}} \times 86,400 \frac{\text{sec}}{\text{d}} \times \frac{1 \text{ MeV}}{1.602 \times 10^{-13} \text{ J}} \times \frac{1 \text{ Fission}}{200 \text{ MeV}} \\ \times \frac{1 \text{ Mole}}{6.02 \times 10^{23} \text{ Atoms}} \times \text{Mass} \frac{\text{MTU}}{\text{Assembly}} \times \frac{\text{Assembly}}{\# \text{ Rods}}$$

Multiplying the number of fissions by 0.3125 (0.25 x 1.25) atoms/fission then derives the quantity of fission gas produced. Olander's "Fundamental Aspects of Nuclear Reactor Fuel Elements" [11] lists the number of gas atoms from a single fission as 0.25. Based on a detailed SAS2H isotope generated fission gas inventory, this fraction is increased by 25% to account for decay chains not included in Olander (particularly those leading to ¹³⁶Xe). By employing a conservative fission gas fraction rather than the SAS2H output itself, the allowable cladding temperature calculation is decoupled from source term calculations.

Based on Sandia Report 90-2406, "A Method for Determining the Spent-Fuel Contribution to Transport Cask Containment Requirements" [10], gas release fractions from the fuel pellets are assumed to be 12% for PWR fuel rods and 25% for BWR fuel rods. Relying on a gas diffusion model (as applied to pre-pressurized light water reactor fuel rods), the Sandia report indicates a release fraction of approximately 1% for PWR rods and approximately 2% for BWR rods [10]. Experimental release fractions reach as high as 16% for PWR rods and 25% for BWR rods [10]. The higher release fractions are associated with unpressurized fuel rods or those rods run at uncharacteristically high temperatures and linear heat generation rates. While these rods show higher release rates, they are not expected to produce higher "burned fuel" pressures, since the partial pressure of the fill gas is not present, thereby allowing a larger number of fission gas molecules to accumulate before reaching limiting cladding pressure. The 12% PWR fission gas release fraction excludes the unpressurized Maine Yankee rod data while including the 43,000 MWD/MTU Calvert Cliff data to approximate the upper bound 45,000 MWD/MTU burnup. An additional analysis is performed comparing the 12% PWR and 25% BWR release fractions to the element specific release fractions in Reg. Guide 1.25 [29]. The 12% PWR release fraction results in gas releases similar to those indicated by the Regulatory Guide, while the BWR 25% release fraction is twice the Regulatory Guide indicated gas release. Note that both the Sandia report and the Regulatory Guide release fractions are for punctured fuel rods where the release of the pressurizing gas allows additional gaseous isotopes to migrate from the fuel matrix. Using the 12% PWR and 25% BWR fuel rod release fractions, therefore, results in a conservative cladding pressurization assumption for the intact rod analysis. For higher burnup PWR fuels (i.e., rod peak burnup up to 50,000 MWD/MTU), Maine Yankee experience is that the maximum gas release rate (fuel pellet to rod plenum in intact fuel rods) is less than 3% [30]. Therefore, the 12% release fraction established for standard PWR fuel burned up to 45,000 MWD/MTU is conservatively applied to the higher burnup PWR fuel.

Fuel rod free volume is calculated based on the fuel characteristics in Tables 3.4-11 and 3.4-12 for PWR and BWR fuel, respectively. Not all assemblies requested for loading are included in the tables, since assemblies with significantly higher free volume or lower fuel mass are bounded by the cladding stress evaluations presented. ■■

Substituting the internal gas pressure resulting from the releasable gas inventories produced by 40,000 MWD/MTU burned fuel into the initial cladding stress ($\sigma_{m,0}$) equation at a temperature of 380°C results in the assembly-specific maximum cladding stresses shown in Table 3.4-11 and

Table 3.4-12. The Westinghouse 14 x 14 and GE 9 x 9 (150-inch fuel region) are the limiting PWR and BWR assembly types at 113.9 and 70.5 MPa stress levels, respectively.

The stress levels in the limiting assemblies are then evaluated at burnups ranging from 35,000 MWD/MTU to 50,000 MWD/MTU for PWR fuel and 35,000 MWD/MTU to 45,000 MWD/MTU for BWR fuel at temperatures of 300°C and 400°C for PWR fuels and 300°C and 450°C for BWR fuel. The evaluation results are presented in Table 3.4-13. This data is overlaid on generic stress versus limiting temperature curves to arrive at cool time and burnup-specific maximum cladding allowable temperatures. The data shown in Table 3.4-14, from which the generic curves are constructed, is taken from Table 3.1 of PNL-6189 [27].

The cladding temperature limit curves for the limiting PWR and BWR fuel assemblies are provided in Figures 3.4-13 and Figure 3.4-14. The intercept of each of the curves represents the maximum allowable cladding temperature at a given cool time and maximum assembly burnup. Fuel rod peak cladding stress level and the allowable cladding temperature are calculated using the assembly average burnup, even though some rods experience a higher burnup than the average. The average burnup is used, since the quantity of fission gas formation and the fuel rod gas temperature are conservatively determined. As shown in Table 3.4-15, allowable cladding temperature varies only slightly over a wide range of burnup for a given required cooling time. Consequently, the variation in cladding stress with burnup is also small.

3.4.6.2 Maximum Allowable Canister Heat Load

Thermal analysis was performed at three heat loads for PWR fuel and one heat load for BWR fuel to determine the corresponding maximum fuel cladding temperature. Only one heat load is analyzed for BWR fuel because the maximum computed clad temperature is 548°F (286.7°C) at the maximum heat load of 16 kW, which is already lower than the minimum allowable temperature limit for any BWR fuel (Table 3.4-15). Therefore, BWR fuel was not further analyzed and a fixed maximum decay heat of 16 kW is allowable for transport of BWR fuel.

The thermal models and methods described in Section 3.4.1, used to determine the temperature of fuel cladding and system components for the design basis heat load are applied to determine the cladding temperature at reduced heat loads. The ANSYS calculated temperatures that provide input for correlating allowable cladding temperature to allowable heat load are

Fuel Type	Fuel Clad Temperature		Heat Load
	(°F)	(°C)	(kW)
PWR	537	280.6	14
PWR	510	261.1	17
PWR	577	358.3	20
BWR	548	286.7	16

The PWR temperature versus heat load curve is plotted in Figure 3.4-15. To provide adequate design margin, the maximum allowable cladding temperatures are reduced by a temperature bias shown in Table 3.4-17, prior to their use in the calculation of maximum allowable canister heat load. Maximum allowable canister heat loads are calculated for initial cool times ranging from 5 to 15 years and burnups ranging from 35,000 MWd/MTU to 50,000 MWd/MTU for PWR fuel and 35,000 MWd/MTU to 45,000 MWd/MTU for BWR fuel. The results of the PWR and BWR analysis are presented in Table 3.4-16. Since these temperatures are based on the PWR and BWR assemblies having the highest cladding stress levels, the maximum heat loads can be applied to all UMS® design basis contents.

3.4.7 Evaluation of Package Performance for Normal Conditions of Transport



Results of thermal analysis of the Universal Transport Cask containing PWR and BWR fuel under normal conditions of transport are summarized in Tables 3.4-1 through 3.4-3. The maximum fuel rod cladding temperature is maintained below 810°F (432°C), temperatures of safety-related cask components are maintained within their safe operating ranges, and thermally induced stresses in combination with pressure and mechanical load stresses are shown in the structural analysis of Chapter 2.0 to be less than the allowable stresses. As shown in Section 3.4.2, the personnel barrier temperature of 153°F is below the allowable temperature of 185°F for exclusive use shipment. Therefore, the Universal Transport Cask can safely transport the design basis fuel under the normal conditions of transport specified in 10 CFR 71.71.



Figure 3.4-1 Three-Dimensional PWR Cask Finite Element Model

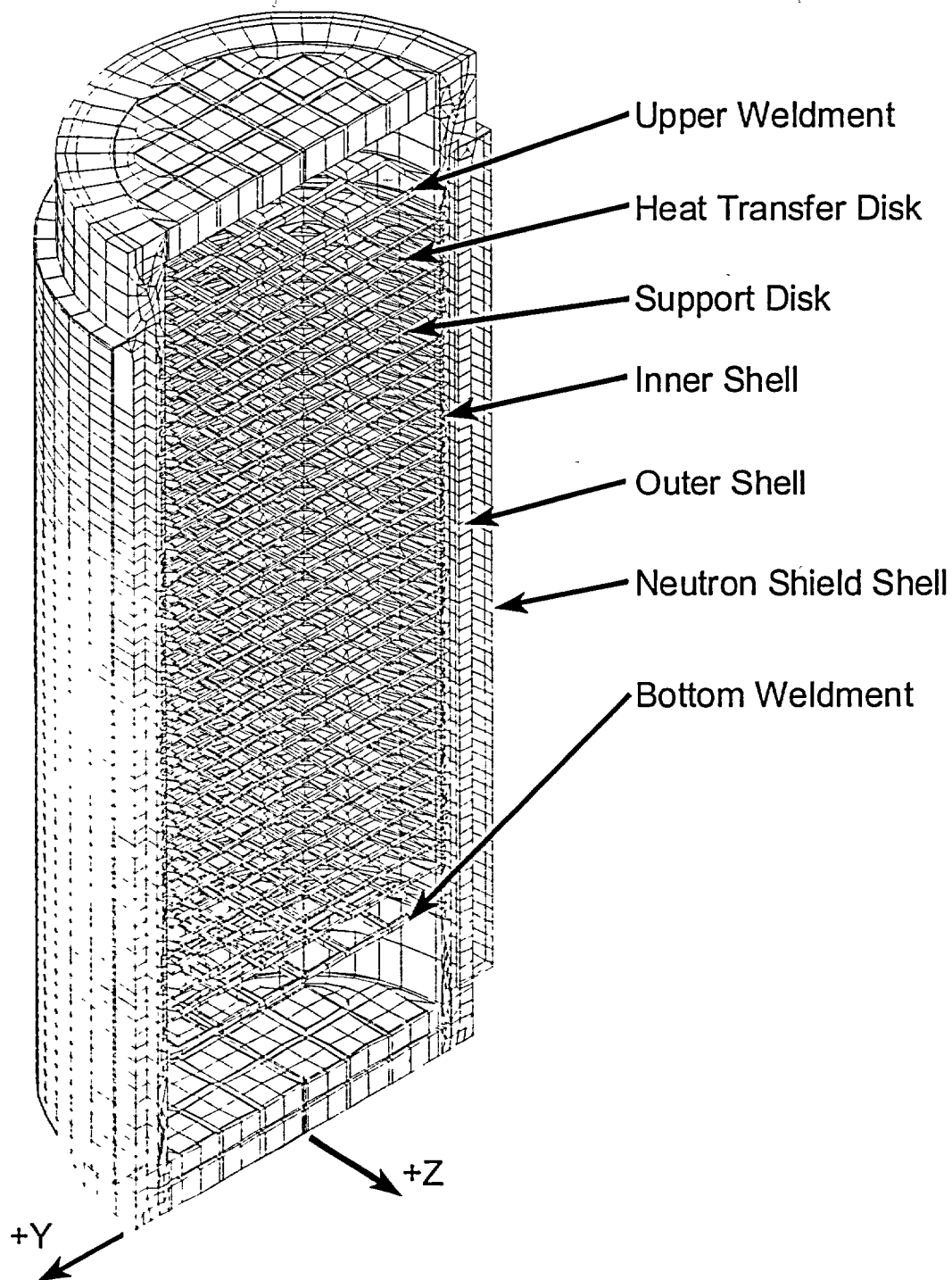


Figure 3.4-2 Design Basis PWR Fuel Assembly Axial Power Distribution

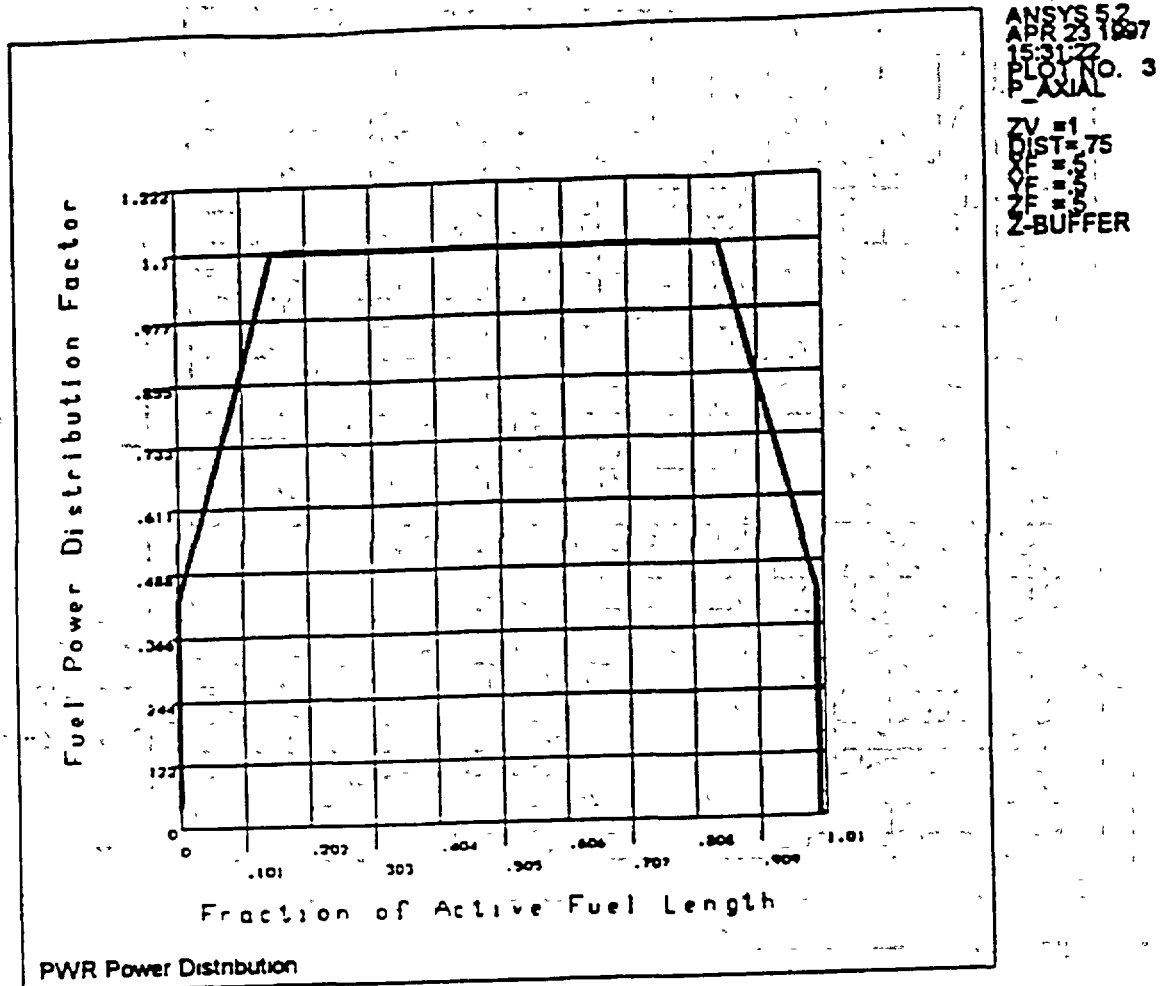


Figure 3.4-3 PWR 14x14 Fuel Assembly Two-Dimensional Finite Element Model

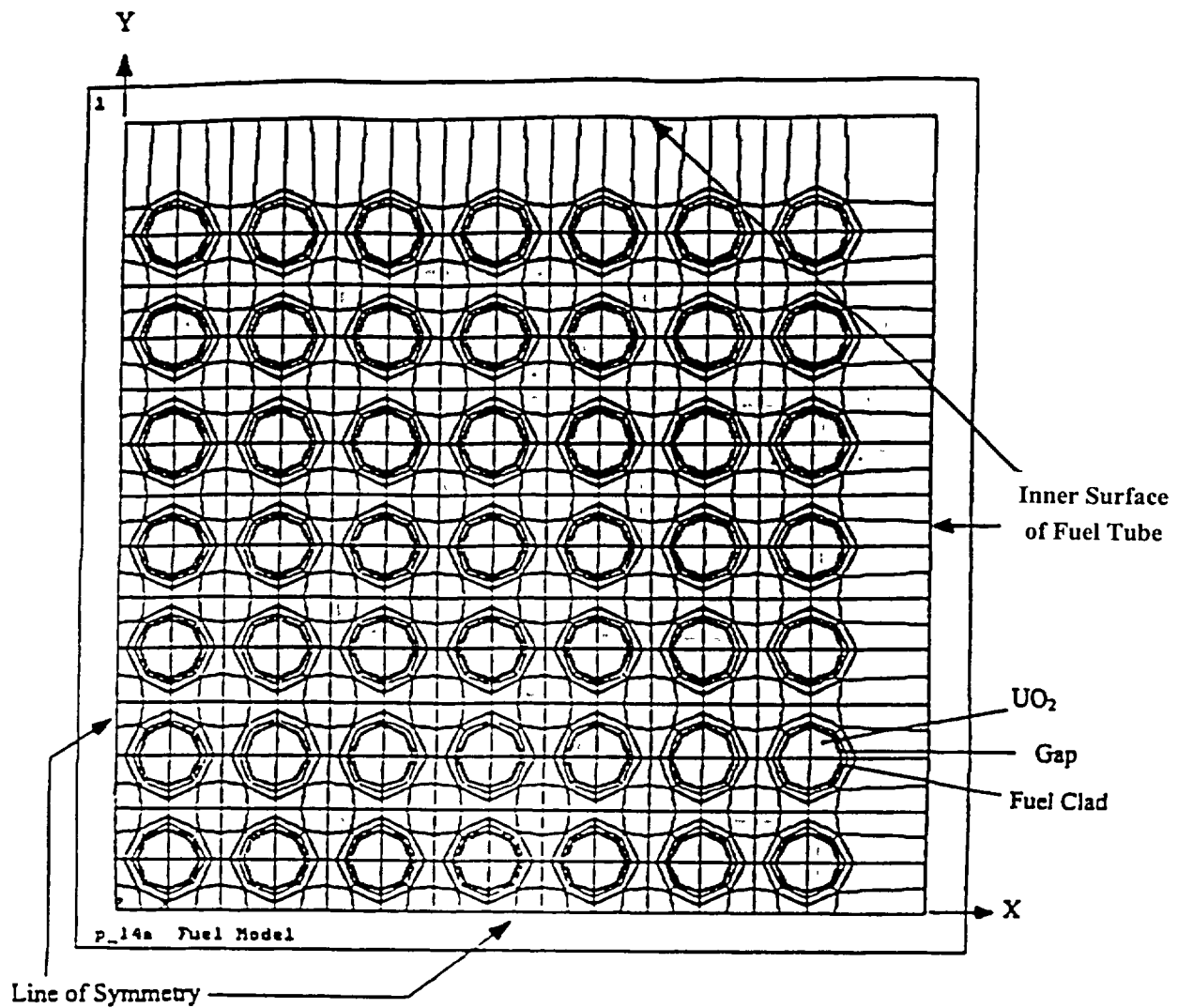


Figure 3.4-4 Two-Dimensional PWR Fuel Tube Model

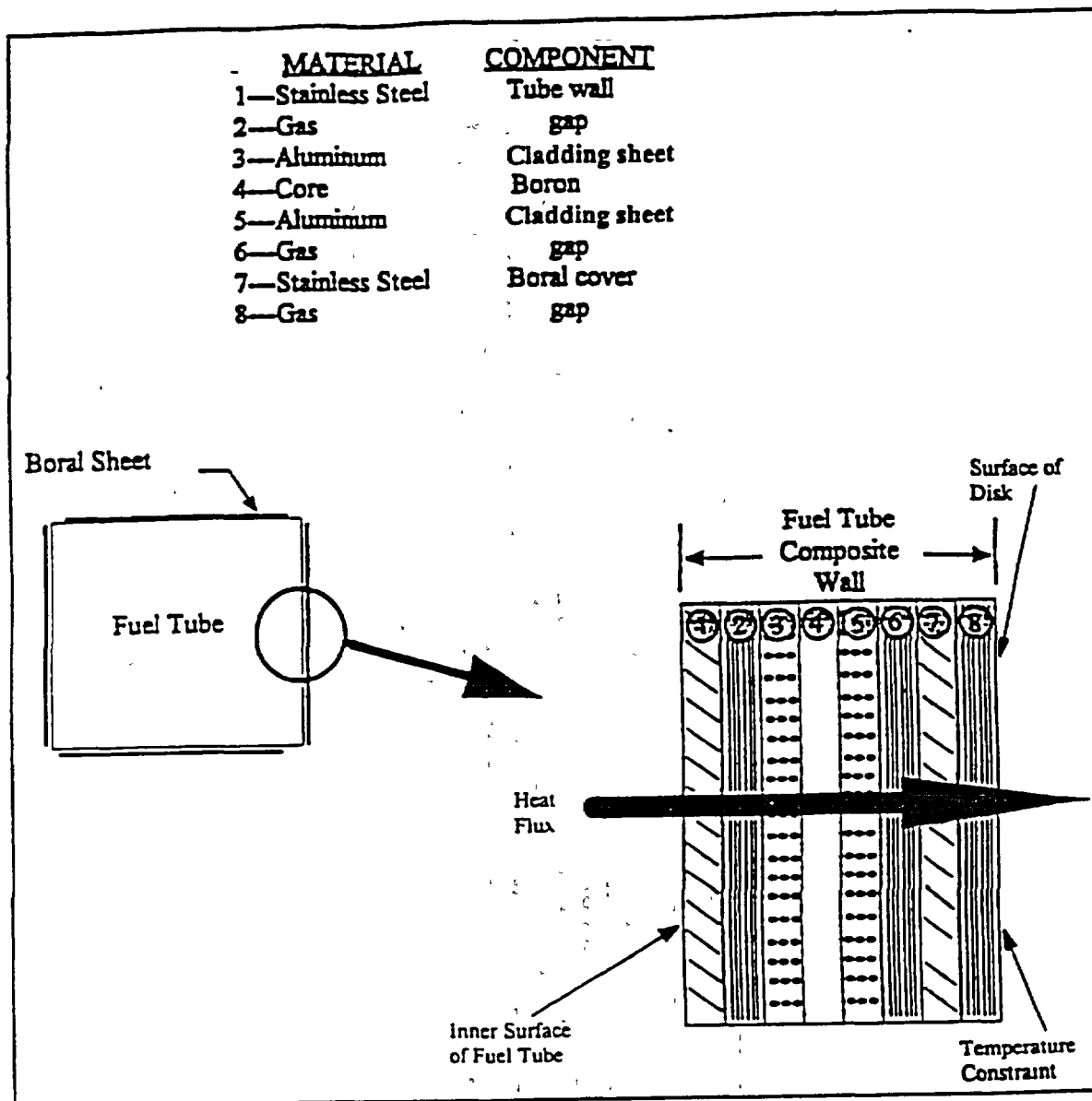


Figure 3.4-5 Three-Dimensional BWR Cask Finite Element Model

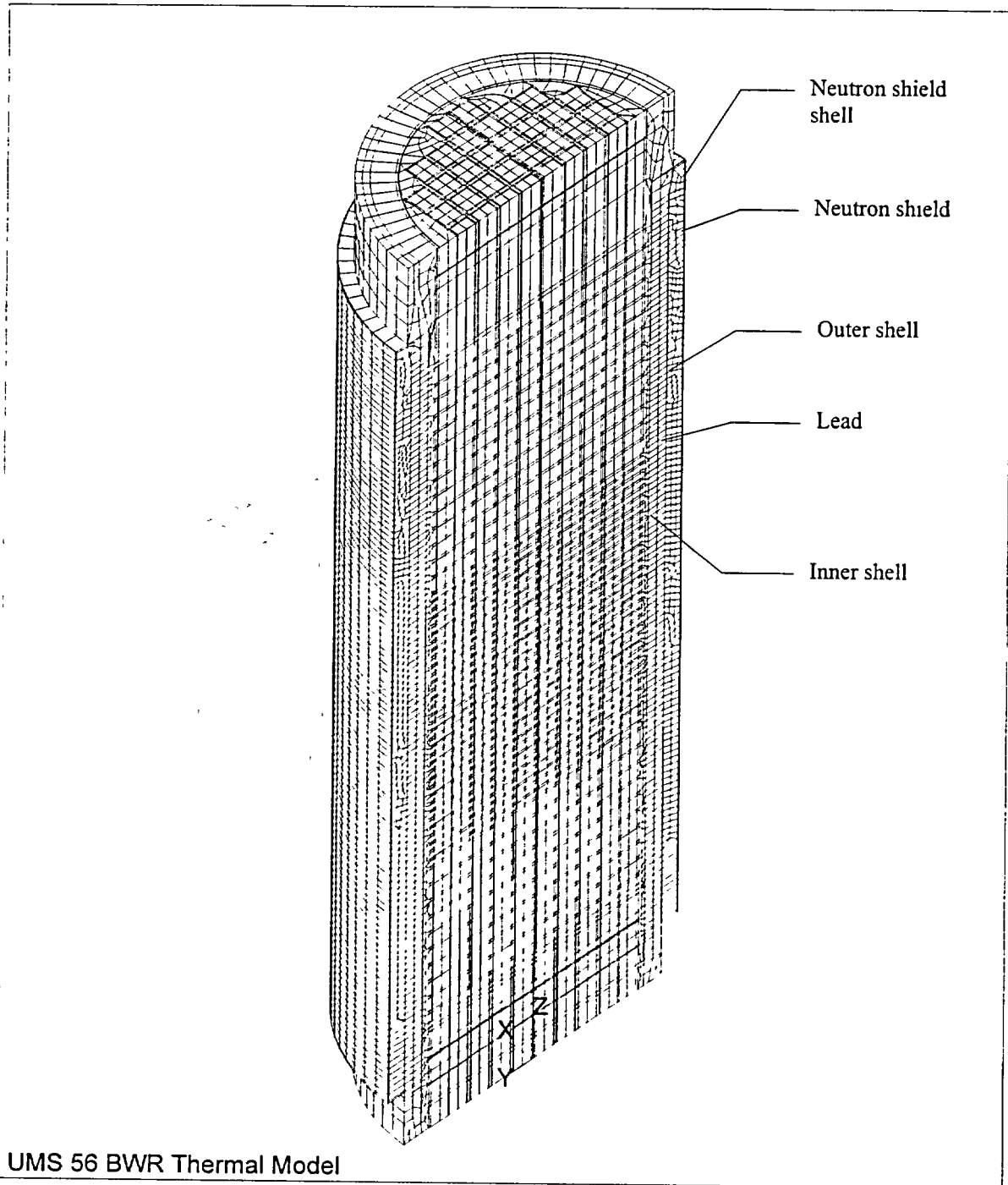


Figure 3.4-6 Design Basis BWR Fuel Assembly Axial Power Distribution

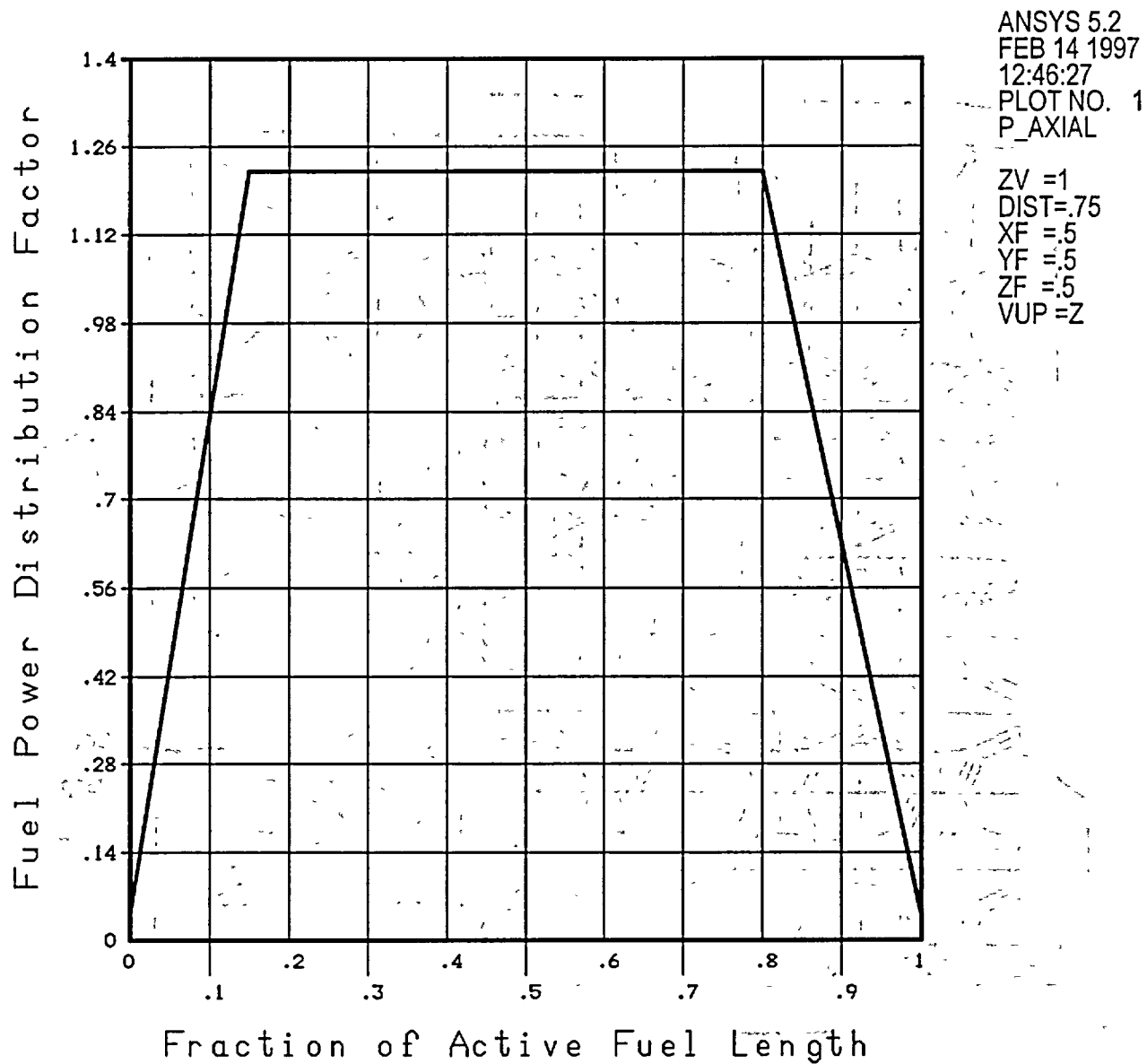


Figure 3.4-7 BWR 9x9 Fuel Assembly Two-Dimensional Finite Element Model

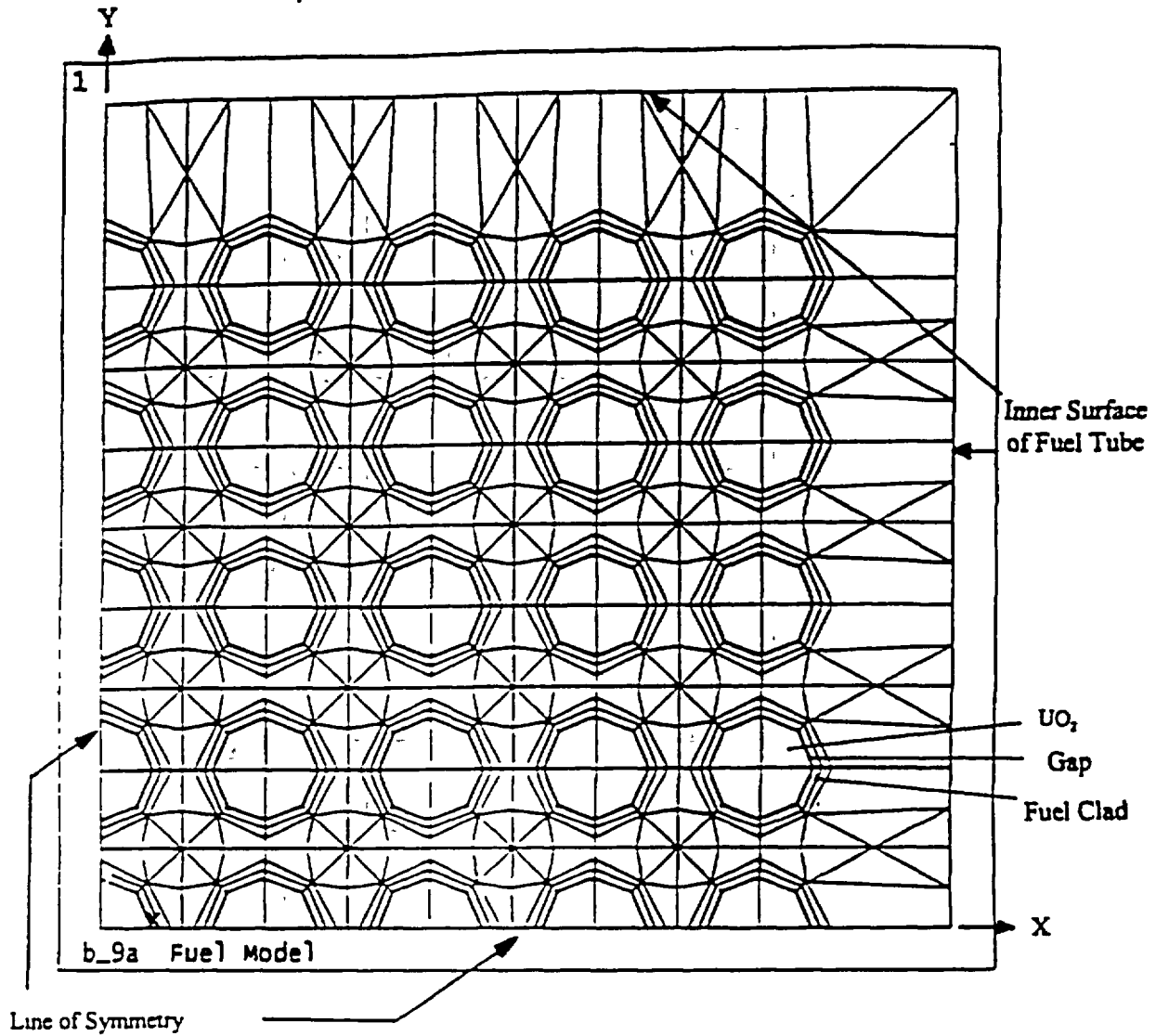


Figure 3.4-8 Two-Dimensional BWR Fuel Tube (with BORAL) Model

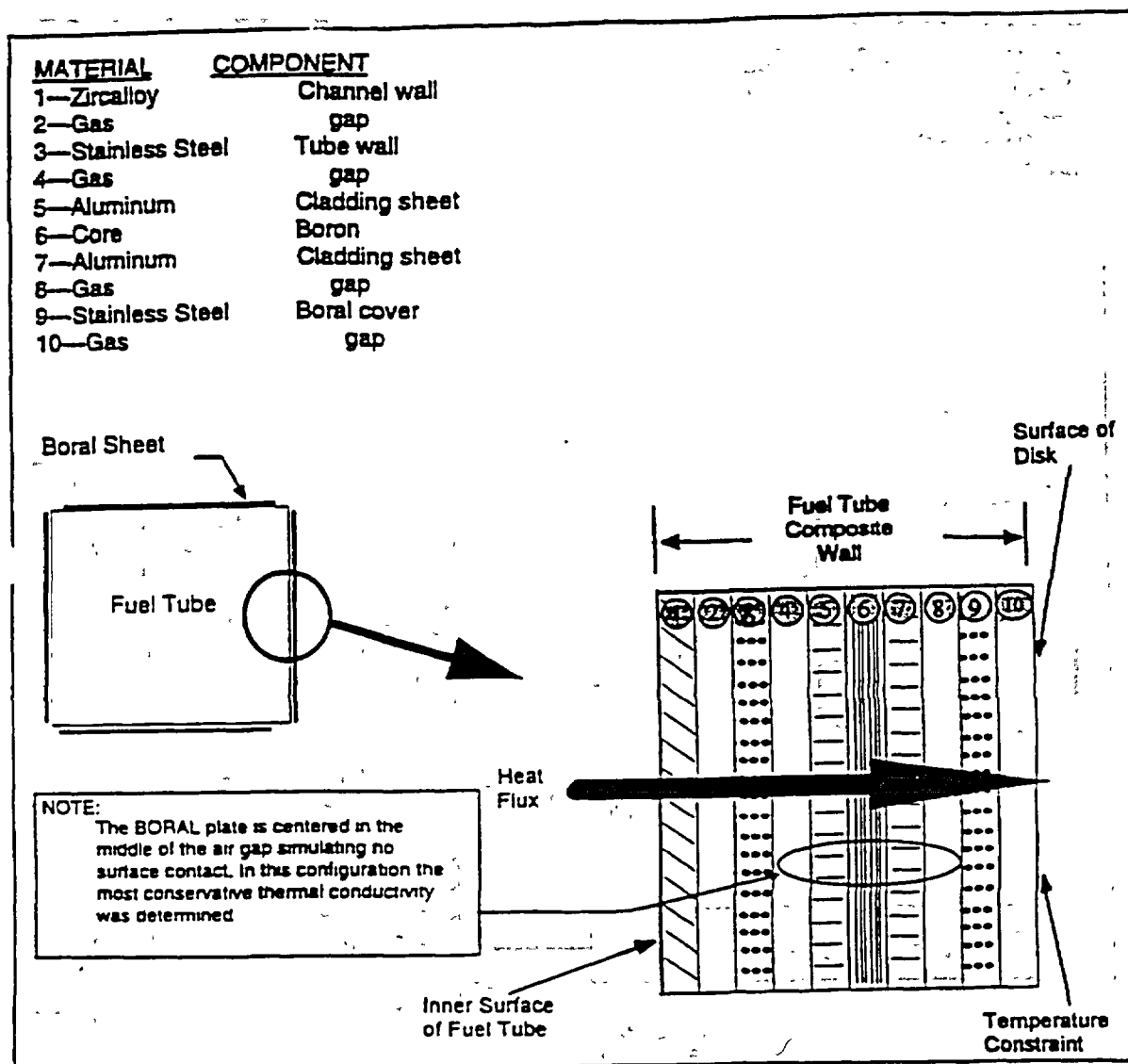


Figure 3.4-9 Two-Dimensional BWR Fuel Tube (without BORAL) Model

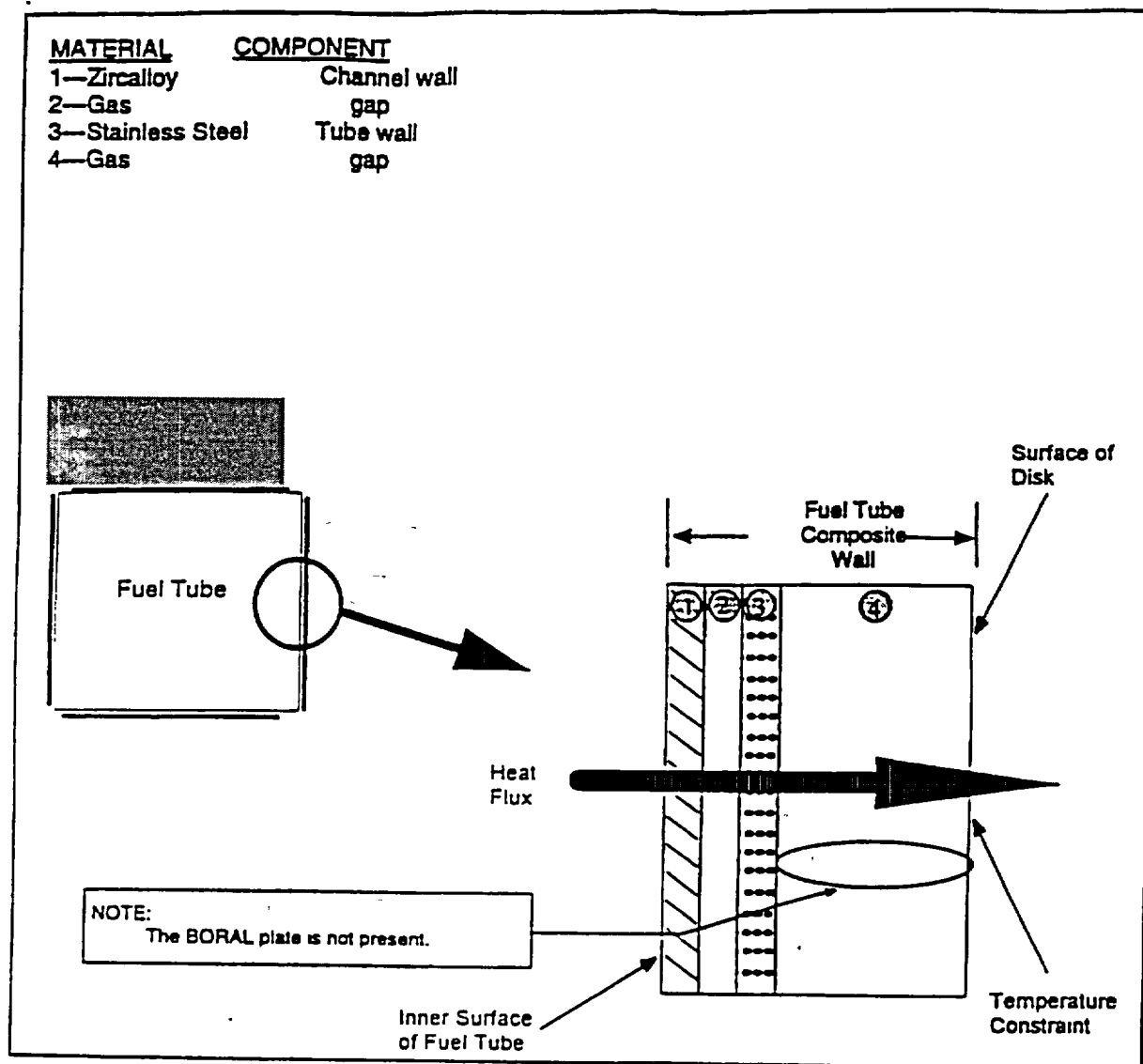


Figure 3.4-10 Cask Impact Limiter Thermal Model

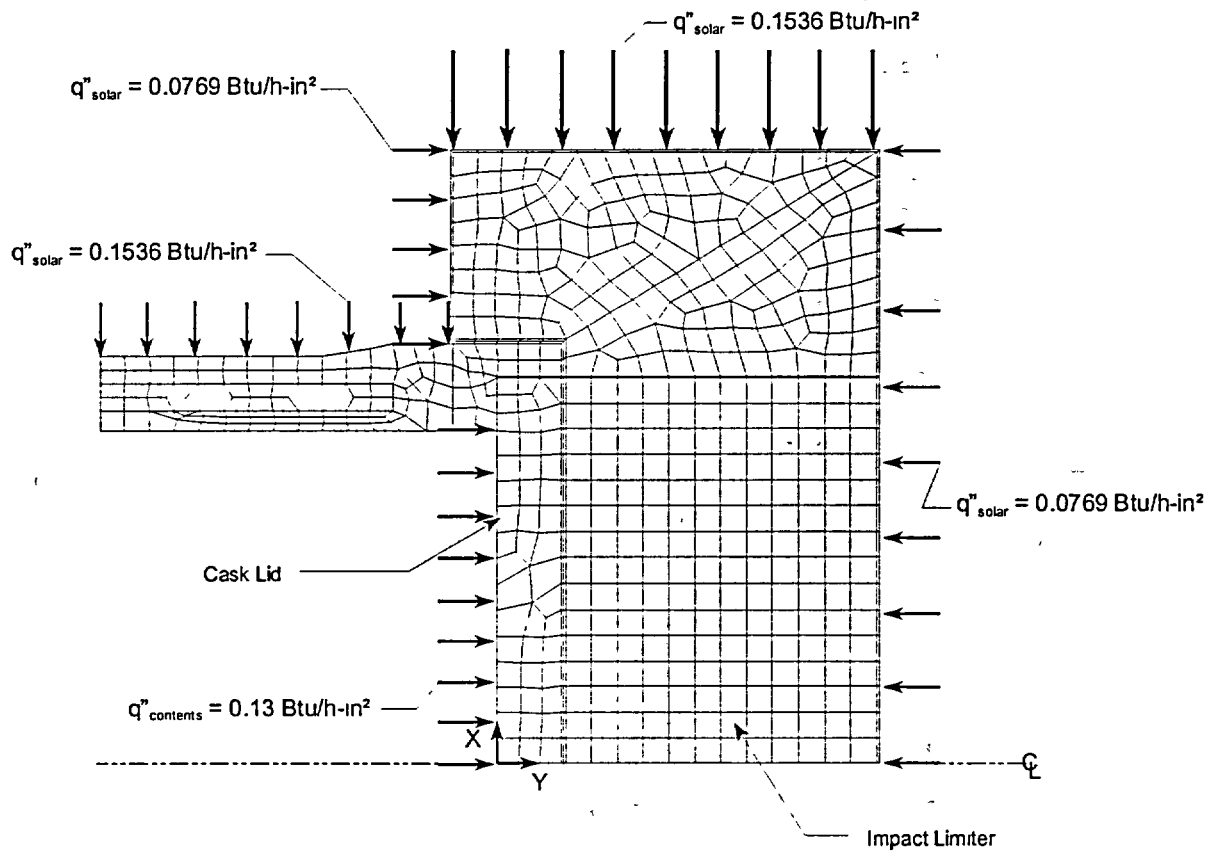


Figure 3.4-11

Personnel Barrier Thermal Mode

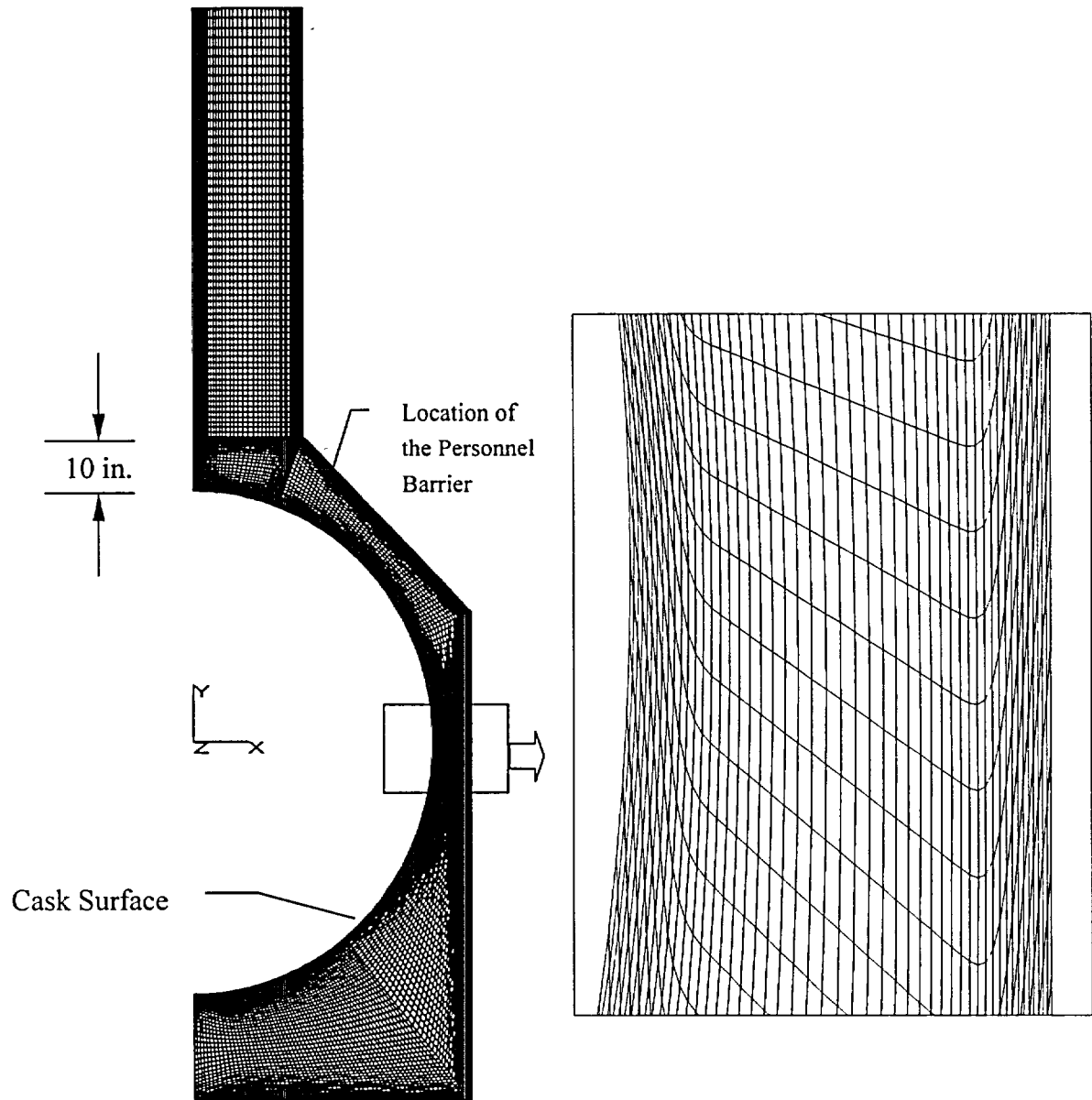
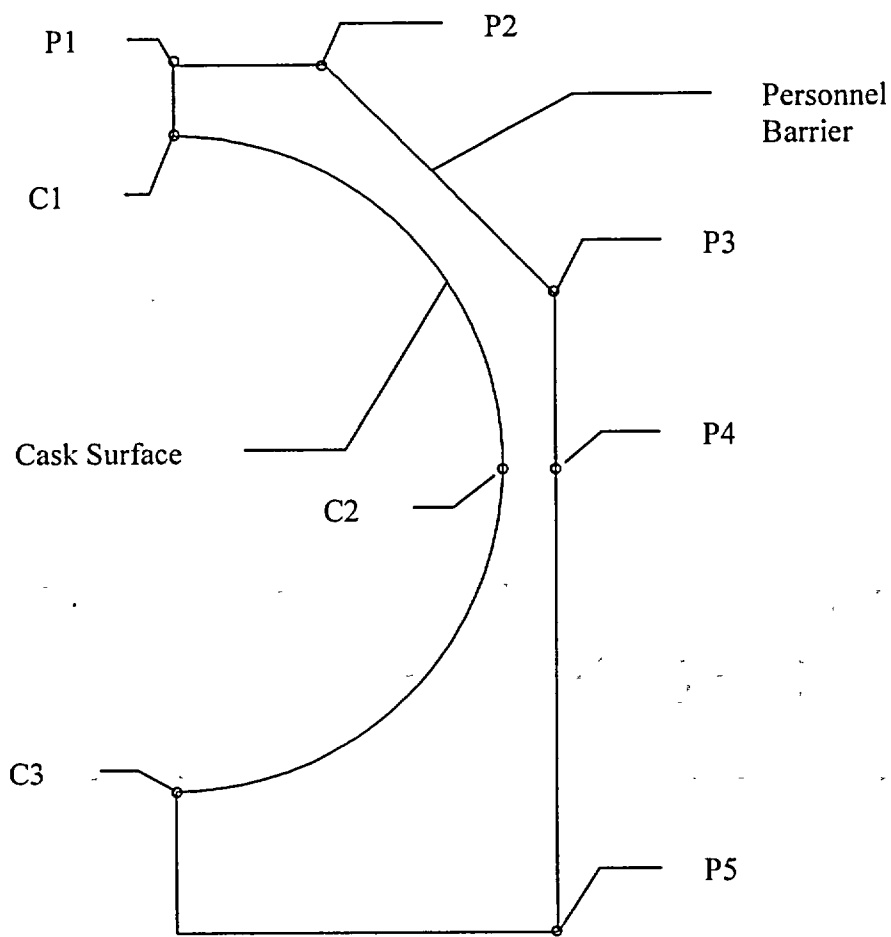


Figure 3.4-12 Temperature Results at Key Points of the Personnel Barrier



	Boundary Conditions			Calculated Temperature (°F)				
Location	C1	C2	C3	P1	P2	P3	P4	P5
Temperature	244	256	267	153	108	133	131	100

Figure 3.4-13

PWR Fuel Dry Storage Temperature versus Cladding Stress

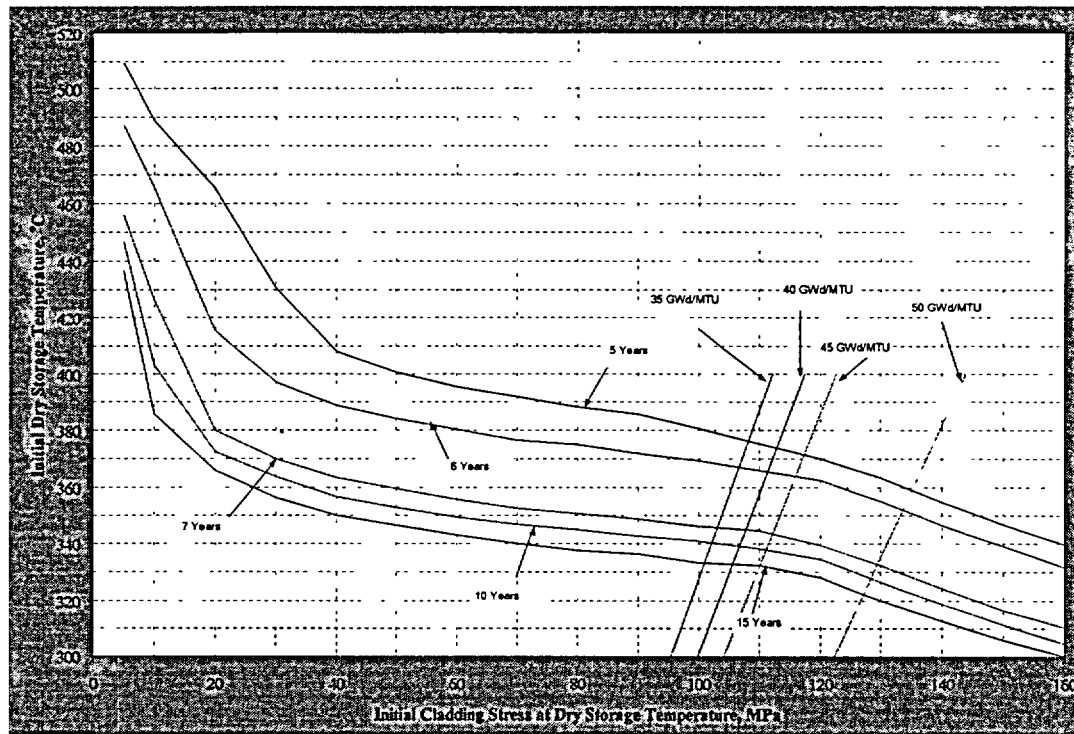


Figure 3.4-14

BWR Fuel Dry Storage Temperature versus Cladding Stress

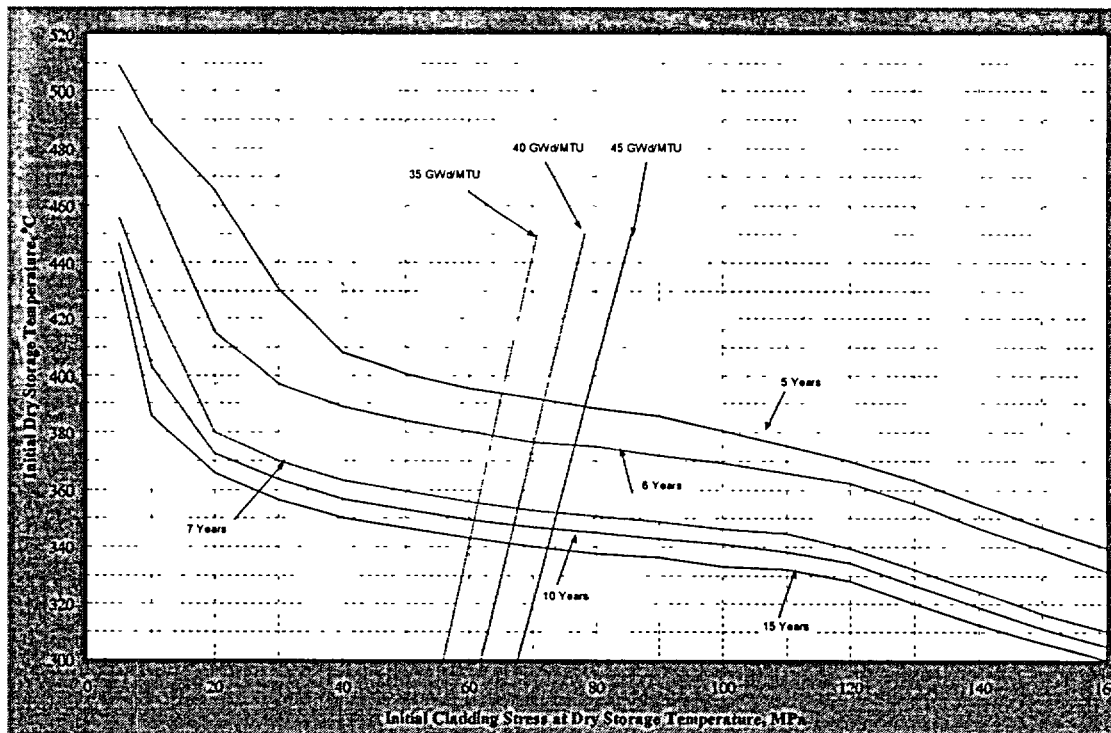


Figure 3.4-15

PWR Fuel Cladding Dry Storage II Temperature versus Basket Heat Load

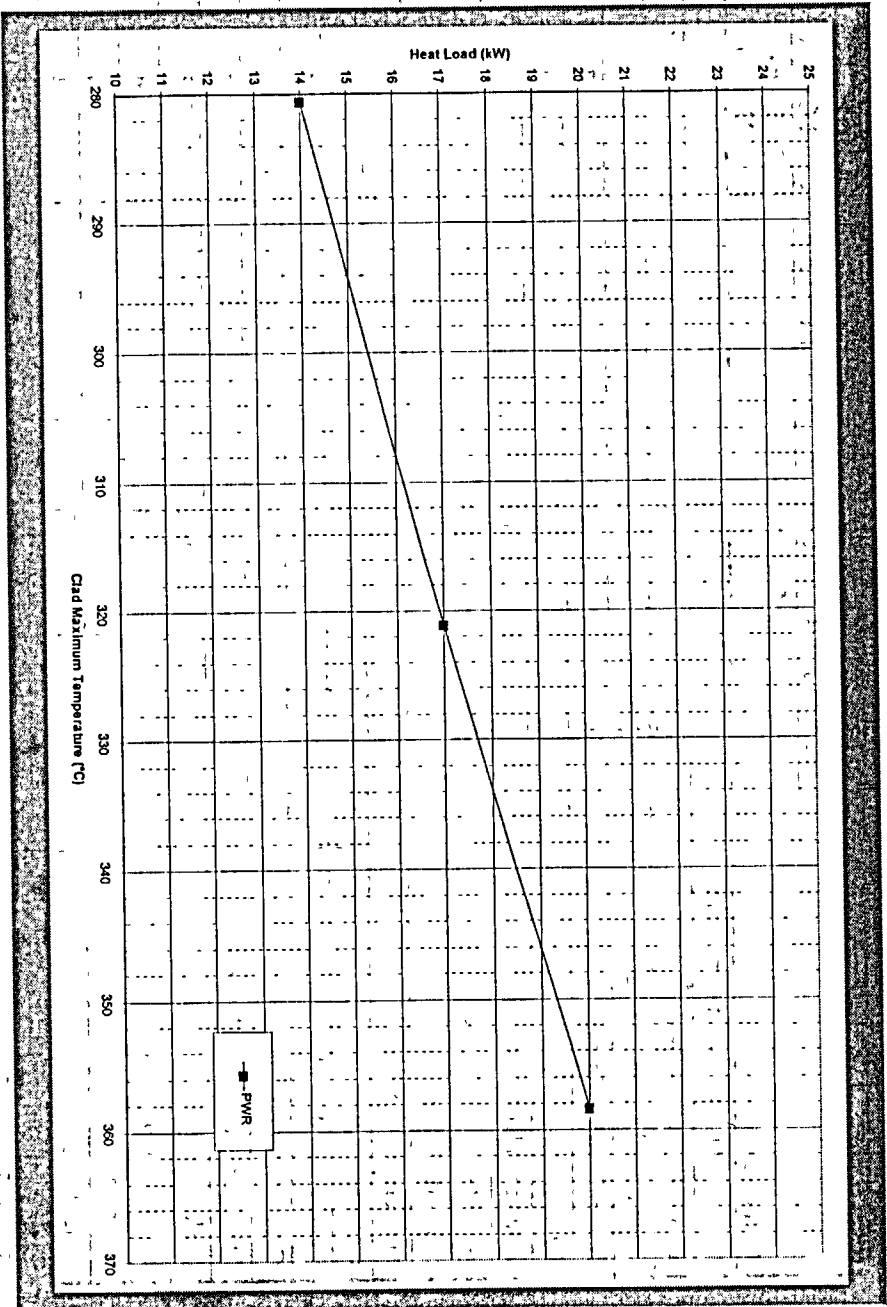




Table 3.4-1 Maximum Component Temperatures - Normal Conditions of Transport,
Maximum Decay Heat, Maximum Ambient Temperature

Component	Temperature (°F) Cask with PWR Fuel Canister		Temperature (°F) Cask with BWR Fuel Canister	
		Canister Gas: Helium		Canister Gas: Helium
Cask Lid O-Rings/Vent Port O-ring ¹		266		204
Lower Drain Port O-ring ⁴		224		230
Cask Radial Outer Surface		266		256
Radial Neutron Shield		293		286
Lead Gamma Shield		306		298
Aluminum Disk Exterior		268		298
Aluminum Disk Interior		309		313
Support Disk Exterior		253		208
Support Disk Interior		308		312
Canister Shell		408		363
Canister Shield Lid		270		208
Canister Bottom Plate		324		262
Maximum Fuel Rod Cladding		673		648
Cask Bottom		214		228
Bottom Forging		224		230
Inner Shell		344		312
Outer Shell		301		293
Top Forging ²		250		192
Cask Lid		266		204
Cask Lid Bolt ³		266		204
Average Gas Temperature in the Canisters ⁵		453		366

Conditions:
100°F ambient temperature
20 kW decay heat load, 1.1 peaking factor - PWR
16 kW decay heat load, 1.22 peaking factor - BWR
Solar insolation
Cask cavity gas: helium
Canister cavity gas:  helium 

1 Cask lid O-rings and vent port O-rings not explicitly modeled—taken to be the maximum cask lid temperature

2 Average temperature

3 Cask lid bolts not explicitly modeled—taken to be the maximum temperature of the cask lid

4 Lower drain port O-ring not explicitly modeled - taken to be the maximum temperature of the bottom forging

5 Calculated as a volumetric average.



Table 3.4-2 Maximum Component Temperatures - Normal Conditions of Transport,
Maximum Decay Heat, Minimum Ambient Temperature

Component	Temperature (°F) Cask with PWR Fuel Canister		Temperature (°F) Cask with BWR Fuel Canister	
		Canister Gas: Helium		Canister Gas: Helium
Cask Lid O-Rings/Vent Port O-ring ¹		140		62
Cask Radial Outer Surface		151		132
Radial Neutron Shield		178		162
Lead Gamma Shield		191		174
Maximum Basket ²		605		404
Canister Shell		289		238
Canister Shield Lid		145		66
Canister Bottom Plate		205		127
Maximum Fuel Rod Cladding		578		440

Conditions:
 -40°F ambient temperature
 20 kW decay heat load, 1.1 peaking factor - PWR
 16 kW decay heat load, 1.22 peaking factor - BWR
 No insulation
 Cask cavity gas: helium
 Canister cavity gas: helium

1. Cask lid O-ring and vent port O-rings not explicitly modeled—taken to be the maximum cask lid temperature

2. Taken to be the greater of the maximum support disk and the maximum aluminum heat transfer disk temperatures

Table 3.4-3 Universal Transport Cask Thermal Performance Summary for Component Operating Temperature

Temperature	Cask with PWR Fuel Canister (helium in cask cavity/helium in canister)	Cask with BWR Fuel Canister (helium in cask cavity/helium in canister)	Allowable Temperature Range
Maximum cladding temperature(°F)	<u>673</u>	<u>548</u>	< <u>705</u>
Component safe operating temperature ranges			
Cask lid O-rings	-40 to <u>266</u> °F	-40 to <u>208</u> °F	-40 to 300°F
Vent port coverplate O-ring	-40 to <u>266</u> °F	-40 to <u>208</u> °F	-40 to 300°F
Drain port coverplate-O-rings	-40 to <u>224</u> °F	-40 to <u>230</u> °F	-40 to 300°F
Radial NS-4-FR neutron shield	-40 to <u>293</u> °F	-40 to <u>286</u> °F	-40 to 300°F
Lead gamma shield	-40 to <u>306</u> °F	-40 to <u>298</u> °F	-40 to 600°F
Aluminum heat transfer disk	-40 to <u>605</u> °F	-40 to <u>515</u> °F	-40 to 700°F
<u>PWR support disk</u>	-40 to <u>608</u> °F		-40 to 650°F
<u>BWR support disk</u>		-40 to <u>517</u> °F	<u>-40 to 700°F</u>

1. The temperature of 705°F (374°C) is based on the maximum allowable cladding temperature established in Table 3.4-15 for the fuels with 5-year cooling time and 40,000 MWD/MTU burnup, which corresponds to maximum allowable canister decay heat of 20 kW for the PWR system (Table 3.4-16). Note that the design basis heat load of 20 kW is used in the thermal evaluation for the PWR fuels. The allowable temperature of 374°C also bounds the allowable temperatures for the design basis heat load for the BWR system (16 kW) as shown in Table 3.4-15.

Table 3.4-4 Maximum Internal Pressures for Transport

Fuel	Cavity	Condition	Pressure (psig)
PWR	Canister	3% fuel rod failure	615
		100% fuel rod failure	743
	Cask	3% fuel rod failure	691
		100% fuel rod failure	693
BWR	Canister	3% fuel rod failure	647
		100% fuel rod failure	438
	Cask	3% fuel rod failure	665
		100% fuel rod failure	428

Table 3.4-5 PWR Per Assembly Fuel Generated Gas Inventory

Array	Assy/Type	MTU	Moles
14x14	WE Standard	0.4144	35.52
15x15	B&W	0.4807	41.32
16x16	GE	0.4417	38.10
17x17	WE Standard	0.4671	40.18

Table 3.4-6 PWR Canister Free Volume (No Fuel or Inserts)

Canister Class	1	2	3
Basket Volume (in ³)	69800	74490	77460
Canister Height (inch)	175.05	184.15	191.75
Canister Free Volume w/o Fuel (liter)	7970	8400	8770
Canister and Cask Free Volume w/o Fuel (liter)	9030	8980	8970

Table 3.4-7 PWR Maximum Normal Condition Pressure Summary

Canister Class	Fuel Type	Canister Pressure (psig)	Cask Pressure (psig)
Class 1	West 17x17 Standard	6.13	6.91
Class 2	B&W 17x17 Mark 6	6.15	6.62
Class 3	GE 16x16	6.81	6.02

Table 3.4-8 BWR Per Assembly Fuel Generated Gas Inventory

Array	Assy Type	MTU	Moles
7x7	GE 7x7 (49 Rods)	D11985	16.78
8x8	GE 8x8 (63 Rods)	D11880	16.07
9x9	GE 9x9 (79 Rods)	D11979	16.86

Table 3.4-9 BWR Canister Free Volume (No Fuel or Inserts)

Canister Class	I	E
Basket Volume (in ³)	73110	74680
Canister Height (inch)	185.55	190.35
Canister Free Volume w/o Fuel (liter)	8500	8740
Canister and Cask Free Volume w/o Fuel (liter)	8710	8930

Table 3.4-10 BWR Maximum Normal Condition Pressure Summary

Canister Class	Fuel Type	Canister Pressure (psig)	Cask Pressure (psig)
Class 4	GE 7x7	8.47	8.65
Class 5	GE 7x7	8.41	8.55
Class 6	GE 9x9	8.38	8.48

Table 3.4-11 PWR Cladding Stress Level Comparison Chart

Fuel Type	B&W 15x15	B&W 17x17	CE 14x14	CE 16x16	WE 14x14	WE 15x15	WE 17x17
Rod OD (inch)	0.43	0.379	0.44	0.382	0.422	0.422	0.374
Cladding Thickness (inch)	0.0265	0.024	0.028	0.025	0.0225	0.0242	0.0225
Pellet OD (inch)	0.3686	0.3239	0.3765	0.325	0.3674	0.3659	0.3225
Active Fuel Length (inch)	144	143	137	150	145.2	144	144
Plenum Length (inch)	7.755	8.318	8.528	9.927	5.790	7.386	6.260
Spring Weight (lb)	0.042	0.026	0.1	0.1	0.07	0.044	0.037
Backfill Pressure (psig)	435	435	500	500	500	500	500
Fuel Mass (MTU)	0.4807	0.4658	0.4037	0.4417	0.4144	0.4646	0.4671
# of Fuel Rods	208	264	176	236	179	204	264
Free Volume (inch ³)	1.427	1.198	1.252	1.052	1.215	1.300	0.882
Pressure (psia) (380°C)	1525	1478	1739	1722	1762	1712	1795
Stress Level (Mpa)	83.1	78.9	91.2	88.5	113.9	101.7	102.1

Table 3.4-12 BWR Cladding Stress Level Comparison Chart

Fuel Type	EX-7x7	EX-8x8	EX-9x9	GE-7x7	GE-8x8a	GE-8x8b	GE-9x9
Rod OD (inch)	0.57	0.484	0.424	0.563	0.493	0.483	0.441
Cladding Thickness (inch)	0.036	0.036	0.03	0.032	0.034	0.032	0.028
Pellet OD (inch)	0.49	0.4045	0.3565	0.487	0.416	0.41	0.376
Active Fuel Length (inch)	144	150	150	144	144	150	150
Plenum Length (inch)	10.200	10.024	9.578	11.190	10.960	9.580	9.580
Spring Weight (lb)	0.13	0.1	0.047	0.083	0.066	0.066	0.047
Backfill Pressure (psig)	44.1	132.0	132.0	44.1	132.0	132.0	132.0
Fuel Mass (MTU)	0.196	0.1793	0.1666	0.1977	0.1855	0.1847	0.1979
# of Fuel Rods	48	62	74	49	63	62	79
Free Volume (inch ³)	2.426	1.708	1.469	3.236	2.181	1.970	1.758
Pressure (psia) (380°C)	1264	1469	1359	971	1236	1345	1286
Stress Level (MPa)	66.7	65.1	65.4	58.2	59.8	68.7	70.5

Table 3.4-13 **Cladding Stress as a Function of Fuel Assembly Average Burnup and Temperature**

Burnup	PWR		BWR	
	300°C	400°C	300°C	450°C
35,000 MWD/MTU	95.4 Mpa	112.3 Mpa	55.9 Mpa	70.8 Mpa
40,000 MWD/MTU	99.9 Mpa	117.4 Mpa	61.8 Mpa	78.2 Mpa
45,000 MWD/MTU	104.2 Mpa	122.6 Mpa	67.6 Mpa	85.5 Mpa
50,000 MWD/MTU	122.3 Mpa	143.9 Mpa	—	—

Table 3.4-14 **Maximum Allowable Initial Storage Temperature (°C) as a Function of Initial Cladding Stress and Initial Cool Time**

MPa	5 years	6 years	7 years	10 years	15 years
5	509.2	487.3	455.9	447	436.5
10	488.8	465.5	426.4	403	385.6
20	465.2	445.5	380.1	372.4	366
30	430.4	397	370.1	363.8	356.5
40	408.1	389	363.2	356.6	350
50	400.6	384	359.7	353.1	346.5
60	395.6	380.4	355.9	349.6	343.1
70	391.9	376.5	352.5	347	340
80	388.2	376	350.8	345.2	337.6
90	385.7	372	348.8	342.8	336.1
100	380.7	369.3	346.2	341	333.2
110	375.2	365.9	344.6	338	332.1
120	370	362.4	339.5	334.3	328.2
130	363.5	355.2	332.2	326.6	320
140	355	346.6	324.2	318.6	312.6
150	346.9	339.1	316.5	311.2	306
160	339.6	331.4	310.3	304.7	299.9

Table 3.4-15 Maximum Allowable Cladding Temperature for PWR and BWR Fuel

Cool Time [years]	PWR Clad Temperature Limit [°C]				BWR Clad Temperature Limit [°C]			
	Burnup (MWD/MTU)				Burnup (MWD/MTU)			
	35,000	40,000	45,000	50,000	35,000	40,000	45,000	50,000
5	376	374	371	359	394	391	389	387
6	367	365	364	352	379	376	376	374
7	346	345	343	333	355	353	352	350
10	340	339	338	328	349	348	346	344
15	333	333	332	322	343	341	339	337

Table 3.4-16 Maximum Allowable Decay Heat for PWR and BWR Systems

Cool Time [years]	PWR Decay Heat Limit [kW]				BWR Decay Heat Limit [kW]			
	Burnup (MWD/MTU)				Burnup (MWD/MTU)			
	35,000	40,000	45,000	50,000	35,000	40,000	45,000	50,000
5	20.00	20.00	19.90	19.30	16.00	16.00	16.00	16.00
6	19.50	19.30	19.20	18.70	16.00	16.00	16.00	16.00
7	17.80	17.80	17.70	17.20	16.00	16.00	16.00	16.00
10	17.40	17.30	17.20	16.80	16.00	16.00	16.00	16.00
15	16.80	16.80	16.70	16.50	16.00	16.00	16.00	16.00

1. Based on maximum clad temperature and biases shown in Table 3.4-17.

Table 3.4-17**Temperature Bias Applied to Maximum Allowable Decay Heats**

Cool Time [years]	PWR Clad Temperature Bias [°C]				BWR Clad Temperature Bias [°C]			
	Burnup (MWD/MTU)				Burnup (MWD/MTU)			
	35,000	40,000	45,000	50,000	35,000	40,000	45,000	50,000
5	-15	-15	-14	-9	-18	-17	-18	-11
6	-15	-15	-16	-10	-18	-17	-19	-11
7	-15	-15	-14	-10	-16	-16	-17	-11
10	-15	-16	-15	-10	-16	-16	-15	-11
15	-16	-16	-16	-9	-16	-16	-16	-11

8. Damaged Fuel Assemblies

Damaged fuel assemblies are standard fuel assemblies with fuel rods that have known or suspected cladding defects greater than hairline cracks or pinhole leaks. Each damaged fuel assembly will be placed in a Maine Yankee fuel can. The primary function of the fuel can is to confine fuel material within the can and to facilitate handling and retrievability. The Maine Yankee fuel can is shown in Drawings 412-501 and 412-502. The placement of the loaded fuel cans is restricted by operating procedures and/or Technical Specifications to loading into the four fuel tube positions at the periphery of the fuel basket as shown in Figure 3.6.1.1-4. The heat load for each damaged fuel assembly is limited to the design basis heat load of 0.833 kW (20 kW/24).

A steady-state thermal analysis is performed using the three-dimensional cask model described in Section 3.4.1.1.1 simulating 100% failure of the damaged fuel rods held in the Maine Yankee fuel can. The canister is assumed to contain twenty (20) design basis PWR fuel assemblies and damaged fuel assemblies in fuel cans in each of the four corner positions.

A debris compaction length of 104 inches is considered in the analysis based on the volume of fuel rods and a 50% compaction of the debris. Additionally, this 104-inch debris region is assumed to be located at the center of the active fuel region of the design basis PWR fuel assemblies, as shown in Figure 3.6.1.1-4. The entire heat load for a single fuel assembly (i.e., 0.833 kW) is considered to be concentrated in the debris region. The effective thermal conductivities for the design basis PWR fuel assembly (Section 3.4.1.1.2) are used for the debris region. This is conservative, since the debris (100% failed rods) is expected to have a higher density (better conduction) and more surface area (better radiation) than an intact fuel assembly. In addition, the thermal conductivity of helium is used for the remainder of the active fuel length. Boundary conditions corresponding to normal transport are used at the outer surface of the cask (see Section 3.4.1.1.1). The results of the steady-state thermal analysis for 100% fuel rod, fuel cladding and guide tube failure are:

Description	Maximum Temperature (°F)			
	Fuel Cladding	Damaged Fuel	Support Disk	Heat Transfer Disk
Configuration with damaged fuel loaded in four basket corner locations	682	633	618	614
Design basis PWR fuel	673	N/A	608	605
Allowable	750	N/A	650	700

As shown in the previous table, the maximum temperatures for the fuel cladding, damaged fuel assembly, support disks, and heat transfer disks for the configuration with damaged fuel loaded in four (4) basket corner locations are within the allowable temperature range. Additionally, the maximum temperature of the support disk remains bounded by that used in the structural analyses of the fuel basket.

Damaged high burnup fuel must be loaded into damaged fuel cans. These fuel assemblies have more than 1% of rods with oxide layers greater than 80 microns or more than 3% of rods with oxide layers greater than 70 microns and burnup greater than 45,000 MWD/MTU. The cask pressure for this condition is used as input to the containment analysis. Consistent with the containment analysis, a basket release fraction of 20% is applied. This release fraction accounts for up to 12 high burnup assemblies, including up to four classified as damaged. Applying this release fraction to the pressure evaluation in Section 3.4.4.1 yields a normal conditions cask pressure of 15.61 psig, calculated using B&W 17x17 Mark C fuel assembly parameters.

Chapter 4

Table of Contents

4.0	CONTAINMENT.....	4-1
4.1	Containment Boundary.....	4.1-1
4.1.1	Containment Vessel.....	4.1-1
4.1.2	Containment Penetrations.....	4.1-2
4.1.3	Seals and Welds.....	4.1-2
4.1.3.1	Seals.....	4.1-2
4.1.3.2	Welds.....	4.1-2
4.1.4	Closure.....	4.1-5
4.2	Containment Requirements for Normal Conditions of Transport.....	4.2-1
4.2.1	Containment of Radioactive Material.....	4.2-1
4.2.1.1	Calculation of Allowable Leak Rates.....	4.2-2
4.2.1.2	Correlation of Allowable Leak Rates to Air Standard.....	4.2-5
4.2.2	Pressurization of Containment Vessel.....	4.2-7
4.2.3	Containment Criteria.....	4.2-8
4.3	Containment Requirements for Hypothetical Accident Conditions.....	4.3-1
4.3.1	Fission Gas Products.....	4.3-1
4.3.2	Containment of Radioactive Materials.....	4.3-2
4.3.2.1	Calculation of Allowable Leak Rates.....	4.3-2
4.3.2.2	Calculation of Allowable Leak Rates to Air Standard.....	4.3-3
4.3.3	Containment Criteria.....	4.3-3
4.4	Special Requirements.....	4.4-1

Table of Contents (Continued)

4.5	Appendices	4.5-1
4.5.1	Containment Evaluation for Site Specific Contents	4.5.1-1
	4.5.1.1 Containment Evaluation for Maine Yankee Contents	4.5.1.1-1
4.5.2	Technical Information on EPDM O-Rings	4.5.2-1
4.5.3	SAS2H Input Output and Group A2 Values for B&W 15×15 and GE 9×9 Assemblies.....	4.5.3-1
4.6	References	4.6-1

List of Figures

Figure 4.1-1	Transport Cask Containment Boundary	4.1-6
Figure 4.5-1	PWR SAS2H Input File for Design Basis Fuel Source Terms	4.5.3-2
Figure 4.5-2	BWR SAS2H Input File for Design Basis Fuel Source Terms	4.5.3-4

List of Tables

Table 4.1-1	Cask Containment Verification Leak Test Requirements and Schedule	4.1-7
Table 4.1-2	Transportable Storage Canister Containment Verification Leak Test Requirements	4.1-7
Table 4.2-1	Release Fractions: Normal and Accident Conditions	4.2-9
Table 4.2-2	Allowable Release Rate Source and A2 Inputs for PWR Cask: Normal Conditions.....	4.2-9
Table 4.2-3	Allowable Release Rate Source and A2 Inputs for BWR Cask: Normal Conditions.....	4.2-10
Table 4.2-4	Leak Rate and Leak Test Sensitivity: Normal Conditions.....	4.2-10
Table 4.2-5	Cask Free Volumes and Pressures: Normal and Accident Conditions	4.2-11
Table 4.2-6	PWR and BWR Containment Parameters - Normal Conditions	4.2-11
Table 4.3-1	Allowable Release Rate Source and A2 Inputs for PWR Cask: Accident Conditions.....	4.3-4
Table 4.3-2	Allowable Release Rate Source and A2 Inputs for BWR Cask: Accident Conditions	4.3-4
Table 4.3-3	Standard Leak Rates: Accident Conditions	4.3-5
Table 4.3-4	PWR and BWR Containment Parameters - Accident Conditions	4.3-5
Table 4.5.3-1	B&W 15×15 SAS2H Output and Group A2 Values (Gas)	4.5.3-6
Table 4.5.3-2	B&W 15×15 SAS2H Output and Group A2 Values (Volatiles)	4.5.3-6
Table 4.5.3-3	B&W 15×15 SAS2H Output and Group A2 Values (Fuel Fines).....	4.5.3-7
Table 4.5.3-4	GE9×9 SAS2H Output and Group A2 Values (Gas)	4.5.3-10
Table 4.5.3-5	GE9×9 SAS2H Output and Group A2 Values (Volatiles)	4.5.3-10
Table 4.5.3-6	GE9×9 SAS2H Output and Group A2 Values (Fuel Fines).....	4.5.3-10

4.1 Containment Boundary

The Universal Transport Cask containment boundary is shown in Figure 4.1-1 and is defined by the following components: (1) inner shell; (2) bottom forging; (3) top forging; (4) cask lid and lid inner EPDM O-ring; (5) vent port coverplate and vent port coverplate inner EPDM O-ring; and (6) drain port coverplate and drain port coverplate inner EPDM O-ring.

There are three possible paths for the escape of radioactive material from the Universal Transport Cask during transport operation. These paths are past the inner EPDM O-ring seals on the lid, on the vent port coverplate and on the drain port coverplate. EPDM O-ring manufacturers data is provided in Section 4.5.2.

The cask containment integrity is verified through leak testing prior to all transport operations. A mass spectrometer leak detector is used to verify that leakage does not exceed the limits established in Section 4.2.3. These limits are in accordance with the requirements of 10 CFR 71.51 and IAEA Safety Series No. 6 (paragraph 548).

The transportable storage canister is designed and analyzed to demonstrate that it maintains its structural integrity in accordance with the 10 CFR 71.63(b) requirement for a separate inner container for damaged fuel or fuel debris, which may contain more than 20 curies of plutonium.

The canister is leak tested at the time of loading to demonstrate that it satisfies the leak tight criteria of ANSI N14.5-1997 and the release limits of 10 CFR 71.63(b).

4.1.1 Containment Vessel

The primary containment vessel for the Universal Transport Cask consists of a 67.61-in. ID, 2-in.-thick inner shell; a 4.25-in.-thick bottom forging; a 8.825-in.-thick top forging; and a closure lid. The containment vessel components are fabricated from Type 304 stainless steel in accordance with the applicable requirements of the ASME Boiler and Pressure Vessel Code, [3].

The transportable storage canister is a right circular cylinder constructed of 5/8-inch thick, Type 304L stainless steel plate. It is closed on the bottom end by a 1.75-inch thick Type 304L stainless steel plate, and at the top by a 7-inch thick Type 304 stainless steel plate (shield lid) and by a 3-inch thick Type 304L stainless steel structural lid.

The canister shell welds are full penetration welds, which are radiographed. The bottom plate is joined to the canister shell by a full penetration groove weld and adjacent fillet weld, which are ultrasonically and liquid penetrant examined. The stainless steel material is selected to be compatible with the DOE MPC program guidelines for future disposal and to minimize the potential for any adverse chemical reactions in the spent fuel pool. The design of the shield lid and structural lid provides a redundant confinement boundary at the top of the canister.

4.1.2 Containment Penetrations

The Universal Transport Cask primary containment boundary is described in Section 4.1. The penetrations in the cask primary containment vessel are the vent and drain ports, and the lid. The penetrations are designed to seal the boundary and to ensure that leakage from the cavity does not exceed the established limits. 10 CFR 71.51 establishes release limits under both normal conditions of transport and hypothetical accident conditions. The quick-disconnects installed in the vent and drain openings and in the lid test port are not considered part of the containment boundary. The vent and drain port coverplates are fabricated from SA-240, Type 304 stainless steel.

The separate inner container (i.e., the transportable storage canister) is a completely welded vessel that has no operable penetrations.

4.1.3 Seals and Welds

4.1.3.1 Seals

The EPDM O-rings of the lid, vent port coverplate, and drain port coverplate are the seals that provide primary containment, as described in Section 4.1. Section 4.5.2 contains the specifications for the EPDM O-rings. The cask is leak tested before acceptance from the manufacturer and after fuel loading. These tests are described in Table 4.1-1. Leak test requirements of the transportable storage canister are included in Table 4.1-2.

4.1.3.1.1 Containment System Fabrication Verification

When fabrication is complete, containment system fabrication verification **leak testing** is performed on the cask containment as described in Section 8.1.3. This leak test verifies that the leak rate of the assembled containment boundary does not exceed the **allowable reference air** leak rate of 1.2×10^{-4} **ref cm³/sec.** **Limiting leak rates are obtained from the evaluation of site-specific contents using a release fraction of 20% under normal conditions of transport. As shown in Table 4.2-4, the allowable leak rate for a PWR cask containing damaged high burnup fuel bounds the allowable leak rate for the cask containing intact PWR fuel and BWR fuel under 45,000 MWD/MTHU burnup.** The maximum allowable leak rates and the corresponding test sensitivities are evaluated in Section 4.2.3 for normal conditions of transport and in Section 4.3.2 for hypothetical accident conditions. Based on the analysis presented in **these sections**, the normal conditions allowable leak rate bounds the **allowable** leak rate for accident conditions. **The transportable storage canister is tested to leak tight conditions per ANSI N14.5-1997.**

4.1.3.1.2 Containment System Periodic Verification

The containment system periodic verification is performed on the Universal Transport Cask package containment boundary seals and components **1**, in accordance with the leak test acceptance criteria established for the containment system fabrication verification **Section 8.1.3**. **This verification leak test conforms to test method A5.4 of Table A1 of ANSI N14.5-1997 [41].**

Whenever a containment seal or component is replaced, the O-ring or containment component is leak tested following replacement according to the requirements of the containment system periodic verification (Section **8.1.3**). This test verifies that the replacement seal or component has been properly installed and that the leak rate meets the allowable leak rate requirements established for the containment system fabrication verification specified in Section 4.2.3.

4.1.3.1.3 Containment System Verification Prior to Transport

As specified in the loading procedure (Section 7.1.3), the containment system is leak tested in accordance with Section 8.1.3 (helium leak tested), if components of the containment boundary are replaced during loading operations. If containment boundary components are not replaced then the containment boundary is pressure tested in accordance with Paragraph 7.6.4 of ANSI

NI4.5-1997 to demonstrate containment boundary assembly in accordance with the operating procedures

For unloaded (empty) transport, pressure testing is used to demonstrate containment boundary assembly.

The assembly pressure test configuration conforms to test method A5.1 of Table A1 of ANSI NI4.5-1997.

4.1.3.2 Welds

Circumferential and longitudinal welds are used to fabricate the **cask** inner shell and to attach it to the top and bottom forgings. The longitudinal welds in the cylindrical sections are staggered circumferentially by 90° or 180°. Containment vessel welds are full penetration bevel or groove welds to ensure structural integrity. Upon completion of the inner shell welds, the welds are radiograph-inspected and accepted in **accordance with** ASME **Code** Section III NB-5320.

Upon completion of containment vessel fabrication, the cask containment boundary is hydrostatically tested in accordance with ASME Code requirements to ensure the integrity of the welds and containment components (Section 8.1.2.3). Following hydrostatic testing, all containment vessel welds are visually inspected by the dye penetrant examination method and evaluated in accordance with ASME Code requirements. **Following fabrication, the containment boundary o-rings are leak tested in accordance with Section 8.1.3. The post-fabrication leak test is based on the bounding PWR fuel allowable leak rate of 4.2×10^{-9} ref cm³/sec as shown in Table 4.2-4. Test equipment and methods are selected to assure a minimum test sensitivity of one-half the reference leak rate, or 2.1×10^{-9} ref cm³/sec. The equivalent allowable helium leak rate is 6.5×10^{-9} cm³/sec at standard conditions. The required helium leak test sensitivity is 3.25×10^{-9} cm³/sec. The helium leak rate at standard conditions is specified since the test is conducted using helium as the detector gas. Specification of standard conditions is conservative since the actual pressure may be higher than the postulated 0 psig (0 atmosphere) pressure that is assumed.**

4.1.4

Closure

The primary closure assembly for the Universal Transport Cask consists of the lid, bolts, and o-rings. The lid is recessed and bolted into the top forging of the cask body. The 6.5-in. thick, 78.17-in. diameter lid is made of ASME SA-336, Type 304 stainless steel. The lid is retained by 48 bolts that are 2-8 UN socket head cap screws fabricated from SB-637, Grade N07718 nickel alloy steel bolting material. The initial torque for installation of the lid bolts is as specified in Table 7-1. The bottom surface of the lid is sealed to the top forging of the cask body by a set of EPDM o-rings with the inner o-ring forming the containment boundary. The second (outer) o-ring provides an annulus to test the inner o-ring seal.

The vent port is recessed into the lid and the drain port is recessed into the bottom forging. The vent and drain port coverplates are secured by four 1/2-13 UNC bolts fabricated from SA-193, Grade B6, Type 410 stainless steel.

Similar to the inner lid configuration, each of the vent and the drain coverplates is sealed by a set of o-rings with the inner o-ring forming the containment boundary. The second (outer) o-ring provides an annulus to test the inner o-ring seal.

Figure 4.1-1

Transport Cask Containment Boundary

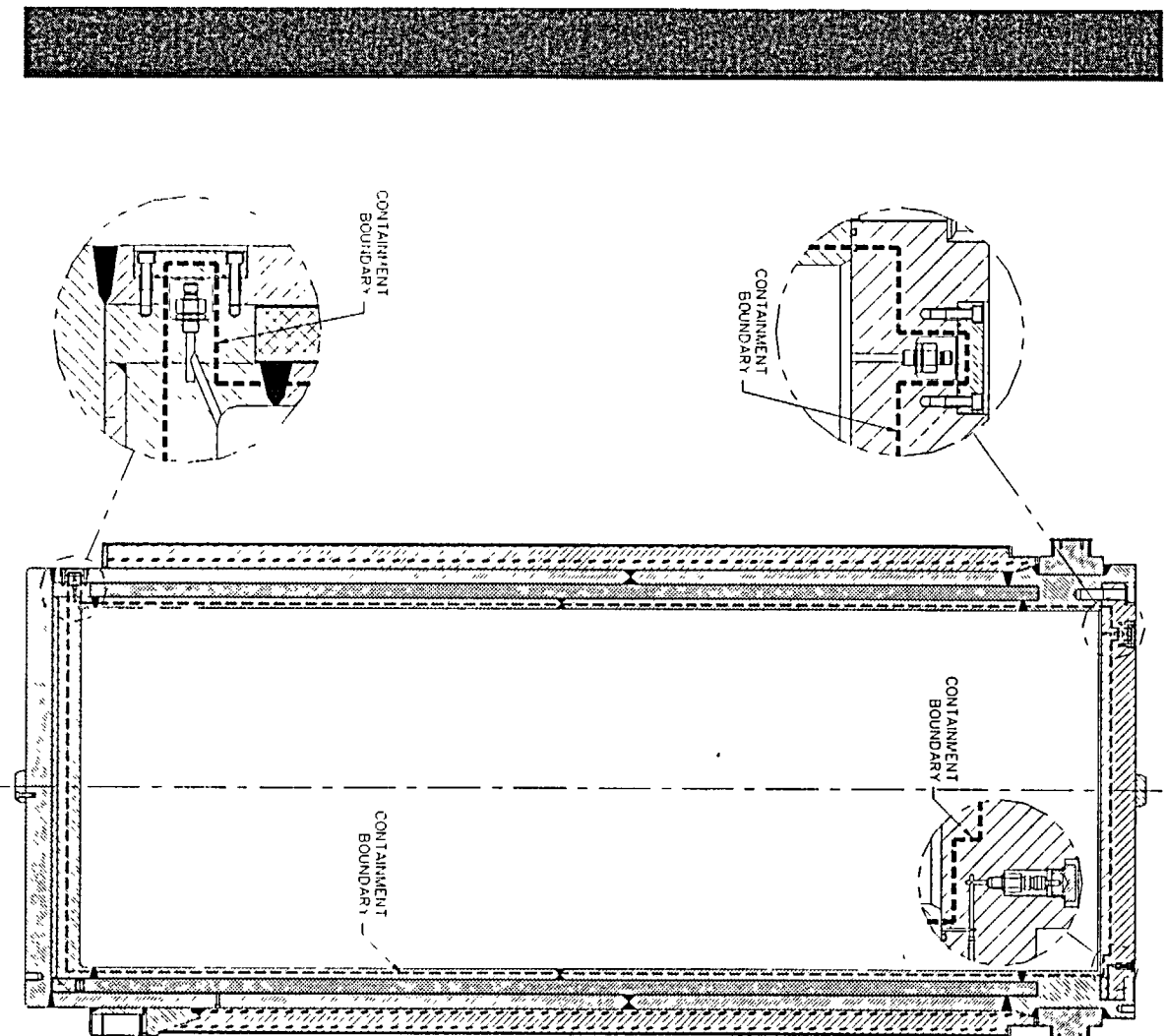


Table 4.1-1 Cask Containment Verification Leak Test Requirements and Schedule

Parameter	Post-Fabrication and Annual Maintenance	Loaded Transport (O-Ring Replacement)	Loaded Transport (No O-Ring Replacement)	Empty Transport
Allowable Reference Leak Rate	4.2×10^{-9} cm ³ /sec	4.2×10^{-9} cm ³ /sec	1×10^{-8} cm ³ /sec	1×10^{-8} cm ³ /sec
Allowable Helium Leak Rate	6.5×10^{-9} cm ³ /sec	6.5×10^{-9} cm ³ /sec	±	±

- 1 All o-rings are replaced during Annual Maintenance.
- 2 The need for o-ring replacement is determined by inspection or by leak test results. Only the appropriate set of o-ring is replaced as necessary prior to transport.
- 3 The allowable leak rate is based on the bounding evaluation containing damaged high burnup PWR fuel assemblies and is the same for the transport of GTCC waste.

Table 4.1-2 Transportable Storage Canister Containment Verification Leak Test Requirements

Parameter	Loading
Allowable Leak Rate	1.0×10^{-7} ref cm ³ /sec
Allowable Helium Leak Rate	2.0×10^{-7} cm ³ /sec (He)
Helium Leak Test Sensitivity	1.0×10^{-7} cm ³ /sec (He)

THIS PAGE INTENTIONALLY LEFT BLANK

4.2 Containment Requirements for Normal Conditions of Transport

The Universal Transport Cask must maintain a radioactivity release rate of not more than 10^{-6} A2/hr under normal conditions of transport, as required by 10 CFR 71.51 and IAEA Safety Series No. 6 (paragraph 548). For the cask containing intact PWR fuel, this condition is satisfied by maintaining a maximum reference (air at standard conditions) leak rate of 5.0×10^{-4} ref cm³/sec, or 6.6×10^{-5} cm³/sec helium at the test condition, which is conservatively considered to be the standard conditions. For the cask containing BWR fuel, the radioactivity release rate requirement is satisfied by maintaining a maximum reference leak rate from the cask of 3.3×10^{-4} ref cm³/sec, or 4.5×10^{-5} cm³/sec helium at the test conditions. For the PWR cask containing PWR damaged high burnup fuel assemblies, the maximum reference leak rate is 4.2×10^{-4} ref cm³/sec or 6.5×10^{-5} cm³/sec helium. Consequently, the PWR high burnup fuel allowable leak rate is conservatively applied as the containment boundary test condition for post-fabrication testing, annual testing, and when containment components are replaced during cask use. Calculations of these limits are provided in this section.

The structural and thermal evaluations of the Universal Transport Cask are provided in Chapters 2.0 and 3.0, respectively. Results of these evaluations also demonstrate that cask containment is maintained during normal conditions of transport. Therefore, the package satisfies the containment requirements of 10 CFR 71.71.

Since the transportable storage canister is tested to demonstrate a leaktight condition, an allowable release rate, based on the gases, fumes, volatiles and particulates that are available for release from the contained spent fuel or GICC waste, is not calculated.

4.2.1 Containment of Radioactive Material

The 10 CFR 71 limit for the release of radioactive material under normal conditions of transport is 10^{-6} A2/hr. In this analysis, A2 for a mixed gas is determined by using the method described in 10 CFR 71, Appendix A. The release fractions for the various radionuclides transported in the Universal Transport Cask are obtained from NUREG/CR-6487 [4] and summarized in Table 4.2-1 (located at the end of this section). The curie content per isotope for 1-year cooled PWR and BWR design basis fuel assemblies is provided in Section 4.5-3.

In addition to the radionuclides produced by the fuel material, fuel assemblies develop a coating of impurities deposited by cooling water during power generation. This coating is known as crud. Crud contains mostly nonradioactive elements but also contains a significant amount of ^{60}Co . NUREG/CR-6487 lists the maximum ^{60}Co concentrations on spent fuel assemblies to be $140 \mu\text{Ci}/\text{cm}^2$ for PWR assemblies and $1,254 \mu\text{Ci}/\text{cm}^2$ for BWR assemblies at initial discharge. The surface areas of the design basis PWR and BWR assemblies (B&W 15×15 and GE 9×9), are calculated to be $3.25 \times 10^5 \text{ cm}^2$ and $1.77 \times 10^5 \text{ cm}^2$, respectively. The total PWR crud activity calculated by the conservative surface area and maximum activity density envelopes assemblies with control components inserted. Fuel assembly characteristics are listed in Tables 1.2-4 and 1.2-5 for PWR and BWR fuel assemblies respectively.

The canister provides the separate inner container (double containment) for the transport of damaged fuel cans containing damaged fuel or fuel debris as required by 10 CFR 71.63

4.2.1.1 Calculation of Allowable Leak Rates

The maximum permissible leak rate from the cask under normal conditions of transport is determined from the 10 CFR 71 limit of $10^{-6} \text{ A}_2/\text{hr}$.

$$R_N = L_N C_N \leq A_2 \times 1 \times 10^{-6} \text{ hr}^{-1} \text{ or}$$
$$R_N = L_N C_N \leq A_2 \times 2.78 \times 10^{-10} \text{ sec}^{-1}$$

where:

- L_N = is the volumetric gas leakage rate [cm^3/s]
 C_N = is the curies per unit volume (termed "activity density") of the radioactive material that passes through the leak path [Ci/cm^3]
 R_N = Release rate for normal transport conditions [Ci/sec]

Activity Density of Radioactive Material (C_N)

The total inventory of fission product gases, volatiles fines and crud are shown in Table 4.5.3-1 through Table 4.5.3-6. These inventories are calculated by using the source terms produced by the SAS2H 6 sequence, the release fractions and the postulated crud (^{60}Co). The ^{60}Co content is decayed 5 years from discharge to the design basis fuel cool time. The PWR analysis is based on 24 design basis fuel assemblies. The BWR analysis is based on 56 design basis fuel assemblies.

$$C_n = C_{\text{Crud}} + C_{\text{Volatiles}} + C_{\text{FissionGas}} + C_{\text{Fines}}$$

$$C_{\text{Crud}} = \frac{f_c M_T}{V} = \frac{f_c S_C N_A (N_R S_{AR} + S_{Ch})}{V}$$

where:

C_{crud} = activity density inside containment vessel resulting from crud spallation [Ci/cm³]

M_T = total crud activity inventory [Ci]

f_c = crud spallation factor

V = free volume inside containment vessel [cm³]

S_C = crud surface activity [Ci/cm²]

N_R = number of fuel rods per assembly

N_A = number of assemblies

S_{AR} = surface area per rod [cm²]

S_{Ch} = channel surface area [cm²] (BWR fuel only).

and,

$$C_{\text{fines}} = \frac{f_F W_R A_R N_R N_A f_B}{V}$$

where:

C_{fine} = activity concentration inside containment vessel resulting from fines released from cladding breaches [Ci/cm³]

f_F = fraction of fuel rod's mass released as fines resulting from cladding breach

f_B = fraction of fuel rods that develop cladding breach

W_R = mass of the fuel in fuel rod [g]

N_R = number of fuel rods per assembly

N_A = number of assemblies

A_R = specific activity of fines emitted from cladding breach in fuel rod [Ci/g]

V = containment vessel void volume [cm³].

and,

$$C_{\text{vg}} = C_{\text{vol}} + C_{\text{gas}} = \frac{N_R N_A f_B W_R (A_V f_V + A_G f_G)}{V}$$

where:

C_{vg}	=	releasable activity concentration inside the containment vessel resulting from gases and volatiles released from cladding breaches [Ci/cm ³]
C_{vol}	=	releasable activity concentration inside the containment vessel resulting from volatiles released from cladding breaches [Ci/cm ³]
C_{gas}	=	releasable activity concentration inside the containment vessel resulting from gases released from cladding breaches [Ci/cm ³]
W_R	=	mass of the fuel in a fuel rod [g]
N_R	=	number fuel rods per assembly
N_A	=	number of assemblies
f_B	=	fraction of rods that develop cladding breaches
A_V	=	specific activity of volatiles in fuel rod [Ci/g]
f_V	=	fraction of volatiles in fuel rod released if rod develops cladding breach
A_G	=	specific activity of gas in fuel rod [Ci/g]
f_G	=	fraction of gas that would escape from fuel rod that develops cladding breach
V	=	is the void volume inside containment vessel [cm ³].

Activity Values for Radionuclides

A₂ values used in this analysis (based on 10 CFR 71 Appendix A) are listed in Section 4.5.3 for all radionuclides produced by the SAS2H analysis (plus ⁶⁰Co). ~~The mixture A₂ values are shown~~ in Tables 4.2-2 and 4.2-3 ~~■~~. For those isotopes for which no specific A₂ values are given ~~in 10~~ ~~CER 71 Appendix A~~, the generic values listed in Table A.2 ~~of Appendix A~~, are applied. A₂ values for mixed isotopes are calculated from the following:

$$A_2 = \frac{1}{\sum \frac{F_i}{A_2}}$$

where:

$$F_i = \frac{S_i}{S_n}$$

and:

F_i = The fraction of isotope i with respect to the entire mixture

S_i = The activity of isotope i [Ci]

S_n = Total group activity [Ci]

Mixture A2 values are determined for gas, volatile, fine, and crud mixtures and are then combined for a total cask mixture A2 value. Tables 4.2-2 and 4.2-3 provide the source term and A2 values per group for PWR and BWR cask systems release rate calculations.

Maximum Allowable Leak Rates

On the basis of the methodology discussed above, the maximum allowable leak rates for the casks containing standard or high burnup PWR and BWR standard fuel under normal conditions of transport are calculated to be 5.5×10^{-1} and 1.5×10^{-1} cm^3/sec , respectively (Table 4.2-4).

The maximum allowable release rates are more restrictive for the cask containing high burnup damaged PWR assemblies because of the higher failure rate associated with the ISG-15 specified failure rate of 50% in normal conditions in fuel with an oxide layer thickness greater than 70 microns. Per ISG-15, no more than 3% of the rods in a high burnup assembly may contain oxide layers over 70 microns. Above this level, assemblies must be placed in damaged fuel cans. The worst case containment analysis UMS® loading is, therefore, 12 intact standard assemblies failing at 3%, 3 high burnup assemblies classified as intact with 50% failure of the 3% high burnup rods, and 50% failure of rods inside the damaged fuel cans. This configuration is bounded by the 20% average release fraction applied to a full canister load of high burnup assemblies.

4.2.1.2 Correlation of Allowable Leak Rates to Air Standard

The volumetric gas leak rate, L , is independent of transport cask pressure and temperature. The maximum allowable release must be correlated with air standard leak rates, which depend on gas temperatures, pressures, and leakage path length and diameter. This correlation requires calculation of the capillary opening diameter through which the flow occurs. Depending on pressure and condition of the flow, a combination of continuum and molecular flow occurs.

Continuum flow ~~and~~ molecular flow equations are obtained from NUREG/CR-6487, Section 2. Both continuum and molecular flow rate equations presented below are adjusted to upstream flow rate ~~in accordance with NUREG/CR-6487 and ANSI N14.5-1997.~~

The continuum volumetric flow rate of the gas (cm³/sec), L_c, is given by:

$$L_c = \frac{2.48 \times 10^6 D^4}{a \mu} (P_u - P_d) * \frac{P_a}{P_u} = F_c * (P_u - P_d) * \frac{P_a}{P_u}$$

where:

- F_c = coefficient for continuum flow [cm³/atm-s]
- D = capillary diameter [cm]
- a = capillary length [cm]
- μ = fluid viscosity [cP]
- P_u = upstream pressure [atm] - pressure inside containment
- P_d = downstream pressure [atm] - pressure outside containment

~~and, the molecular volumetric flow rate of the gas (cm³/sec), L_m, is given by~~

$$L_m = \frac{3.81 \times 10^3 D^3 \sqrt{\frac{T}{M}}}{a P_a} (P_u - P_d) * \frac{P_a}{P_u} = F_m * (P_u - P_d) * \frac{P_a}{P_u}$$

where:

- L_m = is the volumetric flow rate of gas at P_a [cm³/sec]
- F_m = is the coefficient for molecular flow [cm³/atm-s]
- D = is the capillary diameter [cm]
- T = is the gas temperature [K]
- M = is the gas molecular weight [g/mole]
- P_a = is the average pressure (P_u+P_d)/2 [atm]
- P_u = is the upstream pressure [atm]
- P_d = is the downstream pressure [atm].
- a = capillary diameter [cm]

For this analysis, the gas temperature used for molecular flow analysis is identical to the upstream temperature. Pressures and temperatures for PWR and BWR system normal operating conditions are summarized in Table 4.2-5. Based on the pressure, temperature and allowable leakage rate (L_N) the capillary diameter of the leak is determined. The calculated capillary diameter is then used to determine the air standard leak rate and helium test leak rate. Air standard condition leak rates are determined for air leaking from 1 atmosphere to 0.01 atmosphere at a temperature of 298K. The test gas is helium leaking from 1 atmosphere (0 psig) to a vacuum. Table 4.2-4 provides the standard and test leak rates for the Universal Transport Cask loaded with PWR or BWR fuel. The sensitivity for these tests is one-half the air standard leak rate as recommended by ANSI N14.5-1997. Key PWR and BWR containment analysis parameters are summarized in Table 4.2-6.

This analysis is conservative since a higher upstream pressure, which could result from a higher average gas temperature based on decay heat, results in a higher allowable leak rate assuming that the leak path length and the leak path diameter (calculated based on the reference air condition) are held constant. Since the test condition pressure cannot be less than 1 atmosphere and since the average gas temperature does not have a first order effect on calculated leak rate, the helium test condition is conservative with respect to the allowable reference leak rate.

4.2.2 Pressurization of Containment Vessel

The maximum pressure in the canister and cask during normal conditions of transport is calculated by using the methodology presented in Section 3.4.4. Assumptions underlying this calculation are that during normal conditions of transport, 3% of the fuel rods may fail and that 30% of the fission gases in the rods are releasable. The cask cavity under normal conditions of transport is backfilled to 1 atm with at least 99.9% pure helium gas.

The canister does not fail in any of the evaluated normal transport or accident conditions; therefore, there is no pressure increase in the cask cavity except that due to the increase in cavity temperature. Section 3.4.4 determines bounding cask pressures assuming a hypothetical canister failure.

4.2.3 Containment Criteria

The ~~bask reference~~ leak rates provided in Table 4.2-4 for PWR and BWR fuel, represent the maximum leak rate allowed if the o-rings were tested with air at 1 atm and 25°C. ~~The~~ maximum allowable leak rate for the containment system fabrication verification and periodic verification leak tests is described in ~~Sections~~ 4.1.3 and 8.1.3. ~~This allowable leak rate is that for the BWR fuel configuration, which is more restrictive than the allowable leak rate for PWR fuel~~

The sensitivity for these tests is ~~recommended~~ by ANSI N14.5-1997 to be one-half the allowable leak rate.

~~The transportable storage canister welded closure is leak tested at final assembly to leaktight conditions, 1×10^{-7} ref cm³/sec, as defined by ANSI N14.5-1997. To meet this requirement, the allowable leak rate is 2×10^{-7} cm³/sec (helium). The leak test sensitivity applied in testing the canister at the time it is closed is 1×10^{-7} cm³/sec (helium), or less, to account for a test pressure difference. Consequently, the canister provides adequate containment for the spent fuel or GICC waste~~

~~The canister does not fail in any of the evaluated normal conditions of transport. Consequently, the canister provides a leaktight containment for damaged fuel or fuel debris. This configuration meets the requirements of 10 CFR 71.63(b) for a separate inner container (double containment) for radioactive material containing more than 20 curies of plutonium~~

Table 4.2-1 Release Fractions: Normal and Accident Conditions

Radionuclide Origin	Fraction: Normal Conditions	Fraction: Accident Conditions
Volatiles releasable	2.00E-04	2.00E-04
Fission gas releasable	0.3	0.3
Rod mass released	3.00E-05	3.00E-05
Crud spallation factor	0.15	1.0
Fraction of fuel that fails	0.03	1.0

1 PWR fuel is also evaluated at 0.20 to account for high burnup fuel failure during transport.
This failure fraction envelopes damaged fuel can payloads.

Table 4.2-2 Allowable Release Rate Source and A2 Inputs for PWR Cask: Normal Conditions

B&W 15x15	Crud	Gas	Volatiles	Fines	Total
Total Activity per Assembly (Ci)	N/C	3.73E+03	1.49E+05	2.28E+05	3.81E+05
Releasable Activity per Cask (Ci)	3.48E+01	3.06E+02	2.14E+01	4.92E+00	9.17E+02
Cask Volumetric Activity (Ci/cm ³)	1.26E-05	1.20E-04	3.19E-06	7.33E-07	1.36E-04
A2 Value (Ci)	10.80	285.50	3.39	0.114	302.81
Fraction of Activity	0.092	0.879	0.023	0.005	1.000
Fraction of Activity / A2 (1/Ci)	0.0086	0.0031	0.0037	0.0471	0.0624
Mixture A2 Value (Ci)					16.02

1 Based on 3% rod failure

2 Not explicitly calculated.

Table 4.2-3 Allowable Release Rate Source and A2 Inputs for BWR Cask:
Normal Conditions

GE939	Crud	Gas	Volatiles	Fines	Total
Total Activity per Assembly (Ci)	N/C	1.46E+03	5.76E+04	8.82E+04	1.47E+05
Releasable Activity per Cask (Ci)	9.68E+02	7.34E+02	1.94E+01	4.44E+00	1.73E+02
Cask Volumetric Activity (Ci/cm ³)	1.51E-04	1.14E-04	3.02E-06	6.93E-07	2.69E-04
A2 Value (Ci)	10.80	285.60	6.34	0.12	302.84
Fraction of Activity	0.56	0.44	0.01	0.002	1.00
Fraction of Activity / A2 (1/Ci)	0.052	0.001	0.002	0.022	0.078
		Mixture A2 Value (Ci)			12.90

1 Not explicitly calculated

Table 4.2-4 Leak Rate and Leak Test Sensitivity: Normal Conditions

Reactor Type	Assembly Type	Operating Condition	Vol. Activity Ci/cm ³	Leak Rate (cm ³ /sec)		
				Volumetric [L]	Air Reference [L]	Test Sensitivity
PWR	B&W 15x15	Normal	1.4E+04	3.3E-05	5.0E-05	2.5E-06
PWR	B&W 15x15	Normal	3.4E+04	5.5E-06	4.2E-06	2.1E-06
BWR	GE939-2	Normal	2.7E+04	1.3E-05	3.3E-05	1.7E-05

1 The corresponding helium test leak rates and leak test sensitivities for the PWR configuration are 6.6×10^{-5} cm³/sec and 3.3×10^{-5} cm³/sec, respectively, at standard conditions

2 Based on 20% fuel failure to account for high burnup fuel assemblies and damaged fuel cans. The corresponding helium test leak rates and leak test sensitivities for the PWR configuration are 6.5×10^{-5} cm³/sec and 3.25×10^{-5} cm³/sec, respectively, at standard conditions

3 The corresponding helium test leak rates and leak test sensitivities for the BWR configuration are 4.5×10^{-5} cm³/sec and 2.25×10^{-5} cm³/sec, respectively, at standard conditions

Table 4.2-5 Cask Free Volumes and Pressures: Normal and Accident Conditions

Reactor Type	PWR		BWR	
Cask Operating Condition	Normal	Accident	Normal	Accident
Free Gas Volume (liters)	5720	5720	5410	5410
Pressure (atm)	1.47	5.72	1.25	3.91
Average Gas Temperature (K)	507.0	582.0	458.7	542.0

1 The accident condition for this analysis is 100% rod failure in combination with a fire accident raising cask temperature. This hypothetical dual failure accident conservatively maximizes both available releasable material and cask pressure.

2 Bounding values were chosen for free volume (minimum) and pressure (maximum). This conservatively minimizes free volume and capillary diameter.

3 The normal condition pressure assuming 20% fuel rod failure is 2.06 atm.

Table 4.2-6 PWR and BWR Containment Parameters - Normal Conditions

Assembly Type	Grid Surface Activity (Ci/cm ²)	Containment Free Volume (cm ³)	Capillary Length (cm)	Capillary Diameter (cm)	Upstream Pressure (atm)	Gas Temperature (K)
B&W 15x15	73E-5	57E+6	0.287	54E-4	1.47	507
B&W 15x15	73E-5	57E+6	0.287	33E-4	2.06	507
GE 9x9-2	55E-4	54E+6	0.287	57E-4	1.25	459

1 Based on 3% of the fuel rods failing in normal transport conditions.

2 Based on 20% of the fuel rods failing in normal transport conditions.

THIS PAGE INTENTIONALLY LEFT BLANK

4.3 Containment Requirements for Hypothetical Accident Conditions

The 10 CFR 71 requirement for the release of radioactive material under hypothetical accident conditions is met by ensuring that for the cask containing PWR fuel a reference air leak rate limit of 2.0×10^{-4} ref cm³/sec is not exceeded. The corresponding air standard leak rate limit for the cask containing BWR fuel is 2.2×10^{-4} ref cm³/sec. Calculations of these limits are provided in Section 4.3.2.

Assuming a simultaneous occurrence of a fire accident and a 100% rod failure, and on the basis of bulk average gas temperatures of 582K (PWR) and 542K (BWR) resulting from air in the cavity, the pressure within the cask cavity is calculated to be 5.7 atm (PWR) or 3.9 atm (BWR). The hypothetical presence of air in the cask provides an upper bound on the gas temperature. These pressures represent the maximum possible cask internal pressures.

The structural integrity of the cask containment during hypothetical accident conditions is demonstrated in Chapter 2.0. Therefore, the cask containment is maintained under hypothetical accident conditions.

As described in Section 2.7, the transportable storage canister does not fail in any of the evaluated transport accident conditions defined in 10 CFR 71.73. Consequently, its leak tight condition is maintained in the hypothetical accident conditions.

4.3.1 Fission Gas Products

The calculated amounts of fission gases contained in the design basis PWR and BWR fuel assembly are reported in Tables 4.53.1 and 4.53.4. The accident conditions for maximum fission gas release assume 100% rod failure and also assume that 30% of the radioactive fission gases, primarily ⁸⁵Kr, tritium and ¹²⁹I are available for release to the cask cavity. In addition, 100% of the ⁶⁰Co in the crud on the fuel assemblies is conservatively assumed to be available for release as an aerosol. Also released, but not contributing to the cask or canister pressure, are a fraction of the fuel volatile and fine inventory.

4.3.2 Containment of Radioactive Materials

The Universal Transport Cask ~~and transportable storage canister are~~ designed to maintain a release rate of less than 1 A₂/week for the hypothetical accident conditions, as required by 10 CFR 71.51.

~~For the cask, the~~ A₂ ~~value~~ for a mixed gas is determined by using the method described in 10 CFR 71, Appendix A. The release fractions for the various radionuclides found in the cask are obtained from NUREG/CR-6487 and summarized in Table 4.2-1. The curie content per isotope for 5-year cooled PWR and BWR design basis fuel assemblies is provided in Section 4.5.3.

~~As shown in Section 2.7 for the leaktight transportable storage canister, the containment boundary of the canister does not fail during the hypothetical accident events. Consequently, containment is maintained by both the cask and the canister in the hypothetical accident events~~

4.3.2.1 Calculation of Allowable Leak Rates

The allowable leak rates under hypothetical accident conditions are calculated by using the method described in Section 4.2.1.1 for normal conditions of transport. The total inventory of fission product gases, volatiles, fines, and crud are calculated by using the source terms generated by SAS2H and release fractions for the PWR and the BWR fuel. Using the A₂ values from 10 CFR 71, Appendix A (Tables 4.3-1 and 4.3-2 1 ~~■~~), the mixture A₂ values are then determined for gas, volatile, fine, and crud mixtures. Finally, the maximum allowable release rates are calculated by using the hypothetical accident conditions allowable release limit:

$$R_A = L_A C_A \leq A_2 \cdot \text{week}^{-1}$$

or

$$R_A = L_A C_A \leq A_2 \cdot 1.65 \times 10^{-6} \text{sec}^{-1}$$

where:

- L_A = volumetric gas leakage rate [cm³/s]
- C_A = curies per unit volume (termed "activity density") of the radioactive material that passes through the leak path [Ci/cm³]
- R_A = release rate for accident transport conditions

Assumptions underlying the calculations for the hypothetical accident conditions are that 100% of the fuel rods fails and 100% of the crud is released (compared with the assumptions that 3% of the fuel rods fail and 15% of the crud is released in the analysis in Section 4.2.1.1 for normal conditions of transport). The mixture A2 for gas, volatile, fine, and crud mixtures is not changed by the change in the magnitude of releasable material, but the combined A2 changes based on the change in activity fraction in each group.

The calculated maximum permissible release rates for the casks containing design basis PWR and BWR fuel under hypothetical accident conditions are tabulated in Table 4.3-3.

4.3.2.2 Correlation of Allowable Leak Rates to Air Standard

The maximum allowable leak rates for the hypothetical accident conditions are correlated with standard leak rates by using the methodology described in Section 4.2.1.2. The results for casks containing PWR or BWR fuel as shown in Table 4.3-3.

4.3.3 Containment Criteria

The allowable leak rates calculated for the hypothetical accident conditions are much greater than those for the normal conditions of transport calculated in Section 4.2.1. Because the cask containment is demonstrated to be maintained under hypothetical accident conditions (Section 2.7), the maximum permissible leak rates for normal conditions of transport are more limiting and are therefore used for the establishment of the maximum allowable leak rates for the containment system fabrication and periodic verification leak test calculations and test acceptance criteria.

Table 4.3-1 Allowable Release Rate Source and A2 Inputs for PWR Cask: Accident Conditions

B&W 15x15	Crud	Gas	Volatiles	Fines	Total
Total Activity per Assembly (Ci)	N/C	3.73E+03	1.49E+05	2.28E+05	5.81E+05
Releasable Activity per Cask (Ci)	5.65E+02	2.69E+04	7.15E+02	1.64E+02	2.83E+04
Cask Volumetric Activity (Ci/cm ³)	3.41E-05	4.00E-07	1.06E-04	2.44E-05	4.21E-05
A2 Value (Ci)	10.80	285.50	5.39	0.114	302.3
Fraction of Activity	0.020	0.949	0.025	0.006	1.00
Fraction of Activity / A2 (1/Ci)	0.002	0.003	0.004	0.051	0.06
Mixture A2 Value (Ci)					16.68
1. Not explicitly calculated					

Table 4.3-2 Allowable Release Rate Source and A2 Inputs for BWR Cask: Accident Conditions

GE 9x9	Crud	Gas	Volatiles	Fines	Total
Total Activity per Assembly (Ci)	N/C	1.46E+03	5.76E+04	3.82E+04	1.47E+05
Releasable Activity per Cask (Ci)	6.45E+02	2.45E+04	6.45E+02	1.48E+02	3.17E+04
Cask Volumetric Activity (Ci/cm ³)	1.01E-03	3.82E-05	1.01E-04	2.31E-05	4.95E-03
A2 Value (Ci)	10.80	285.60	5.34	0.115	302.35
Fraction of Activity	0.203	0.772	0.0204	0.006	1.00
Fraction of Activity / A2 (1/Ci)	0.019	0.003	0.003	0.041	0.065
Mixture A2 Value (Ci)					15.31
1. Not explicitly calculated					

4.4 Special Requirements

The containment provided by the Universal Transport cask and leaktight canister constitute the double containment (separate inner container) required by 10 CFR 71.63(b) for the damaged fuel cans, which could contain more than 20 curies of plutonium. Double containment is maintained during both normal transport conditions and the hypothetical accident conditions.

THIS PAGE INTENTIONALLY LEFT BLANK

Chapter 5

List of Figures

Figure 5.1-1	Location of Maximum Dose Rates for Normal Conditions of Transport ...	5.1-7
Figure 5.1-2	Location of Maximum Dose Rates for Hypothetical Accident Conditions	5.1-8
Figure 5.2-1	Enveloping Axial Burnup Profile for PWR Design Basis Fuel	5.2-8
Figure 5.2-2	Enveloping Axial Burnup Profile for BWR Design Basis Fuel	5.2-8
Figure 5.2-3	PWR Photon and Neutron Axial Source Profiles	5.2-9
Figure 5.2-4	BWR Photon and Neutron Axial Source Profiles	5.2-9
Figure 5.3-1	Illustration of SAS4 Axial Surface Detector Partitioning	5.3-10
Figure 5.3-2	Illustration of SAS4 Radial Surface Detector Partitioning	5.3-10
Figure 5.3-3	One-Dimensional Radial Shielding Regions	5.3-11
Figure 5.3-4	Equivalent Homogenized Cylindrical Source: PWR Dimensions in cm	5.3-12
Figure 5.3-5	Equivalent Homogenized Cylindrical Source: BWR (Dimensions in cm)	5.3-13
Figure 5.3-6	Design Basis PWR (WE 17×17) Fuel Assembly Source Region Elevations	5.3-14
Figure 5.3-7	Design Basis BWR (GE 9×9-2) Fuel Assembly Source Region Elevations	5.3-15
Figure 5.3-8	One-Dimensional Top Axial Model: BW 15×15 Fuel Assembly Dimensions in cm	5.3-16
Figure 5.3-9	One-Dimensional Bottom Axial Model: BW 15×15 Fuel Assembly Dimensions in cm	5.3-16
Figure 5.3-10	Transport Cask Bottom Model – PWR Design Basis (Dimensions in cm)	5.3-17
Figure 5.3-11	Transport Cask Bottom Model – BWR Design Basis (Dimensions in cm)	5.3-18
Figure 5.3-12	Transport Cask Top Model – PWR Design Basis (Dimensions in cm)	5.3-19
Figure 5.3-13	Transport Cask Top Model – BWR Design Basis (Dimensions in cm) ...	5.3-20
Figure 5.3-14	PICTURE Representation of PWR Top Model – Normal Conditions – Showing Trunnion Recesses and Lid Vent	5.3-21
Figure 5.3-15	PICTURE Representation of PWR Bottom Model – Normal Conditions – Slice Through Lower Rotation Pockets	5.3-22
Figure 5.3-16	Radial Lead Slump Model (Dimensions in Inches)	5.3-23
Figure 5.3-17	PICTURE Representation of PWR Top Model – Accident Conditions ...	5.3-24

List of Figures (Continued)

FIGURE 5.3-18	Representation of BWR Fuel Region and Heat Transfer Fin Models at Fuel Axial Midplane	5.3-25
Figure 5.4-1	PWR Total Dose Rate - Side - Normal Conditions	5.4-11
Figure 5.4-2	PWR Total Dose Rate - Top - Normal Conditions	5.4-11
Figure 5.4-3	PWR Total Dose Rate - Bottom - Normal Conditions	5.4-12
Figure 5.4-4	BWR Total Dose Rate - Side - Normal Conditions	5.4-12
Figure 5.4-5	BWR Total Dose Rate - Azimuthal Profile at Rotation Pocket Elevation - Normal Conditions	5.4-13
Figure 5.4-6	BWR Total Dose Rate - Top - Normal Conditions	5.4-13
Figure 5.4-7	BWR Total Dose Rate - Bottom - Normal Conditions	5.4-14
Figure 5.4-8	Effect of Heat Transfer Fins on Cask Surface Fuel Neutron and Gamma Dose Rates [mrem/hr]	5.4-14
Figure 5.4-9	PWR Canister with No Spacer Assembly - Side Total Dose Rate Profile (Lower Half)	5.4-15
Figure 5.5.1.1-1	SAS2H Model Input File - CE14x14	5.5.1-17

List of Tables (Continued)

Table 5.3-18	Isotopic Composition of Additional Shielding Materials [atom/b-cm]	5.3-34
Table 5.3-19	Isotopic Composition of Additional Shielding Materials [atom/b-cm]	5.3-35
Table 5.4-1	SAS4 Runs Performed for Each Source Region	5.4-16
Table 5.4-2	PWR Surface Average Dose Rates – Top Model – Radial Detectors – Normal Conditions	5.4-16
Table 5.4-3	PWR Surface Average Dose Rates – Top Model – Axial Detectors – Normal Conditions	5.4-17
Table 5.4-4	PWR Maximum Subdetector Dose Rates – Top Model – Radial Detectors – Normal Conditions	5.4-17
Table 5.4-5	PWR Maximum Subdetector Dose Rates – Bottom Model – Radial Detectors – Normal Conditions	5.4-17
Table 5.4-6	PWR Maximum Subdetector Dose Rates – Top Model – Axial Detectors – Normal Conditions	5.4-18
Table 5.4-7	PWR Maximum Subdetector Dose Rates – Bottom Model – Axial Detectors – Normal Conditions	5.4-18
Table 5.4-8	BWR Maximum Subdetector Dose Rates – Top Model – Radial Detectors – Normal Conditions	5.4-19
Table 5.4-9	BWR Maximum Subdetector Dose Rates – Top Model – Axial Detectors – Normal Conditions	5.4-19
Table 5.4-10	BWR Maximum Subdetector Dose Rates – Bottom Model – Radial Detectors – Normal Conditions	5.4-20
Table 5.4-11	BWR Maximum Subdetector Dose Rates – Bottom Model – Axial Detectors – Normal Conditions	5.4-20
Table 5.4-12	PWR Surface Average Dose Rates – Top Model – Radial Detectors – Accident Conditions	5.4-21
Table 5.4-13	PWR Maximum Subdetector Dose Rates – Top Model – Radial Detectors – Accident Conditions	5.4-21
Table 5.4-14	PWR Maximum Subdetector Dose Rates – Bottom Model – Radial Detectors – Accident Conditions	5.4-21
Table 5.4-15	PWR Maximum Subdetector Dose Rates – Top Model – Axial Detectors – Accident Conditions	5.4-22

List of Tables (Continued)

Table 5.4-16	PWR Maximum Subdetector Dose Rates – Bottom Model – Axial Detectors – Accident Conditions	5.4-22
Table 5.4-17	BWR Maximum Subdetector Dose Rates – Top Model – Radial Detectors – Accident Conditions	5.4-22
Table 5.4-18	BWR Maximum Subdetector Dose Rates – Bottom Model – Radial Detectors – Accident Conditions	5.4-23
Table 5.4-19	BWR Maximum Subdetector Dose Rates – Top Model – Axial Detectors – Accident Conditions	5.4-23
Table 5.4-20	BWR Maximum Subdetector Dose Rates – Bottom Model – Axial Detectors – Accident Conditions	5.4-23
Table 5.4-21	Loading Table for PWR Fuel	5.4-24
Table 5.4-22	Loading Table for BWR Fuel	5.4-25
Table 5.4-23	Results of Verification Study for Normal Conditions	5.4-26
Table 5.4-24	Results of Verification Study for Accident Conditions	5.4-26
Table 5.5.1.1-1	CEA Exposure History by Group – Maine Yankee	5.5.1-18
Table 5.5.1.1-2	CE14x14 CEA Hardware Spectra – 5, 10, 15, and 20 Years Cool Time – Maine Yankee	5.5.1-19
Table 5.5.1.1-3	Maine Yankee ICI Thimble Exposure History and Total Source Rate by Group	5.5.1-20
Table 5.5.1.1-4	Maine Yankee Core Exposure History by Cycle of Operation	5.5.1-21
Table 5.5.1.1-5	Maine Yankee Fuel Assemblies with Stainless Steel Replacement Rods (SSR) Showing Cycles of Operation and Burnup Received	5.5.1-22
Table 5.5.1.1-6	Contents of Maine Yankee Consolidated Fuel Lattices CN-1 and CN-10	5.5.1-22
Table 5.5.1.1-7	Maine Yankee CE14x14 Homogenized Fuel Region Isotopic Composition	5.5.1-23
Table 5.5.1.1-8	Isotopic Compositions of Maine Yankee CE14x14 Fuel Assembly Non-Fuel Source Regions	5.5.1-23

List of Tables (Continued)

Table 5.5.1.1-9	Isotopic Compositions of Maine Yankee CE14x14 Canister Annular Region Materials (One-Dimensional Analysis Only)	5.5.1-24
Table 5.5.1.1-10	Loading Table for Maine Yankee CE14x14 Fuel with No Non-Fuel Material – Required Cool Time in Years Before Assembly is Acceptable	5.5.1-24
Table 5.5.1.1-11	Three-Dimensional Shielding Analysis Results for Various Maine Yankee CEA Configurations Establishing One-Dimensional Dose Rate Limits for Loading Table Analysis	5.5.1-25
Table 5.5.1.1-12	Loading Table for Maine Yankee CE14x14 Fuel Containing CEA Cooled to Indicated Time	5.5.1-26
Table 5.5.1.1-13	Design Basis Maine Yankee CEA Source Rate at Each Cool Time Analyzed	5.5.1-27
Table 5.5.1.1-14	Establishment of Dose Rate Limit for Maine Yankee ICI Thimble Analysis	5.5.1-27
Table 5.5.1.1-15	Loading Table for Maine Yankee CE14x14 Fuel Containing ICI Thimble	5.5.1-27
Table 5.5.1.1-16	Required Cool Time for Maine Yankee Fuel Assemblies with Activated Stainless Steel Replacement Rods	5.5.1-28
Table 5.5.1.1-17	Maine Yankee Consolidated Fuel Model Parameters	5.5.1-28
Table 5.5.1.1-18	Maine Yankee Source Rate Analysis for CN-10 Consolidated Fuel Lattice	5.5.1-28
Table 5.5.1.1-19	Loading Table for Maine Yankee CE 14x14 Damaged Fuel	5.5.1-29
Table 5.5.1.1-20	Additional Maine Yankee Non-Fuel Hardware Characterization – Non-Neutron Sources	5.5.1-29
Table 5.5.1.1-21	Additional Maine Yankee Non-Fuel Hardware Characterization – Neutron Sources	5.5.1-29
Table 5.5.1.1-22	Pu-Be Assy Hardware Spectra (Cycles 11-13) – 9-Year Cool Time from 1/1/1997	5.5.1-30
Table 5.5.1.1-23	Additional Maine Yankee Non-Fuel Hardware – Hardware Assembly Spectra (Class 2 Canister) – 10-Year Cool Time from 1/1/1997	5.5.1-31

List of Tables (Continued)

Table 5.5.1.1-24	Additional Maine Yankee Non-Fuel Hardware – Source Assembly Spectra – 10-Year Cool Time 1/1/1997	5.5.1-32
Table 5.5.1.1-25	Additional Maine Yankee Non-Fuel Hardware – Hardware Assembly Dose Rates (Class 2) – 10-Year Cool Time from 1/1/1997	5.5.1-33
Table 5.5.1.1-26	Additional Maine Yankee Non-Fuel Hardware – Transport Cask Source Assembly Surface Dose Rates – Normal Conditions – 2m + Railcar Dose – 10-Year Cool Time from 1/1/1997	5.5.1-34
Table 5.5.1.1-27	Additional Maine Yankee Non-Fuel Hardware – Transport Cask Source Assembly Surface Dose Rates – Accident Conditions – 1m Dose – 10-Year Cool Time from 1/1/1997	5.5.1-35
Table 5.5.2-1	Neutron Dose Response Factors	5.5.2-2
Table 5.5.2-2	Photon Dose Response Factors	5.5.2-3

5.0 SHIELDING EVALUATION

The Universal Transport Cask meets the 10 CFR 71 [1] requirements for transportation dose rate limits. The optimized multiwall design provides an efficient shielding arrangement for the transportation of 24 PWR or 56 BWR spent fuel assemblies. This chapter describes the shielding design and the analysis used to establish bounding radiological dose rates for the transport of various PWR and BWR fuels.

The Universal Transport Cask is assigned a nominal Transport Index for shielding of 20 (TI=20) based on the requirement of 10 CFR 71.4 and the analysis of Section 5.4. The maximum dose rate at 1 meter from the Universal Transport Cask in normal conditions of transport is 19.3 mrem per hour, based on the analysis of the Westinghouse 17x17 Std assembly in a Class 3 canister.

The shielding design criteria for the Universal Transport Cask are in accordance with the requirements established in 10 CFR Parts 71.47 and 71.51 and IAEA Safety Standard Series No. ST-1 for normal conditions of transport and hypothetical accident conditions. The 10 CFR 71.47 and IAEA Safety Standard Series No. ST-1 (paragraph 572) requirements for the exclusive use transport of spent fuel under normal conditions of transport include the following:

- The dose rate on the surface of the enclosed package must not exceed 1000 mrem/hr.
- The dose rate on the outer surfaces of the transport vehicle must not exceed 200 mrem/hr.
- The dose rate on a plane two meters from the lateral surfaces of the railcar must not exceed 10 mrem/hr.
- The dose rate in any normally occupied positions of the railcar must not exceed 2 mrem/hr.

The 10 CFR 71.51 and IAEA Safety Standard Series No. ST-1 (paragraph 656) requirements state that the dose rate under hypothetical accident conditions must not exceed 1,000 mrem/hr at 1 meter from the surface of the cask. A summary description of the modeling methodology and dose rate results is provided in Section 5.1.

The shielding analysis is performed on the basis of design basis fuel descriptions for both PWR and BWR fuel. The design basis PWR fuel is a Westinghouse 17×17 assembly with a burnup of 45,000 MWD/MTU, an initial enrichment of 3.7 wt % ^{235}U , and a 10-year cooling time. The design basis BWR fuel is a GE 9×9 assembly design with a burnup of 40,000 MWD/MTU, an initial enrichment of 3.25 wt % ^{235}U , and a 10-year cooling time. A detailed description of the source term specification is provided in Section 5.2.

In the Universal Transport Cask design, the spent fuel assemblies are surrounded by a multiwalled arrangement of shielding materials. However, structural design requirements lead to cask extremity regions, such as rotation pockets, in which shield materials are reduced or penetrated. Detailed analytical treatment of these shield transition regions is required to assess the radiological consequences of the design. Section 5.3 describes the three-dimensional shielding models employed in this analysis.

Dose rate results are obtained for both normal conditions of transport and hypothetical accident conditions. Under accident conditions, the cask is analyzed for the simultaneous effects of complete loss of radial neutron shielding including loss of the outer neutron shield shell; loss of impact limiters; and combined radial and axial lead slumps resulting from postulated cask side and end drops. Analytical details and dose rate results are given in Section 5.4. Under all postulated conditions, the fully loaded cask is shown to meet regulatory radiological limits.

The design basis fuel descriptions characterize Universal Transport Cask dose and heat generation rates at nominal conditions of burnup and initial enrichment for a particular PWR and BWR fuel type. In order to extend the results to other fuel types and various combinations of initial enrichment and burnup, a detailed analysis is conducted that determines, for any given fuel type, enrichment, and burnup combination, the cool time required for radiation dose and heat generation rates to fall below the design basis values. The analysis explicitly models the source term for the various fuel combinations based on SAS2H results, and the dose rate evaluation is made on the basis of computed one-dimensional dose rates which explicitly consider the effects of radiation spectrum and cask shielding properties rather than a simple source rate comparison.

For clarity, the various fuel assembly types considered are classified according to array size, with the results for the most limiting fuel type within each array size taken as the minimum required cool time for all assemblies within that size. The result of the analysis is a fuel assembly loading table showing the required cool time for any combination of fuel array size, initial enrichment and burnup. Results are summarized in Section 5.1.3.

An analysis is performed for fuel at various combinations of burnup and initial enrichment to determine the required cool time for the fuel to fall below the design basis dose and decay heat levels. The bounding cool time is determined considering the cask normal and accident condition dose rates and total decay in the cask. This analysis is presented in Section 5.4.3.

Site specific fuel and GTCC waste is evaluated in Section 5.5.1.

THIS PAGE INTENTIONALLY LEFT BLANK

In the tabulated results, computed dose rates are reported along with the relative uncertainty associated with each computed value expressed as a percentage. The relative uncertainty corresponds to plus or minus one standard deviation in the quoted value.

5.1.3.1 Normal Conditions of Transport

The maximum radial and axial dose rates calculated for the PWR and BWR casks under normal conditions of transport are shown in Table 5.1-1 and Table 5.1-3, respectively. The locations of the maximum dose rates in normal conditions of transport relative to the cask body and transporter are shown in Figure 5.1-1. The tables present the maximum computed dose rates and corresponding relative uncertainties on radial and axial surfaces outside the cask. Dose rates indicated at the personnel barrier correspond to the maximum values computed on a cylindrical surface extending between the top and bottom impact limiters and surrounding the cask at a radius of 53.5 in. In the radial case, dose rates indicated at the "2 m position" correspond to a position 2 m from the edge of a 124 in. wide standard railcar. For axial results, this position corresponds to a dose location 2 m from the top or bottom impact limiter surface.

For the PWR cask, the maximum normal conditions surface dose rate is 167.2 (±1.8%) mrem/hr, occurring on the surface of the upper forging at the upper trunnion recess. (Values in parentheses following a dose rate result indicate the relative uncertainty in the value.) If a Class 3 canister is loaded, the dose rate at the outer shell surface in the inaccessible 1.25-inch wide gap between the neutron shield shell and lower impact limiter is computed to be 393.0 (±2.6%) mrem/hr. However, this dose rate is not considered significant due to the inaccessibility of the location. Furthermore, the dose rate at the gap opening coplanar with the neutron shield radius is well below 200 mrem/hr as demonstrated in Figure 5.1-1. All other cask surface dose rates are less than 200 mrem/hr. At the surface of the personnel barrier, the dose rate is much less than 200 mrem/hr with a maximum computed dose rate of 46.6 (±1.6%) mrem/hr. In addition, the 10 mrem/hr criterion is met at all locations 2 m from the railcar, 2 m above or below the cask, and 2 m from the axial surfaces of the impact limiters.

For the BWR cask, the maximum normal conditions surface dose rate is 34.8 (±2.0%) mrem/hr, occurring on the surface of the upper forging at the upper trunnion recess. The dose rate at the outer shell surface in the inaccessible 1.25-in. wide gap between the neutron shield shell and lower impact limiter, is computed to be 225.6 (±3.5%) mrem/hr. However, this dose rate is not

considered significant due to the inaccessibility of the location. Furthermore, the dose rate at the gap opening coplanar with the neutron shield radius is well below 200 mrem/hr as demonstrated in Figure 5.1-1. All other cask surface dose rates are less than 200 mrem/hr. At the personnel barrier, the maximum dose rate is much less than 200 mrem/hr, with a maximum computed dose rate of 40.4 (±1.5%) mrem/hr. The 10 mrem/hr criterion is met at all locations 2 m from the railcar and from the axial surfaces of the impact limiters.

5.1.3.2 Hypothetical Accident Conditions

Table 5.1-2 and Table 5.1-4 provide accident dose rates that could occur in the event of the loss of the neutron shield, shield shell, and impact limiters in the PWR and BWR casks, respectively. The location of the maximum hypothetical accident dose rates relative to the transport cask body is shown in Figure 5.1-2. An accident involving the complete loss of the impact limiters or neutron shielding is not credible for the Universal Transport Cask, although some of the neutron shielding capability may be lost as a result of a fire. Nonetheless, the shielding analysis conservatively assumes a complete loss of radial neutron shielding. In addition, axial and radial lead slumps resulting from postulated cask side and end drop accidents are modeled in the accident condition analysis

In the event of a cask end drop, the lead gamma shielding could slump and fill the annular gap (if one exists) created by the cooling of the lead after fabrication. This accident could create a 3.05 in. gap at the top of the lead annulus. The major radiation concern in this event is the “shine through” of the activated end-fittings. If the cask is subjected to a side drop, the lead gamma shielding could slump and create a void on the upper side of the cask. An evaluation of this side drop accident shows that the lead may sag at the opposite side by a maximum 0.91 in. Figure 5.1-3

The dose rates presented here and in more detail in Section 5.4 show that neither the loss of the neutron shielding nor the lead slump conditions will result in a dose rate that exceeds the hypothetical accident dose rate limit of 1000 mrem/hr at 1 m from the surface of the cask.

Figure 5.1-1

Location of Maximum Dose Rates for Normal Conditions of Transport

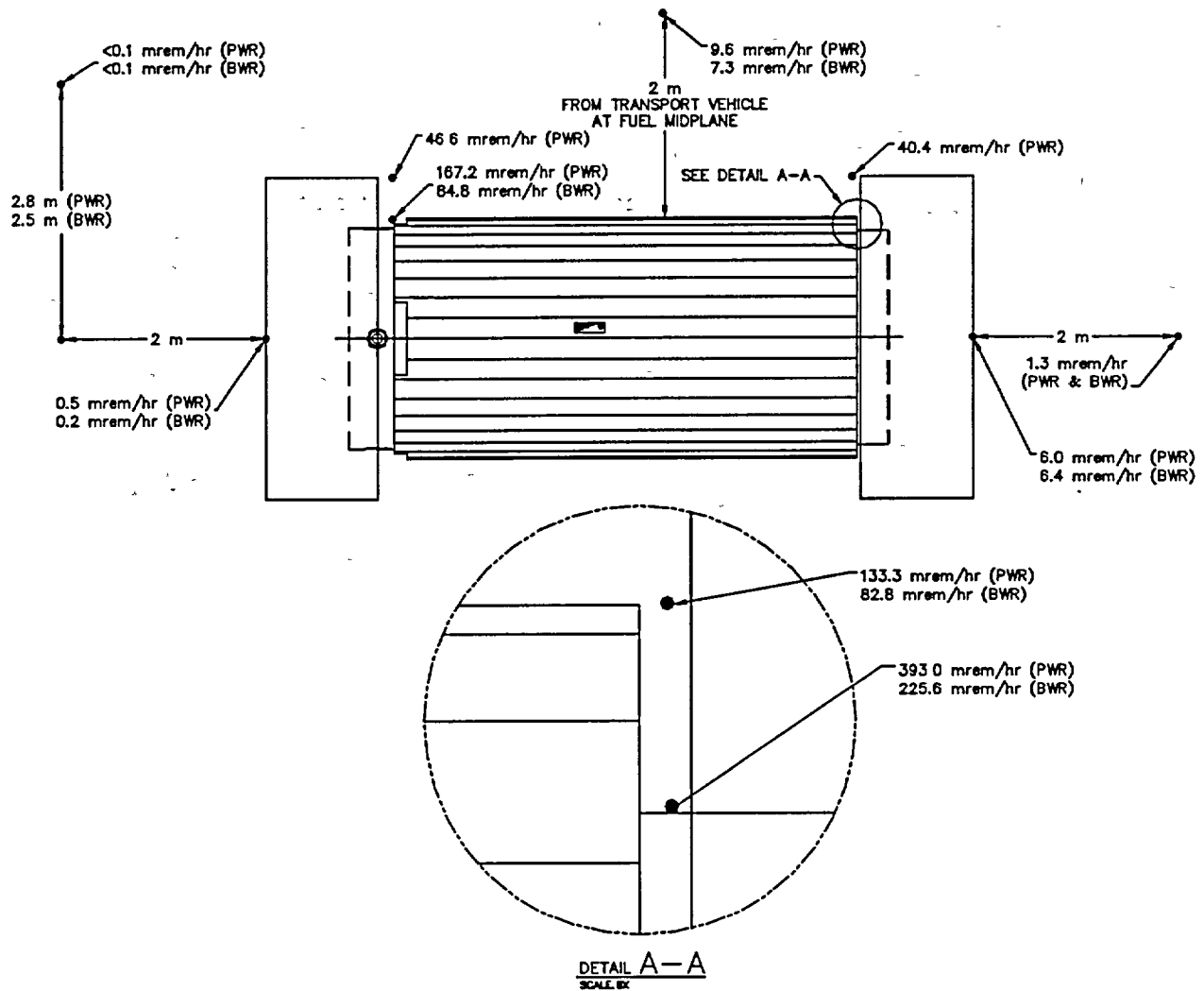


Figure 5.1-2 Location of Maximum Dose Rates for Hypothetical Accident Conditions

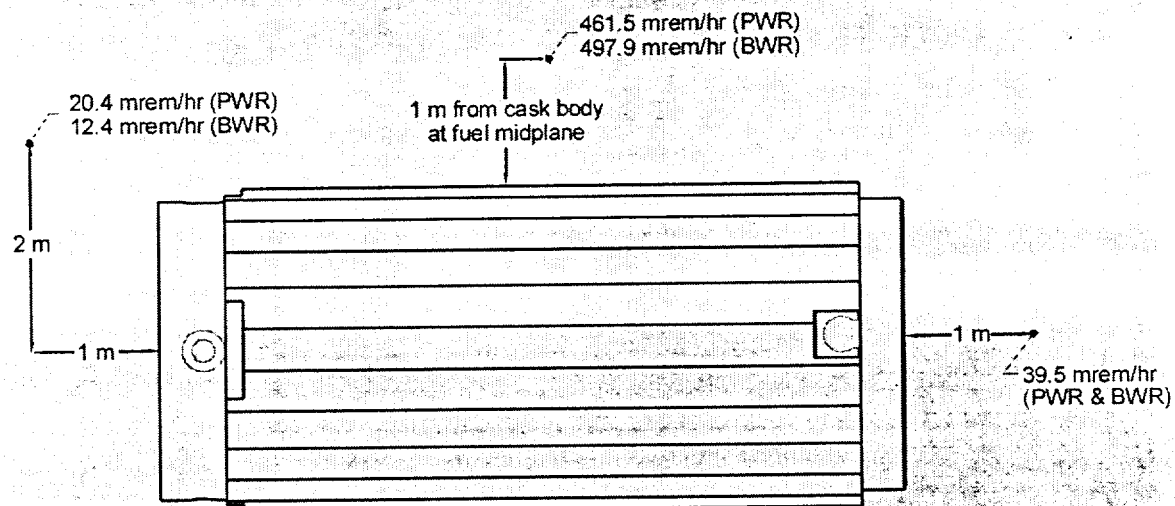


Table 5.1-1 PWR Maximum Total Dose Rate Summary – Normal Conditions [mrem/hr]

Location	Dose Type	Radial	Top Axial	Bottom Axial
Surface	Gamma	66.2 (0.6%)	0.5 (2.0%)	6.0 (0.4%)
	Neutron	101.1 (2.9%)	<0.1 (1.4%)	<0.1 (1.7%)
	Total	167.2 (1.8%)	0.5 (1.9%)	6.0 (0.4%)
Personnel Barrier	Gamma	23.5 (0.5%)	-	-
	Neutron	23.2 (3.1%)	-	-
	Total	46.6 (1.6%)	-	-
2 m Position	Gamma	6.4 (0.3%)	<0.1 (3.5%)	1.3 (1.0%)
	Neutron	3.2 (0.9%)	<0.1 (14.9%)	<0.1 (3.2%)
	Total	9.6 (0.4%)	<0.1 (11.4%)	1.3 (1.0%)

(1) The bounding dose rate occurs for Class 3 canisters at the forging surface inside gap between lower limiter and shield shell and is 393.0 mrem/hr (2.6%)

Table 5.1-2 PWR Maximum Total Dose Rate Summary – Accident Conditions [mrem/hr]

Location	Dose Type	Radial	Top Axial	Bottom Axial
1 m Position	Gamma	44.8 (0.5%)	<0.1 (8.6%)	28.7 (0.4%)
	Neutron	416.7 (0.2%)	20.3 (2.9%)	10.9 (0.6%)
	Total	461.5 (0.2%)	20.4 (2.8%)	39.5 (0.4%)

Table 5.1-3 **BWR Maximum Total Dose Rate Summary – Normal Conditions [mrem/hr]**

Location	Dose Type	Radial		Top Axial		Bottom Axial	
Surface	Gamma	50.4	(1.1%)	0.2	(2.8%)	6.4	(0.4%)
	Neutron	34.5	(4.6%)	<0.1	(1.6%)	<0.1	(2.0%)
	Total	84.8 ⁽¹⁾	(2.0%)	0.2	(2.7%)	6.4	(0.4%)
Personnel Barrier	Gamma	20.7	(0.5%)	-	-	-	-
	Neutron	19.8	(3.0%)	-	-	-	-
	Total	40.4	(1.5%)	-	-	-	-
2 m Position	Gamma	4.0	(0.4%)	<0.1	(3.9%)	1.3	(1.0%)
	Neutron	3.4	(0.8%)	<0.1	(24.1%)	<0.1	(4.3%)
	Total	7.3	(0.4%)	<0.1	(15.3%)	1.3	(1.0%)

⁽¹⁾ Dose rate at forging surface inside gap between lower limiter and shield shell is 225.6 (3.5%)

Table 5.1-4 **BWR Maximum Total Dose Rate Summary – Accident Conditions [mrem/hr]**

Location	Dose Type	Radial		Top Axial		Bottom Axial	
1 m Position	Gamma	25.3	(0.8%)	<0.1	(8.9%)	30.8	(0.4%)
	Neutron	472.7	(0.2%)	12.3	(3.9%)	8.7	(0.7%)
	Total	497.9	(0.2%)	12.4	(3.9%)	39.5	(0.4%)

5.1-9

5.1-10

5.1-11

5.1-12

5.5.1 Site Specific Contents Shielding Evaluations

This section describes fuel assembly characteristics and configurations, or waste configurations, which are unique to specific reactor sites. These site specific content configurations result from conditions that occurred during reactor operations, participation in research and development programs, testing programs intended to improve reactor operations, and from decommissioning activities.

Site specific fuel assembly configurations are either shown to be bounded by the analysis of the standard design basis fuel assembly configuration of the same type (PWR or BWR), or are shown to be acceptable contents by specific evaluation of the configuration.

5.5.1.1 Maine Yankee Site Specific Spent Fuel

This analysis considers both assembly fuel sources and sources from activated non-fuel material such as control element assemblies (CEA), in-core instrument (ICI) thimbles, and fuel assemblies containing activated stainless steel replacement (SSR) rods and other non-fuel material, including start-up neutron sources. It also considers the consolidated fuel present in the Maine Yankee spent fuel inventory, as well as damaged fuel and fuel debris.

The Maine Yankee spent fuel inventory also contains fuel assemblies with hollow zirconium rods, removed fuel rods, axial blankets, poison rods, variable radial enrichment, and low enriched substitute rods. These components do not result in additional sources to be considered in shielding evaluations and are, therefore, enveloped by the standard fuel assembly evaluation. For shielding considerations of the variably enriched rods, the planar-average enrichment should be employed in determining minimum cool times.

5.5.1.1.1 Fuel Source Term Description

Maine Yankee utilized 14x14 array size fuel based on designs provided by Combustion Engineering, Westinghouse, and Exxon Nuclear. The previously analyzed Combustion Engineering GE14x14 Standard fuel design is selected as the design basis for this analysis because its potential Uranium loading is the highest of the three vendor fuel types, based on a 0.3765-inch nominal fuel pellet diameter, a 137 inch active fuel length, and a 95% theoretical fuel density. This results in a fuel mass of 0.4907 MTU. This exceeds the maximum reported Maine Yankee fuel mass of 0.397 MTU, and therefore, produces bounding source terms. The

SAS2H model of the CE14x14 assembly at a nominal burnup of 45,000 MWD and initial enrichment of 3.7 wt %, based on data provided in Table 1.2-4, is shown in Figure 5.5.1.1-1.

Source terms for various combinations of burnup and initial enrichment discussed in Section 5.4.3.1 are computed by adjusting the SAS2H BURN parameter to model the desired burnup and specifying the initial enrichment in the Material Information Processor input for UO₂. For Maine Yankee CE 14 x 14 fuel, the burnup is increased to 50,000 MWD/MTU.

5.5.1.1.1 Control Element Assemblies (CEA)

For the CEA evaluation, the assumptions are:

- 1 The irradiated portion of the CEA assembly is limited to the CEA tips, as during normal operation, the elements are retracted from the core and only the tips are subject to significant neutron flux.
- 2 The CEA tips are defined as that portion present in the "Gas Plenum" neutron source region in the Characteristics Database (CDB) [9].
- 3 Material subject to activation in the CEA tips is limited to stainless steel, Inconel, and the AgInCd absorber material present in the lower eight inches of the CEA.
- 4 All stainless steel and Inconel material is assumed to have a concentration of 1.2 g/kg ⁶⁰Co. The CDB indicates that a total of 2,495 kg/CEA of this material is present in the Gas Plenum region of the core during operation.
- 5 The mass of AgInCd present in each CEA tip is 2.767 kg/CEA [9]. The AgInCd material is modeled as 80 wt % Ag, 15.35 wt % In, and 5.35 wt % Cd. Note that the composition sums to a value greater than 100%, but this only means that conservatively more mass is represented than is actually present.
- 6 The irradiated CEA material is assumed to be present in the bottom eight inches of the active fuel region when inserted in the assembly.
- 7 The decay heat generated in the most limiting CEA at a 5-year cool time is 2.16 W/kg of stainless steel or Inconel and 3.11 W/kg of AgInCd. For a cask fully loaded with fuel assemblies containing design basis CEAs, the additional heat generation due to the CEAs amounts to: $[(2.16 \text{ W/kg SS or Inconel})(2,495 \text{ kg/CEA}) + (3.11 \text{ W/kg AgInCd})(2.767 \text{ kg/CEA})](24 \text{ CEA/cask}) = 336 \text{ W/cask}$. This value is conservatively rounded up to 350 W. Although longer cool times are considered in this analysis for the fuel source terms, this decay heat generation rate is conservatively used for all longer CEA cool times.

source term. Hence, no adjustment to the one-dimensional dose rate limits is required as in previous analyses involving added non-fuel sources. The results of the cool time analysis for each assembly are shown in Table 5.5.1.1-16.

5.5.1.1.4.4 Consolidated Fuel

There are two consolidated fuel lattices intended for shipment in the Universal Transport Cask. The lattices house fuel rods taken from assemblies as shown in Table 5.5.1.1-6. The consolidated fuel rods have decayed for over twenty years and do not represent a significant shielding issue.

A limiting cool time analysis is conducted by identifying a fuel assembly description analyzed in the loading table analysis which bounds the parameters of the fuel rods in the consolidated fuel lattices. The parameters of those fuel rods are shown in Table 5.5.1.1-17. The CE14x14 fuel at 30,000 MWD/MTU and 1.9 wt % enrichment represents a bounding assembly type since it has a significantly higher burnup and a lower enrichment than the original assemblies. This fuel requires six years cool time before it can be loaded in the transport cask as shown in Table 5.5.1.1-10. The consolidated fuel has been cooled for at least 24 years. For container CN-1 lattice, one can immediately conclude that dose rates are bounded by the limiting fuel.

However, the CN-10 lattice contains significantly more fuel rods than an intact assembly. Neglecting the mitigating effects of additional self-shielding, this configuration is addressed by comparing the radiation source strength of the limiting fuel at six and 24 years cool time. Conservatively assuming that all fuel rods present in CN-10 are at the limiting conditions of 30,000 MWD/MTU and 1.9 wt %, the ratio of the source rate in the CN-10 to the source rate in the limiting fuel assembly is shown to be less than one for each source type in Table 5.5.1.1-18. For each source type, the ratio is computed as:

$$\text{Ratio} = (\text{Num Rods in CN-10})(\text{Source Rate at 24 Yr}) / (\text{Num Rods in F/A})(\text{Source Rate at 6 Yr})$$

Hence, CN-10 is also bounded by the limiting case and the consolidated fuel is eligible for shipment in the transport cask as of January 1, 2001.

5.5.1.1.4.5 Damaged Fuel

To provide minimum cool times for Maine Yankee damaged fuel inserted in Maine Yankee fuel cans in the four corner locations of the basket, an analysis is performed that determines, for any given enrichment and burnup combination, the minimum cool time required for dose rates to fall below the design basis values for these locations. The analysis models the source term for combinations of enrichment, burnup, and cool time based on SAS2H results. The dose rate evaluation is made on the basis of computed three-dimensional dose rates that explicitly consider the effects of radiation spectrum and cask shielding properties. The analysis considers the migration of damaged fuel from the active fuel region into the upper end-fitting and upper plenum assembly regions.

5.5.1.1.4.5.1 Damaged Fuel Loading Table Analysis

The loading table analysis extends the applicability of the initial 10-year-cooled, 45,000 MWD/MTU PWR design basis shielding evaluation by providing minimum cool times for 30,000 to 50,000 MWD/MTU burned fuel assemblies in increments of 5,000 MWD/MTU. In addition to the burnup range, the loading table evaluation includes minimum initial enrichment limits ranging from 1.9 to 3.7 wt.% ^{235}U in 0.2 wt.% ^{235}U increments.

A complete set of source spectra for the design basis Maine Yankee CE 14x14 fuel assembly is computed using the SAS2H code at various initial enrichment, burnup, and cool times representative of the fuel inventory intended for shipment. Next, the damaged fuel material descriptions are computed for the upper end-fitting and upper plenum assembly regions. The volume of void space in each region is calculated and is then assumed completely filled with UO_2 . Thus, 56% of the assembly fuel mass is assumed to migrate into the upper assembly region with no reduction in fuel modeled over the active fuel length.

With the damaged fuel defined, gamma and neutron source spectra for the four corner basket locations are constructed based on the mass of UO_2 in each fuel assembly region for seven sources: active fuel gamma, active fuel neutron, active fuel hardware, upper end-fitting gamma, upper end-fitting neutron, upper plenum gamma, and upper plenum neutron.

Because of the migration of the fuel out of the active fuel region, the one-dimensional dose response approach outlined in Section 5.4.3.1 cannot be used. Therefore, a three-dimensional

dose response methodology is used to generate the large number of dose rates required. Thus, seven sets of three-dimensional response cases are run to generate the groupwise contribution to dose rates at the dose rate locations of interest.

For each enrichment, burnup, cool time, and source region, the product of the normalized source spectrum and the response spectrum is multiplied by the total source to calculate the dose rates at the detector locations of interest. The dose rates from all sources are then summed. With the dose rates calculated for each possible combination, the exclusive use dose limits are used in conjunction with the four corner location results of the design basis PWR fuel to compute required cool times.

The SCALE computer code system is used to evaluate radiation source terms and to perform three-dimensional shielding calculations. Source terms are evaluated using the SAS2H code, which provides a simplified interface to the ORIGEN-S code, including burnup-dependent cross-section processing. The SAS4 code sequence is used to determine three-dimensional dose rate response functions. All SCALE analyses are conducted using the SCALE 27N18G group library.

SAS2H runs are executed for the CE 14x14 assembly at the following combinations of burnup, initial enrichment, and cool time:

Burnup: 30, 35, 40, 45, 50 MWD/MTU

Enrichment: 1.9, 2.1, 2.3, 2.5, 2.7, 2.9, 3.1, 3.3, 3.5, 3.7 wt % ²³⁵U

Cool Time: 5, 6, 7, 8, 9, 10, 12, 14, 16, 18, 20, 22, 24, 26, 28, 30, 35, 40 years

Final cool times are established by interpolating between results calculated for each cool time listed above. This interpolation procedure is conservative due to the exponentially decreasing behavior of radiation source rates with time. The maximum cool time (that is, the cool time that ensures the dose rate limit is met) is always rounded up to the next whole year.

The various combinations of enrichment and burnup shown above define a discrete mesh of possible combinations. When considering the required cool time for a particular assembly, the actual enrichment of the assembly should be rounded down to the next lower analyzed value, and the assembly burnup should be rounded up to the next higher analyzed value in order to ensure that a conservative value is obtained from the loading table.

5.5.1.1.4.5.2 Establishment of Limiting Values

Normal condition dose rate limits are established using the SAS4 code by computing the contribution of the sources in the four corner basket locations to the total dose rate for the design basis PWR fuel. The SAS4 geometric models are described in Section 5.3.2. The dose rate limits are established based on the difference between the total design basis Westinghouse 17x17 fuel dose rate and the Westinghouse 17x17 fuel four corner dose rate contribution and the exclusive use dose rate limits. The limiting detector location for maximum cool times is at a distance 2m from the edge of a 124-inch wide railcar (357.48 cm from the cask centerline) for the exclusive use surface dose rate limit of 1000 mrem/hr. The resulting three-dimensional dose rate limit for damaged fuel in the four corner basket locations is 2.65 mrem/hr at the limiting detector location.

5.5.1.1.4.5.3 Damaged Fuel Cool Time Determination

The strategy used to determine the limiting cool times for a given initial enrichment and burnup combination is

1. Determine dose rate values at each cool time step
2. Interpolate in the resulting collection of data to find the minimum cool time required to meet the limiting dose rate (total of 10 mrem/hr at 2m from the edge of the railcar)

The minimum cool times required to meet the dose rate limit are rounded up to the next whole year. The results of the Maine Yankee damaged fuel loading table analysis are shown in Table 5.5.1.1-19.

5.5.1.1.4.6 Additional Non-Fuel and Neutron Source Material

Additional non-fuel material consists of

1. Three plutonium-beryllium (Pu-Be) neutron sources, two irradiated and one unirradiated
2. Two antimony-beryllium (Sb-Be) neutron sources, both irradiated
3. Control element assembly (CEA) fingertips
4. ICI string segment

The five neutron sources will be inserted into the center guide tubes of five different assemblies and loaded into Class 1 canisters. These five assemblies must be loaded in five different canisters. The CEA fingertips and ICI string segment may be inserted into the guide tubes of one fuel assembly, but the assembly must be loaded into a Class 2 canister to accommodate a flow mixer to plug the guide tubes holding the non-fuel components.

The characterization of the additional non-fuel hardware is provided in Tables 5.5.1.1-20 and 5.5.1.1-21. The data is divided into two separate categories:

1. Non-neutron producing radiation sources – this category includes the CEA fingertips, ICI string segment, and the Sb-Be neutron sources (the neutron production rate of these is negligible)
2. Neutron producing radiation sources – this category includes the two irradiated and one unirradiated Pu-Be neutron sources.

The masses of ^{238}Pu and ^{239}Pu given for the unirradiated Pu-Be source are used in conjunction with the delivery date of May 1972 to generate source terms.

The neutron sources have an additional source component due to the irradiation of the stainless steel rod encasing the source. The quantity of irradiated steel is taken as 10 lbs (4.54 kg).

From the waste characterization, it is apparent that the Sb-Be sources already include the contribution of irradiated stainless steel. Therefore, only the Pu-Be irradiated stainless steel requires activation. The hardware source spectra for the irradiated Pu-Be sources are based on the Maine Yankee exposure history shown in Table 5.5.1.1-4. The combined Pu-Be assembly hardware irradiation for Cycles 1-13 is shown in Table 5.5.1.1-22 at a cool time of nine years from 1/1/1997.

The waste characterizations given in Table 5.5.1.1-20 and 5.5.1.1-21 are used to generate source terms using ORIGEN-S [8]. For the non-neutron producing sources, the total curie content is assigned to ^{60}Co to provide bounding source terms. Also, only one Sb-Be spectrum is produced, based on the higher curie content source. For the neutron-producing sources, the given curie contents are used for the irradiated sources, whereas the plutonium masses are used for the unirradiated Pu-Be source.

Based on the loading plan, there are two areas of application of both spectra and dose rates. The CEA fingertips and ICI strapping segment may be loaded into one assembly. Therefore, the gamma spectra of these items are summed and only one gamma spectrum is used to calculate the dose rates due to this loaded assembly. Each of the five neutron sources will be loaded into different fuel assemblies, and the spectra are presented accordingly. The single assembly spectra are presented in Table 5.5.1.1-23, and the neutron source assembly spectra are presented in Table 5.5.1.1-24.

Dose rates are calculated by simply groupwise multiplying the spectra and CEA 4x4 dose rate response functions and adjusting by a factor of $24/(10E+10 \times 5.6193E+06)$ to remove the volume component and the calculation scaling factor. Dose rates are presented in Tables 5.5.1.1-25 through 5.5.1.1-27 and show the minimal dose rate contribution due to the inclusion of the additional non-fuel material.

Figure 5.5.1.1-1 SAS2H Model Input File - CE 14x14

```
-SAS2H      PARM=(HALT03,SKIPSHIPDATA)
CE 14X14 3.7 W/O U235, 45000 MWD/MTD 12.0-22.0 YEAR COOLING
27GROUPNDF4 LATTICECELL
UO2      1 0.950 900 92235 3.7 92238 96.3 END
ZIRCALLOY 2 1.0 620 END
H2O      3 DEN=0.725 1.0 580 END
ARM-BORMOD 0.725 1 1 0 5000 100 3 550.0E-6 580 END
END COMP
SQUAREPITCH 1.4732 0.9563 1 3 1.1176 2 0.9754 0 END
NFIN=176 FUEL=347.98 NCYC=3 NLIB=1 PRIN=6 LIGH=5
INPL=1 NUMH=20 NUMI=0 ORTU=0.5588 SRU=0.49285 END
POWER=13.065 BURN=463.5350 DOWN=60.0 END
POWER=13.065 BURN=463.5350 DOWN=60.0 END
POWER=13.065 BURN=463.5350 DOWN=1461.00 END
FE 0.672 CR 0.190 NI 0.115 MN 0.020 CO 0.0012
END
```


Table 5.5.11-1

CEA Exposure History by Group – Maine Yankee

CEA Group	First Cycle	Last Cycle	Maximum Exposure (MWD/MTU)	Number of Cycles	Exposure Per Cycle (MWD/MTU)	Cool Time as of 1/1/2001 (y)
A1-A8	7	15	60239	9	6693	4
B1-B5	9	15	48909	7	6987	4
C1-C11, C13-C15	10	15	44315	6	7386	4
D1-D15	11	15	35283	5	7057	4
E1-E17, GN, 78, 101, 102, 138-153	12	15	29367	4	7342	4
F1, F2	13	15	18663	3	6221	4
4A	12	12	9786	1	9786	8
C12	10	12	24309	3	8103	8
NA	11	11	75444	1	6859	10
1-69	11	8	53258	8	6657	15

The asterisk is added to CEA 78* to distinguish it from the original CEA 78.

Table 5.5.1.1-2 CE14x14 CEA Hardware Spectra – 5, 10, 15 and 20 Years Cool Time
Maine Yankee

Group	5 year (γ/sec)	10 year (γ/sec)	15 year (γ/sec)	20 year (γ/sec)
1	0.0000E+00	0.0000E+00	0.0000E+00	0.0000E+00
2	0.0000E+00	0.0000E+00	0.0000E+00	0.0000E+00
3	0.0000E+00	0.0000E+00	0.0000E+00	0.0000E+00
4	0.0000E+00	0.0000E+00	0.0000E+00	0.0000E+00
5	1.3479E-04	4.4697E-06	1.4822E-07	4.9154E-09
6	7.1467E+06	2.6384E+06	1.3598E+06	7.0431E+05
7	4.0337E+09	1.6979E+09	8.7691E+08	4.5422E+08
8	3.7246E+10	2.3434E+08	1.4804E+06	1.5188E+04
9	1.8642E+14	7.1649E+13	3.6955E+13	1.9142E+13
10	4.8840E+14	2.5265E+14	1.3086E+14	6.7790E+13
11	1.3804E+14	9.4554E+11	4.7779E+10	3.7897E+10
12	1.1469E+15	9.3808E+14	9.1172E+14	3.8714E+14
13	4.3885E+14	4.2316E+14	4.1174E+14	4.0065E+14
14	9.1526E+11	5.5505E+11	5.2913E+11	5.0949E+11
15	1.2039E+12	3.4093E+11	3.0140E+11	7.6939E+11
16	3.8479E+12	2.9855E+12	2.7489E+12	2.5803E+12
17	5.1828E+13	4.4134E+13	4.2118E+13	4.0659E+13
18	3.4899E+14	2.7741E+14	2.6393E+14	2.5520E+14
SS Source Rate	6.3886E+14	3.2951E+14	1.7066E+14	3.8413E+13
AgInCd Source Rate	2.1666E+15	1.6829E+15	1.6308E+15	1.5861E+15
Total Source Rate	2.8055E+15	2.0124E+15	1.8014E+15	1.6745E+15
SFA	5.6110E+15	4.0249E+15	3.6029E+15	3.3490E+15

1 = SAS4 file input value

Table 5.5-1.1-2 **Maine Yankee ICI Thimble Exposure History and Total Source Rate by Group**

Group	Quantity	Cycles Exposed	Number of Cycles	Total Source r/sec
A	41	1-1A-2	3	9.1881E-11
B	1	1	1	2.3775E-11
C	2	1-1A	2	3.6244E-11
D	1	1A-2	2	6.8106E-11
E	3	2	1	5.5637E-11
F	15	3 thru 11-13	10	1.1695E-11
G	12	3 thru 11-14	10	1.2126E-11
H	12	3 thru 11-15	10	1.1454E-11
I	3	3 thru 9-14-15	9	1.1309E-11
J	2	10 thru 15	6	1.4940E-11
K	1	10 thru 12	3	6.1296E-12
L	25	12 thru 15	4	1.1491E-11
M	17	12	1	2.6801E-12
N	3	13 thru 15	3	3.8105E-12

Table 5.5.1-1-4 Maine Yankee Core Exposure History by Cycle of Operation

Cycle	Discharge Date	Cycle Burnup MWD/MTU	Core Average Enrichment wt. %
1	6/29/74	10367	2.44
1A	5/2/75	4492	2.30
2	4/9/77	17365	2.45
3	7/14/78	11105	2.59
4	1/11/80	10500	2.84
5	5/8/81	10799	2.98
6	9/24/82	11585	3.01
7	3/31/84	12483	3.10
8	3/17/85	12504	3.20
9	3/28/87	14424	3.29
10	10/15/88	12675	3.36
11	4/7/90	13786	3.50
12	2/14/92	15364	3.62
13	7/30/93	13668	3.68
14	1/14/95	13075	3.75
15	12/6/96	7859	3.76

**Table 5.5.1-1-5 Maine Yankee Fuel Assemblies with Stainless Steel Replacement Rods (SSR)
Showing Cycles of Operation and Burnup Received**

Assembly Number	1 st Cycle	2 nd Cycle	3 rd Cycle	1 st Cycle Burnup	2 nd Cycle Burnup	3 rd Cycle Burnup	Number SSR
N420	9	10	11	16,428	13,467	11,893	5
N842	9	10	11	18,420	13,885	0	1
N868	9	10	11	18,622	13,386	4,919	1
R032	12	13	14	16,464	15,386	12,168	1
R439	12	13	14	20,371	14,779	11,685	1
R444	12	13	14	20,371	14,779	11,685	4
U01	15	1	1	7,339	0	0	1
U05	15	1	1	7,339	0	0	1
U16	15	1	1	10,598	0	0	1
U37	15	1	1	9,005	0	0	1
U51	15	1	1	8,288	0	0	1
U60	15	1	1	8,288	0	0	5

1. MWD/MTU

Table 5.5.1-1-6 Contents of Maine Yankee Consolidated Fuel Lattices CN-1 and CN-10

C4E Lattice	Original Fuel Assembly	Number Rods	Actual Burnup MWD/MTU	Initial Enrichment wt. %
CN-1	EF0039	172	5150	1.929
CN-10	EF0045	176	17150	1.953
	EF0046	107	17150	1.953

Table 5.5.1-7

Maine Yankee CE14x14 Homogenized Fuel Region Isotopic Composition

Isotope	CE14x14 [atom/b-cm]
ALUMINUM	2.051114E-03
BORON-10	1.90898E-04
BORON-11	7.68387E-04
CARBON-12	2.39821E-04
CHROMIUM(SS304)	7.19369E-04
IRON(SS304)	2.4501E-03
MANGANESE	7.16674E-05
NICKEL(SS304)	3.18674E-04
OXYGEN-16	3.72597E-03
URANIUM-234	2.39964E-07
URANIUM-235	3.14155E-05
URANIUM-238	4.33153E-03
ZIRCALLOY	3.06324E-03

Table 5.5.1-8

Isotopic Compositions of Maine Yankee CE14x14 Fuel Assembly Non-Fuel

Source Regions

Isotope	Upper Plenum [atom/b-cm]	Upper End Fit [atom/b-cm]	Lower End Fit [atom/b-cm]
CHROMIUM(SS304)	1.59190E-03	1.39910E-03	3.08125E-03
MANGANESE	1.58594E-04	1.39199E-04	3.06971E-04
IRON(SS304)	5.42166E-03	5.46791E-03	1.04941E-02
NICKEL(SS304)	7.05196E-04	8.41284E-04	1.36497E-03
ZIRCALLOY	3.22036E-03		

Table 5.5.1.1-9 Isotopic Compositions of Maine Yankee CE14x14 Canister Annular Region Materials (One-Dimensional Analysis Only)

Isotope	Fuel Annulus [atom/b-cm]	Upper Plenum Annulus [atom/b-cm]	Upper End Fit Annulus [atom/b-cm]	Lower End Fit Annulus [atom/b-cm]
ALUMINUM	5.96817E-03			
CHROMIUM(SS304)	1.77895E-03	9.31065E-04	2.53529E-03	4.13797E-03
MANGANESE	1.77228E-04	9.27577E-05	2.52579E-04	4.12247E-04
IRON(SS304)	6.05870E-03	3.11710E-03	8.63463E-03	1.40930E-02
NICKEL(SS304)	7.88057E-04	4.12453E-04	1.12311E-03	1.83308E-03

Table 5.5.1.1-10 Loading Table for Maine Yankee CE14x14 Fuel with No Non-Fuel Material – Required Cool Time in Years Before Assembly is Acceptable

Loading Table for CE14x14 Fuel with No Non-Standard Fuel Material					
Enrichment [wt %]	Burnup (B) [GWD/MTU]				
	B ≤ 30	30 < B ≤ 35	35 < B ≤ 40	40 < B ≤ 45	45 < B ≤ 50
1.9 ≤ E < 2.1	6 years	8 years	11 years	18 years	27 years
2.1 ≤ E < 2.3	6 years	7 years	10 years	15 years	24 years
2.3 ≤ E < 2.5	6 years	7 years	9 years	14 years	22 years
2.5 ≤ E < 2.7	6 years	7 years	9 years	12 years	19 years
2.7 ≤ E < 2.9	6 years	6 years	8 years	11 years	17 years
2.9 ≤ E < 3.1	5 years	6 years	8 years	10 years	15 years
3.1 ≤ E < 3.3	5 years	6 years	7 years	10 years	15 years
3.3 ≤ E < 3.5	5 years	6 years	7 years	9 years	15 years
3.5 ≤ E < 3.7	5 years	6 years	7 years	9 years	14 years
3.7 ≤ E < 4.2	5 years	6 years	7 years	9 years	14 years

Table 5.5.1-1-11

Three-Dimensional Shielding Analysis Results for Various Maine Yankee
CEA Configurations Establishing One-Dimensional Dose Rate Limits for
Loading Table Analysis

CEA Cool Time [yr]	Dose Rate [mrem/hr]	FSD	Ratio [%]	Limit [mrem/hr]
Class I Result	7.70	0.72%	1	6.71
No Cea	7.92	0.63%	97.2%	6.53
5V	9.41	0.55%	81.9%	6.49
10V	8.53	0.59%	90.3%	6.06
15V	8.22	0.60%	93.6%	6.28
20V	8.08	0.61%	95.3%	6.39

Table 5.5.1-1-12 Loading Table for Maine Yankee CEI4x14 Fuel Containing CEA Cooled to Indicated Time

Loading Table for ce14x14 Fuel - Minimum Required Cool Time in Years						
Burnup 30 GWD/MTU		Minimum Cool Time (yr) for				
Enrichment	No CEA (Class 1)	No CEA (Class 2)	5 Yr CEA	10 Yr CEA	15 Yr CEA	20 Yr CEA
1.9	6	6	7	6	6	6
2.1	6	6	7	6	6	6
2.3	6	6	6	6	6	6
2.5	6	6	6	6	6	6
2.7	6	6	6	6	6	6
2.9	5	6	6	6	6	6
3.1	5	5	6	6	6	5
3.3	5	5	6	6	5	5
3.5	5	5	6	5	5	5
3.7	5	5	6	5	5	5

Burnup 35 GWD/MTU		Minimum Cool Time (yr) for				
Enrichment	No CEA (Class 1)	No CEA (Class 2)	5 Yr CEA	10 Yr CEA	15 Yr CEA	20 Yr CEA
1.9	8	8	9	8	8	8
2.1	7	7	9	8	8	8
2.3	7	7	8	7	7	7
2.5	7	7	8	7	7	7
2.7	6	7	7	7	7	7
2.9	6	6	7	7	6	6
3.1	6	6	7	6	6	6
3.3	6	6	7	6	6	6
3.5	6	6	6	6	6	6
3.7	6	6	6	6	6	6

Burnup 40 GWD/MTU		Minimum Cool Time (yr) for				
Enrichment	No CEA (Class 1)	No CEA (Class 2)	5 Yr CEA	10 Yr CEA	15 Yr CEA	20 Yr CEA
1.9	11	12	14	13	12	12
2.1	10	10	13	11	11	11
2.3	9	9	12	10	10	10
2.5	9	9	10	9	9	9
2.7	8	8	10	9	8	8
2.9	8	8	9	8	8	8
3.1	7	7	8	8	8	8
3.3	7	7	8	7	7	7
3.5	7	7	8	7	7	7
3.7	7	7	7	7	7	7

Burnup 45 GWD/MTU		Minimum Cool Time (yr) for				
Enrichment	No CEA (Class 1)	No CEA (Class 2)	5 Yr CEA	10 Yr CEA	15 Yr CEA	20 Yr CEA
1.9	18	18	21	19	18	18
2.1	15	16	19	17	17	16
2.3	14	14	18	16	15	15
2.5	12	13	16	14	14	13
2.7	11	12	14	13	12	12
2.9	10	11	13	12	11	11
3.1	10	10	12	11	10	10
3.3	9	9	11	10	10	10
3.5	9	9	10	10	10	10
3.7	9	9	10	10	10	10

Burnup 50 GWD/MTU		Minimum Cool Time (yr) for				
Enrichment	No CEA (Class 1)	No CEA (Class 2)	5 Yr CEA	10 Yr CEA	15 Yr CEA	20 Yr CEA
1.9	27	27	29	27	27	27
2.1	24	24	27	25	24	24
2.3	22	22	25	23	22	22
2.5	19	19	23	21	20	20
2.7	17	17	21	19	18	18
2.9	15	16	19	18	18	18
3.1	15	15	18	17	17	17
3.3	15	15	17	17	17	17
3.5	14	14	15	15	15	15
3.7	14	14	15	15	15	15

Table 5.5.1.1-13 Design Basis Maine Yankee CEA Source Rate at Each Cool Time Analyzed

CEA Cool Time [Y]	Source Strength [γ/sec/CEA]
5	1.1690E+14
10	3.3851E+13
15	7.5060E+13
20	6.9771E+13

Table 5.5.1.1-14 Establishment of Dose Rate Limit for Maine Yankee ICI Thimble Analysis

Case	Bottom		Top	
	Rate [mrem/hr]	ESD	Rate [mrem/hr]	ESD
No ICI	3.50	0.7%	9.78	0.8%
4 Yr Cooled ICI	3.50	0.7%	9.87	0.8%
Delta			0.08	
Original Limit			6.71	
Adjusted Limit			6.63	

Table 5.5.1.1-15 Loading Table for Maine Yankee CE14x14 Fuel Containing ICI Thimble

Enrichment [wt %]	Burnup [GWD/MTU]				
	30	35	40	45	50
1.9	6 years	8 years	11 years	18 years	27 years
2.1	6 years	7 years	10 years	16 years	24 years
2.3	6 years	7 years	9 years	14 years	22 years
2.5	6 years	7 years	9 years	13 years	19 years
2.7	6 years	6 years	8 years	11 years	17 years
2.9	5 years	6 years	8 years	10 years	15 years
3.1	5 years	6 years	7 years	10 years	15 years
3.3	5 years	6 years	7 years	9 years	15 years
3.5	5 years	6 years	7 years	9 years	14 years
3.7	5 years	6 years	7 years	9 years	14 years

Table 5.5.1.1-16 Required Cool Time for Maine Yankee Fuel Assemblies with Activated Stainless Steel Replacement Rods

Assy Number	Burnup [GWD/MTU]	Enrichment [wt %]	SSR Source [g/s/assy]	Cool Time [y]	Earliest Loadable
N420	45	3.2	2.1602E+13	10	Jan 2001
N842	35	3.3	3.1396E+12	8	Jan 2001
N868	40	3.2	5.2444E+12	7	Jan 2001
R032	45	3.5	1.4550E+12	8	Jan 2005
R439	50	3.5	1.3998E+13	14	Jan 2010
R444	50	3.5	5.5993E+13	19	Jan 2015

Table 5.5.1.1-17 Maine Yankee Consolidated Fuel Model Parameters

Lattice	Assy	Num Rods	Actual		Modeled		Required Cool Time [y]	Cool Time 1/1/01 [y]
			Burnup [MWD/MTU]	Enrichment [wt %]	Burnup [MWD/MTU]	Enrichment [wt %]		
CN-1	EF0039	172	5150	1.929	30000	1.9	8	26
CN-10	EF0045	176	17150	1.953	30000	1.9	6	24
	EF0046	107	17150	1.953	30000	1.9	6	24

Table 5.5.1.1-18 Maine Yankee Source Rate Analysis for CN-10 Consolidated Fuel Lattice

Cool Time [y]	Num Rods Present	Decay Heat [kW/cask]	Fuel Neutron [n/s/assy]	Fuel Gamma [g/sec/assy]	Fuel Hardware [g/sec/assy]
6	176	13.9	1.63E+08	3.16E+15	9.28E+12
24	283	7.42	3.41E+07	1.28E+15	3.67E+11
Src Ratio 24/6		0.86	0.83	0.65	0.15

Table 5.5.1.1-19

Loading Table for Maine Yankee GE 14x14 Damaged Fuel

Enrichment [wt.% ²³⁵ U]	Burnup [MWD/MTU]				
	30,000	35,000	40,000	45,000	50,000
1.9	7 years	11 years	19 years	28 years	37 years
2.1	6 years	9 years	16 years	26 years	34 years
2.3	6 years	8 years	14 years	23 years	32 years
2.5	6 years	8 years	12 years	21 years	30 years
2.7	6 years	7 years	11 years	19 years	27 years
2.9	6 years	7 years	10 years	17 years	25 years
3.1	5 years	7 years	9 years	15 years	23 years
3.3	5 years	6 years	8 years	13 years	21 years
3.5	5 years	6 years	8 years	12 years	19 years
3.7	5 years	6 years	7 years	11 years	17 years

Table 5.5.1.1-20

Additional Maine Yankee Non-Fuel Hardware Characterization – Non-Neutron Sources

Item	Waste Volume [ft ³]	Total Curies	⁶⁰ Co Curies
Sb-Be Source 1H1	0.020	4.15E+02	2.22E+02
Sb-Be Source 6H4	0.020	4.32E+02	2.31E+02
CEA Fingertips	0.100	1.06E+02	8.90E+01
ICI String Segment	0.007	2.82E+01	1.76E+01

Table 5.5.1.1-21

Additional Maine Yankee Non-Fuel Hardware Characterization – Neutron Sources

Item	²³⁸ Pu Grams	²³⁸ Pu Curies	²³⁹ Pu Grams	²³⁹ Pu Curies
Pu-Be Unirradiated Source	1.16	1	0.24	1
Pu-Be Irradiated Sources	1.16	5.10E-02	0.24	5.88E-05

Table 5.5.11-22

Pu-Be Assy Hardware Spectra (Gy/cds 1E13) - 9-Year Cool Time from 1A/1997

Group	Pu-Be Assy HW [g/sec]
1	0.0000E+00
2	0.0000E+00
3	0.0000E+00
4	0.0000E+00
5	0.0000E+00
6	1.6598E+15
7	2.1099E+05
8	1.3607E+08
9	5.5885E+09
10	5.7338E+12
11	2.0304E+13
12	1.3362E+09
13	2.3989E+07
14	6.9076E+07
15	1.0929E+09
16	8.3300E+08
17	1.6776E+10
18	6.9545E+10
19	3.5629E+11
TOTAL	4.9691E+12

Table 5.5.1-1-23

Additional Maine Yankee Non-Fuel Hardware – Hardware Assembly
Spectra (Class 2 Canister) – 10-Year Cool Time from 1/1/1997

Group	ICI String [g/sec]	CEA Fingertips [g/sec]	Total Gamma [g/sec]
1	0.0000E+00	0.0000E+00	0.0000E+00
2	0.0000E+00	0.0000E+00	0.0000E+00
3	0.0000E+00	0.0000E+00	0.0000E+00
4	0.0000E+00	0.0000E+00	0.0000E+00
5	0.0000E+00	0.0000E+00	0.0000E+00
6	7.7679E+03	2.9198E+04	3.6966E+04
7	5.0096E+06	1.8830E+07	2.3840E+07
8	0.0000E+00	0.0000E+00	0.0000E+00
9	2.1109E+11	7.9347E+11	1.0046E+12
10	7.4750E+11	2.8098E+12	3.5573E+12
11	3.3302E+07	1.2518E+08	1.5848E+08
12	3.8318E+05	3.3197E+06	4.2029E+06
13	2.5431E+06	9.5592E+06	1.2102E+07
14	4.0238E+07	1.5125E+08	1.9149E+08
15	3.0668E+07	1.1528E+08	1.4595E+08
16	6.1764E+08	2.3216E+09	2.9392E+09
17	2.5600E+09	9.6228E+09	1.2183E+10
18	1.2840E+10	4.8265E+10	5.1105E+10
Total	9.7472E+11	3.6639E+12	4.6386E+12

Table 5.5.1-1-24 Additional Maine Yankee Non-Fuel Hardware – Source Assembly Spectra – 10-Year Cool Time from 1/1/1997

Group	Sb-Be Source	Pu-Be Unirradiated Source		Pu-Be Irradiated Source			
	Gamma [g/sec]	Gamma [g/sec]	Neutron [n/sec]	Gamma [g/sec]	Hw Gamma [g/sec]	Total Gamma [g/sec]	Neutron [n/sec]
1	0.0000E+00	1.7724E+00	4.5780E+01	5.6750E-03	0.0000E+00	5.6750E-03	1.4660E-01
2	0.0000E+00	8.6878E+00	3.0620E+03	2.7817E-02	0.0000E+00	2.7817E-02	9.8050E+00
3	0.0000E+00	4.6818E+01	7.7810E+03	1.4991E-01	0.0000E+00	1.4991E-01	2.4920E+01
4	0.0000E+00	1.2370E+02	2.2600E+03	3.9608E-01	0.0000E+00	3.9608E-01	7.2370E+00
5	0.0000E+00	3.9121E+02	1.5280E+03	1.2526E+00	1.6598E-15	1.2526E+00	4.8930E+00
6	1.1900E+05	4.5986E+02	7.9540E+02	1.4722E+00	2.1099E+05	2.1099E+05	2.5470E+00
7	7.6742E+07	8.3349E+02	1.4320E+02	2.6552E+00	1.3607E+08	1.3607E+08	4.5850E-01
8	0.0000E+00	1.4479E+03	—	4.6003E+00	5.5885E-09	4.6003E+00	—
9	3.2338E+12	6.7259E+00	—	1.0044E-04	5.7338E+12	5.7338E+12	—
10	1.1451E+13	3.6431E+03	—	2.7632E+01	2.0304E+13	2.0304E+13	—
11	5.1015E+08	3.7894E+04	—	1.2132E+02	1.3362E+09	1.3362E+09	—
12	1.3530E+07	2.9010E+05	—	9.2911E+02	2.3989E+07	2.3990E+07	—
13	3.8958E+07	3.7568E+03	—	3.4472E+01	6.9076E+07	6.9076E+07	—
14	6.1641E+08	2.6912E+04	—	1.0610E+02	1.0929E+09	1.0929E+09	—
15	4.6980E+08	2.4539E+04	—	3.1311E+01	3.3300E+08	3.3300E+08	—
16	9.4617E+09	1.9698E+07	—	6.3049E+04	1.6776E+10	1.6776E+10	—
17	3.9217E+10	2.7826E+07	—	3.9027E+04	6.9545E+10	6.9545E+10	—
18	1.9670E+11	2.9816E+10	—	9.5465E+07	3.5629E+11	3.5639E+11	—
Total	1.4932E+13	2.9864E+10	1.562E+04	9.5618E+07	2.6484E+13	2.6484E+13	5.001E+01

Table 5.5-1-25

Additional Maine Yankee Non-Fuel Hardware – Hardware Assembly
Dose Rates (Class 2) – 10-Year Cool Time from 1/1/1997

Group	Normal – Railcar + 2m Dose	Accident – 1m Dose
	Gamma Dose	Gamma Dose
	mrem/hr	mrem/hr
1	0.00E+00	0.00E+00
2	0.00E+00	0.00E+00
3	0.00E+00	0.00E+00
4	0.00E+00	0.00E+00
5	0.00E+00	0.00E+00
6	7.43E-09	3.42E-08
7	2.39E-06	1.18E-05
8	0.00E+00	0.00E+00
9	1.18E-02	5.91E-02
10	6.70E-03	4.38E-02
11	2.01E-08	1.52E-07
12	2.44E-11	2.08E-10
13	1.28E-13	1.31E-12
14	1.30E-18	1.72E-17
15	1.21E-34	1.99E-33
16	0.00E+00	0.00E+00
17	0.00E+00	0.00E+00
18	0.00E+00	0.00E+00
Total	1.85E-02	1.13E-01

Table 5.5.1-1-26 Additional Maine Yankee Non-Fuel Hardware – Transport Cask Source Assembly Surface Dose Rates – Normal Conditions – 2m + Railcar Dose – 10-Year Cool Time from 1/1/1997

Group	Sb-Be Source	Pu-Be Unirradiated Source		Pu-Be Irradiated Source	
	Dose	Dose		Dose	
	Gamma mrem/hr	Gamma mrem/hr	Neutron mrem/hr	Gamma mrem/hr	Neutron mrem/hr
1	0.00E+00	1.16E-12	1.12E-07	3.71E-15	3.59E-10
2	0.00E+00	6.35E-12	4.09E-06	2.03E-14	1.31E-08
3	0.00E+00	3.16E-11	9.39E-06	1.01E-13	3.01E-08
4	0.00E+00	6.62E-11	1.93E-06	2.12E-13	6.20E-09
5	0.00E+00	1.43E-10	1.04E-06	4.57E-13	3.33E-09
6	2.39E-08	9.25E-11	4.13E-07	4.24E-08	1.32E-09
7	7.69E-06	3.35E-11	3.55E-08	1.36E-05	1.14E-10
8	0.00E+00	5.46E-11	—	1.73E-14	—
9	3.80E-02	7.90E-14	—	6.73E-02	—
10	2.16E-02	1.63E-11	—	3.83E-02	—
11	6.49E-08	4.82E-12	—	1.70E-07	—
12	7.84E-11	1.68E-12	—	1.39E-10	—
13	4.13E-13	9.28E-17	—	7.32E-13	—
14	4.17E-18	1.82E-22	—	7.39E-18	—
15	3.90E-34	2.04E-38	—	6.91E-34	—
16	0.00E+00	0.00E+00	—	0.00E+00	—
17	0.00E+00	0.00E+00	—	0.00E+00	—
18	0.00E+00	0.00E+00	—	0.00E+00	—
Total	5.96E-02	5.01E-10	1.70E-05	1.06E-01	5.45E-08

Table 5.5.1-1-27

Additional Maine Yankee Non-Fuel Hardware – Transport Cask Source
Assembly Surface Dose Rates – Accident Conditions – 1m Dose = 10-
Year Cool Time from 1/1/1997

Group	Sb-Be Source	Pu-Be Unirradiated Source		Pu-Be Irradiated Source	
	Dose	Dose		Dose	
	Gamma mrem/hr	Gamma mrem/hr	Neutron mrem/hr	Gamma mrem/hr	Neutron mrem/hr
1	0.00E+00	4.04E-12	7.22E-06	1.29E-14	2.31E-08
2	0.00E+00	2.27E-11	3.80E-04	7.28E-14	1.22E-06
3	0.00E+00	1.18E-10	9.62E-04	3.79E-13	3.08E-06
4	0.00E+00	2.63E-10	2.43E-04	3.42E-13	7.78E-07
5	0.00E+00	6.06E-10	1.46E-04	1.94E-12	4.67E-07
6	1.10E-07	4.25E-10	6.96E-05	1.95E-07	2.23E-07
7	3.79E-05	4.12E-10	3.61E-06	3.73E-05	1.80E-08
8	0.00E+00	2.94E-10	—	9.33E-13	—
9	2.22E-01	4.63E-13	—	3.94E-01	—
10	1.41E-01	1.06E-10	—	2.50E-01	—
11	4.89E-07	3.64E-11	—	1.28E-06	—
12	6.70E-10	1.44E-11	—	1.19E-09	—
13	4.23E-12	9.50E-16	—	7.49E-12	—
14	3.52E-17	2.41E-21	—	9.79E-17	—
15	6.41E-33	3.35E-37	—	1.14E-32	—
16	0.00E+00	0.00E+00	—	0.00E+00	—
17	0.00E+00	0.00E+00	—	0.00E+00	—
18	0.00E+00	0.00E+00	—	0.00E+00	—
Total	3.63E-01	2.30E-09	1.81E-03	6.44E-01	5.81E-06

THIS PAGE INTENTIONALLY LEFT BLANK

Chapter 6

List of Figures

Figure 6.3-1	Universal Transport Cask KENO-Va PWR Basket Cell Model	6.3-9
Figure 6.3-2	Universal Transport Cask KENO-Va BWR Basket Cell Model.....	6.3-10
Figure 6.3-3	Universal Transport Cask PWR KENO-Va Cask Model.....	6.3-11
Figure 6.3-4	Universal Transport Cask BWR KENO-Va Cask Model	6.3-12
Figure 6.3-5	PWR Basket Criticality Control Design.....	6.3-13
Figure 6.3-6	BWR Basket Criticality Control Design	6.3-14
Figure 6.4-1	Visage Slice – Hypothetical Shifting of PWR Fuel	6.4-26
Figure 6.4-2	Visage Slice – Hypothetical Shifting of BWR Fuel	6.4-27
Figure 6.5-1	KENO-Va Validation - 27 Group Library Results: Frequency Distribution of k_{eff} Values.....	6.5-11
Figure 6.5-2	KENO-Va Validation - 27 Group Library Results: k_{eff} versus Enrichment	6.5-12
Figure 6.5-3	KENO-Va Validation - 27 Group Library Results: k_{eff} versus Rod Pitch	6.5-13
Figure 6.5-4	KENO-Va Validation - 27 Group Library Results: k_{eff} versus H/U Volume Ratio	6.5-14
Figure 6.5-5	KENO-Va Validation - 27 Group Library Results: k_{eff} versus Average Group of Fission.....	6.5-15
Figure 6.5-6	KENO-Va Validation - 27 Group Library Results: k_{eff} versus β/Λ Loading for Flux Trap Criticals.....	6.5-16
Figure 6.5-7	KENO-Va Validation - 27 Group Library Results: k_{eff} versus Flux Trap Critical Gap Thickness.....	6.5-17

List of Figures (Continued)

Figure 6.5-8	USLSTATS Output for Fuel Enrichment Study	6.5-18
Figure 6.5-9	MONK8A – JEF 2.2 Library Validation Statistics - k_{eff} versus Fuel Enrichment	6.5-20
Figure 6.5-10	MONK8A – JEF 2.2 Library - k_{eff} versus Rod Pitch	6.5-21
Figure 6.5-11	MONK8A – JEF 2.2 Library - k_{eff} versus H/U (fissile) Atom Ratio	6.5-22
Figure 6.5-12	MONK8A – JEF 2.2 Library - k_{eff} versus ^{10}B Loading	6.5-23
Figure 6.5-13	MONK8A – JEF 2.2 Library - k_{eff} versus Mean Neutron Log(E) Causing Fission	6.5-24
Figure 6.5-14	MONK8A – JEF 2.2 Library - k_{eff} versus Cluster Gap Thickness	6.5-25
Figure 6.5-15	MONK8A – JEF 2.2 Library - k_{eff} versus Fuel Pellet Outside Diameter	6.5-26
Figure 6.5-16	MONK8A – JEF 2.2 Library - k_{eff} versus Fuel Rod Outside Diameter	6.5-27
Figure 6.5-17	USLSTATS Output - k_{eff} versus Gap Thickness	6.5-28
Figure 6.6.1.1-1	24 Removed Fuel Rods – Diamond Shaped Geometry, Maine Yankee Site Specific Fuel	6.6.1-12
Figure 6.6.1.1-2	Consolidated Fuel Geometry, 113 Empty Fuel Rod Positions, Maine Yankee Site Specific Fuel	6.6.1-13
Figure 6.6.2-1	CSAS Input & Output for Normal Conditions Criticality Analysis: PWR Fuel	6.6.2-2
Figure 6.6.2-2	CSAS Input & Output for Accident Conditions Criticality Analysis: PWR Fuel	6.6.2-25

List of Tables (Continued)

Table 6.4-15	BWR Cask Array Analysis Criticality Results - Variable Exterior	6.4-36
Table 6.4-16	Heterogeneous vs. Homogeneous Enrichment Analysis Results (GE)	6.4-36
Table 6.4-17	PWR Lattice Parameter Study Criticality Analysis Results	6.4-37
Table 6.4-18	BWR Lattice Parameter Study Criticality Analysis Results	6.4-38
Table 6.4-19	Transport Cask Top End Impact Bounding Exposed Fuel Heights	6.4-39
Table 6.4-20	Fuel Assembly Minimum Intact Hardware Dimension Limits	6.4-39
Table 6.5-1	KENO-Va and 27-Group Library Validation Statistics	6.5-30
Table 6.5-2	Correlation Coefficient for Linear Curve-Fit of Critical Benchmarks	6.5-33
Table 6.5-3	Most Reactive Configuration System Parameters	6.5-33
Table 6.5-4	Range of Correlated Parameters for Design Basis Fuel	6.5-34
Table 6.5-5	MONK8A - Correlation Coefficient for Linear Curve-Fit of Critical Benchmarks	6.5-34
Table 6.5-6	MONK8A - JEF 2.2 Library Validation Statistics	6.5-35
Table 6.6.1.1-1	Maine Yankee Standard Fuel Characteristics	6.6.1-14
Table 6.6.1.1-2	Maine Yankee Most Reactive Fuel Dimensions	6.6.1-14
Table 6.6.1.1-3	Maine Yankee Pellet Diameter Study	6.6.1-15
Table 6.6.1.1-4	Maine Yankee Annular Fuel Results	6.6.1-15
Table 6.6.1.1-5	Maine Yankee Removed Rod Results with Small Pellet Diameter	6.6.1-16
Table 6.6.1.1-6	Maine Yankee Removed Fuel Rod Results with Maximum Pellet Diameter	6.6.1-17

List of Tables (Continued)

Table 6.6.1.1-7	Maine Yankee Fuel Rods in Guide Tubes Results	6.6.1-18
Table 6.6.1.1-8	Maine Yankee Consolidated Fuel Empty Fuel Rod Position Results	6.6.1-19
Table 6.6.1.1-9	Fuel Can Infinite Height Model Results of Fuel – Water Mixture Between Rods	6.6.1-20
Table 6.6.1.1-10	Fuel Can Finite Model Results of Fuel – Water Mixture Outside BORAL Coverage	6.6.1-21
Table 6.6.1.1-11	Fuel Can Finite Model Results of Replacing All Rods with Fuel – Water Mixture	6.6.1-22
Table 6.6.1.1-12	Maine Yankee Fuel Can Preferential Flooding Evaluation	6.6.1-23
Table 6.6.1.1-13	Infinite Height Analysis of Maine Yankee Start-up Sources	6.6.1-24

Fuel Assembly Minimum Intact Hardware Dimension Limits

Based on limiting the exposed height of active fuel to 4.52 inches for the PWR fuel assemblies and to 7.625 inches for the BWR fuel assemblies, intact fuel assembly hardware limits are defined to assure compliance with the safety basis of the analysis. These limits consider zero PWR top end-fitting deformation, 2.371 inches of BWR top end-fitting (lifting bail) deformation and a BWR plenum spring rebound height of 1.729 inches. The limits for each UMS® canister class containing PWR fuel are calculated by subtracting the height of exposed fuel, 4.52 inches, from the distance between the canister lid and the top of the neutron absorber. The limits for each UMS® canister class containing BWR fuel are calculated by subtracting the sum of the height of exposed fuel, 7.625 inches, and the plenum spring rebound height, 1.729 inches, from the sum of the lifting bail deformation, 2.371 inches, and the distance between the canister lid and the top of the neutron absorber. These resulting limits are provided in Table 6.4-20.

Each minimum axial assembly dimension is a generic limit that all fuel types in the respective fuel class shall meet. Compliance with these limits will ensure that the exposed fuel heights evaluated and found to result in a subcritical system will not be exceeded. For PWR fuel, the minimum intact assembly hardware dimension above the active fuel shall be calculated by summing the top end-fitting height, the top end cap height, and the solid height of the plenum spring. For BWR fuel, the minimum axial assembly dimension above the active fuel shall be calculated by summing the intact top end-fitting height, the portion of the top end-cap height below the tie plate when the fuel rod is shifted up, and the solid height of the plenum spring. Tolerances on these components shall be conservatively considered when calculating the subject dimension.

Evaluation of Bottom End Axial Fuel Shifting

Similar to the top end evaluation, a bounding hypothetical axial fuel-shifting condition is considered in which all of the fuel rods are shifted to the bottom of each assembly. For PWR fuel assemblies with a lower plenum, the fuel within every rod is assumed to shift downward to contact a fully compressed plenum spring. Each fuel assembly is assumed to remain in contact with the canister bottom plate. The basket dimensions used assume conservative tolerances, and the basket is conservatively assumed to be shifted upward to contact the canister shield lid. This bounding axial shifting scenario results in the maximum distance from the canister bottom plate to the lower end of the neutron absorber panels. For all UMS® PWR canister classes, this distance is limited to 5.22 inches. For all UMS® BWR canister classes, the distance is limited to 8.19 inches. However, all PWR and BWR fuel assembly types have rod bottom end caps, tie

plates and/or components of the bottom end-fitting/nozzle that will not deform to a total height of less than 0.7 inches. Consequently, the top end axial fuel shifting condition, which considers exposed fuel lengths of 4.52 inches for PWR fuel and 7.625 inches for BWR fuel, bounds the bottom end axial fuel shifting condition.

End Impact Accident Condition Effect on System Reactivity

The bounding PWR system end impact event does not significantly affect the reactivity of the system. Therefore, poison sheet coverage is adequate for all allowed PWR fuel contents of the UMS® system. The bounding BWR end impact event increases the reactivity of the system. This increase in reactivity, a Δk_{eff} of 0.0249, is added to the most reactive accident condition system reactivity, $k_{eff} \pm 2\sigma$, of 0.9108 ± 0.0008 as determined in Section 6.4.3.3, to establish a maximum BWR system reactivity, $k_{eff} \pm 2\sigma$, of 0.9357 ± 0.0008 . This value is less than the USL of 0.9426 identified in Section 6.5.5. Including code bias, code bias uncertainty, and statistical uncertainty (2σ) in accordance with Equation 6 in Section 6.5.3, the resulting system k_{eff} of 0.9497 is less than 0.95. Thus, poison sheet coverage is adequate for all allowed BWR fuel contents of the UMS® system.

6.4.6 Regulatory Compliance

The licensing requirements for criticality analyses are provided in 10 CFR 71.55 and 10 CFR 71.59 for shipment of radioactive material.

10 CFR 71.55 and 10 CFR 71.59 require that the fissile material package be subcritical under any credible condition, e.g., optimum interior/exterior moderation and reflection and credible configuration of the material. A criticality transport index is to be assigned to the fissile material package. This transport index must be based on the number of packages (casks in this context) remaining subcritical in an array configuration.

Additional requirements imposed include the reduction in poison plate ^{10}B from 100 to 75 percent and water in the pellet-to-cladding gap.

NUREG/CR-6361. However, if no strong correlation can be determined, then a constant bias adjustment can be made. This is typically done with a one-side tolerance factor that guarantees 95% confidence in the uncertainty in the bias. This is the approach taken in the UMS criticality analysis.

Both NUREG/CR-6361 and the NAC evaluation perform regression analysis on key system parameters. For all of the major system parameters, the evaluation found no strong correlation. This is based on the observation that the correlation coefficients are all much less than ± 1 . Thus a constant bias with a 95/95 confidence factor is applied to the system k_{eff} . NAC's statistical analysis of the k_{eff} results produced a bias of 0.0052 and a 95/95 uncertainty of 0.0087. Adding the two together and subtracting from 0.95 yields an effective constant USL of 0.9361.

To assure compliance with NUREG/CR-6361, an upper safety limit is generated using USLSTATS and is compared to the constant NAC bias and bias uncertainty used in Section 6.5.2.

To evaluate the relative importance of the trend analysis to the upper safety limits, correlation coefficients are required for all independent parameters. Table 6.5-2 contains the correlation coefficient, R , for each linear fit of k_{eff} versus experimental parameter (data is extracted from Figure 6.5-2 through Figure 6.5-7 by taking the square root of the R^2 value). Based on the highest correlation coefficient and the method presented in NUREG/CR-6361, a USL is established based on the variation of k_{eff} with enrichment. Note that even the enrichment function shows a low statistical correlation coefficient (an $|R|$ equal or near 1 would indicate a good fit). The output generated by USLSTATS is shown in Figure 6.5-8.

The NAC applied USL of 0.9361 bounds the calculated upper safety limits for all enrichment values above 3.0 wt % ^{235}U . Since the maximum reactivities in the UMS® are calculated at enrichments well above this level, the existing bias bounds the NUREG calculated USL. The parameters of the most reactive configurations for the UMS® design basis PWR and BWR fuels and for the Maine Yankee fuel are presented in Table 6.5-3. This table also compares the most reactive fuel parameters to the minimum and maximum benchmark values to demonstrate the applicability of the critical benchmarks.

6.5. MONK Validation in Accordance with NUREG/CR-6361

NUREG/CR-6361, "Criticality Benchmark Guide for Light-Water-Reactor Fuel in Transportation and Storage Packages" (NUREG), provides a guide to LWR criticality benchmark calculations and the determination of bias and subcritical limits in critical safety evaluations. Section 6.5.1 contains detail on the implementation of the NUREG in subcritical limit evaluations for the UMS Transport Cask. This section implements the ULSTATS method of the NUREG for MONK8A application with JEF 2.2 point energy libraries in LWR transport and storage applications.

SERCO Assurance (SERCO, previously AEA Technologies) has performed an extensive benchmarking of MONK8A. The cross-section set and key geometry features employed in the critical benchmark models are reflected in the transport cask evaluation models. Consequently, the SERCO produced critical benchmark models are applicable to the evaluation of the UMS System. The critical benchmarks relevant to LWR fuel evaluations were extracted from the total benchmark set and listed in Table 6.5-6. The range of the parameters to be benchmarked is summarized in Table 6.5-4. Trending in k_{eff} was evaluated for the following independent variables: enrichment, rod pitch, fuel pellet diameter, fuel rod diameter, H/U ratio, average neutron group causing fission, ^{10}B loading for flux trap cases, and flux trap gap thickness. The data is plotted in Figures 6.5-9 through 6.5-16.

To evaluate the relative importance of the trend analysis to the upper safety limits, correlation coefficients are required for all independent parameters. Table 6.5-5 contains the correlation coefficient, R , for each linear fit of k_{eff} versus experimental parameter (data is extracted from Figure 6.5-9 through Figure 6.5-16 by taking the square root of the R^2 value). Based on the highest correlation coefficient and the method presented in NUREG/CR-6361, a USL is established based on the variation of k_{eff} with flux trap thickness. Note that even the flux trap function shows a low statistical correlation coefficient (an $|R|$ equal or near 1 would indicate a good fit). The output generated by USLSTATS is shown in Figure 6.5-17.

The NAC applied USL is 0.9426, and bounds the calculated upper safety limits for the typical flux trap spacing found in multi-purpose casks. The parameters of the most reactive fuel are included in Table 6.5-4.

6.6.1 Criticality Evaluation for Site Specific Contents

This section describes fuel assembly characteristics and configurations, or waste configurations, which are unique to specific reactor sites. These site specific content configurations result from conditions that occurred during reactor operations, participation in research and development programs, testing programs intended to improve reactor operations, and from decommissioning activities.

Site specific fuel assembly configurations are either shown to be bounded by the analysis of the standard design basis fuel assembly configuration of the same type (PWR or BWR), or are shown to be acceptable contents by specific evaluation of the configuration.

6.6.1.1 Criticality Evaluation for Maine Yankee Site Specific Spent Fuel

Loading the transport cask with the standard CE 14x14 fuel assembly is shown in Section 6.4 to be less reactive than loading the cask with the most reactive Westinghouse 17x17 OFA criticality design basis spent fuel. This analysis addresses variations in fuel assembly dimensions, variable enrichment, axial zoning patterns, annular axial fuel blankets, removed fuel rods or empty rod positions, fuel rods placed in guide tubes, fuel assemblies with an inserted startup source or other component, consolidated fuel assemblies and damaged fuel or fuel debris. These configurations are not included in the standard fuel analysis, but are present in the site fuel inventory that must be transported.

6.6.1.1.1 Maine Yankee Fuel Criticality Model

The criticality evaluations of the Maine Yankee fuel inventory require the basket cell and basket in cask models described in Section 6.3 and 6.4. The basket cell model is principally employed in the most reactive dimension evaluation for the Maine Yankee intact fuel types. The basket cell model represents an infinite array of fuel tubes separated by one-inch flux traps and neglects the radial neutron leakage of the basket. This will result in k_{eff} values greater than 0.95. The basket cell model is, therefore, only used to determine relative reactivities of the various physical dimensions of the Maine Yankee fuel inventory, not to establish maximum k_{eff} values for the basket loaded with Maine Yankee fuel assemblies. The basket in cask model is used for the evaluation of the remaining fuel configurations. The basket criticality model uses the nominal basket configuration with full moderation under accident conditions, where accident conditions

imply the loss of fuel cladding integrity and flooding of the pellet to cladding gap in all fuel rods. The analyses presented are performed using the UMS® transport cask shield geometry.

Transport Cask Model

The infinite array geometry is used only to determine the most reactive dimensions. The most reactive lattice dimensions determined by the basket cell model are incorporated into the basket in cask model. The Universal Transport Cask geometry is evaluated using the nominal basket configuration with full moderation. The Transport Cask accident event is modeled assuming that the fuel clad gap is flooded, the basket is flooded and the neutron shield material is replaced with water. Evaluating 24 hybrid 14x14 fuel assemblies with the most reactive pellet diameter for the accident condition produces a $k_{eff} + 2\sigma$ of 0.91014. This is less reactive than the accident condition for the transport cask loaded with the Westinghouse 17x17 OFA assemblies ($k_{eff} + 2\sigma$ of 0.9210). Therefore, the Westinghouse 17x17 OFA fuel criticality evaluation is bounding.

6.6.1.1.2 Maine Yankee Intact Spent Fuel

The evaluation of the intact Maine Yankee spent fuel inventory demonstrates that under all conditions the maximum reactivity of the UMS® basket loaded with Maine Yankee fuel assemblies is bounded by the Westinghouse 17x17 OFA evaluation presented in Section 6.4. The intact fuel assembly evaluation includes the determination of maximum reactivity dimensions of the Maine Yankee fuel assemblies, and the reactivity effects of variably enriched assemblies, annular axial end blankets, removed rods, fuel in guide tubes, and consolidated fuel assemblies. Where necessary, loading restrictions are applied to limit the number and location of the basket payload evaluated.

Fuel Assembly Lattice Dimensional Variations

Maine Yankee 14x14 PWR fuel has been provided by Combustion Engineering, Exxon/ANF and Westinghouse. The range of fuel assembly dimensions evaluated for Maine Yankee are shown in Table 6.6.1.1-1.

Most Reactive Fuel Dimensions

Bounding fuel assembly dimensions are determined using the guidelines set in Section 6.4.4 and are reported in Table 6.6.1.1-2. The dimensional perturbations that can increase the reactivity of any undermoderated array of fuel assemblies in a flooded system (including flooding the fuel-clad gap) are:

loading restriction, the Westinghouse 17 x 17 OFA fuel criticality evaluation is bounding.

6.6.1.1.8 Damaged Fuel and Fuel Debris in the Maine Yankee Fuel Can

Damaged fuel assemblies are placed in a Maine Yankee fuel can prior to loading in the basket (see Drawings 412-501 and 412-502). The Maine Yankee fuel can has screened openings in the baseplate and the lid to permit drainage, vacuum drying and inerting of the can. This evaluation conservatively considers 100% of the fuel rods in the fuel can as damaged.

Fuel debris must be loaded in a rod or tube structure that is subsequently loaded into a Maine Yankee fuel can. The mass of fuel debris placed in the rod or tube is restricted to the mass equivalent of a fuel rod of an intact fuel assembly.

The Maine Yankee spent fuel inventory includes fuel assemblies with fuel rods inserted in the guide tubes of the assembly. If the integrity of the cladding of the fuel rods in the guide tubes cannot be ascertained, then those fuel rods are assumed to be damaged.

Damaged Fuel Evaluation

All of the spent fuel classified as damaged and all of the spent fuel not in its original lattice are stored in a Maine Yankee fuel can. This fuel is analyzed using a 100% fuel rod failure assumption. The screened fuel can is designed to preclude the release of pellets and gross particulates into the canister cavity. Evaluation of the canister with four Maine Yankee fuel cans containing CE 14x14 fuel assemblies that have up to 176 damaged fuel rods, or consolidated fuel consisting of up to 289 fuel rods, considers 100% dispersal of the fuel from these rods within the fuel can. The Maine Yankee fuel can is restricted to loading in one of the four corner positions of the basket.

All loose fuel in each analysis is modeled as a homogeneous mixture of fuel and water, of which the volume fractions of the fuel versus the water are varied from 0-100%. By varying the fuel fraction up to 100%, this evaluation addresses fuel masses significantly larger than those available in a standard or consolidated fuel assembly. First, loose fuel from damaged fuel rods within a fuel assembly is evaluated between the remaining rods of the most reactive missing rod array. The results of this analysis, provided in Table 6.6.1.1-9, show a slight decrease in the reactivity of the system. Adding fuel to the already optimized H/U ratio of the bounding missing rod array reduces the reactivity of the system as this effectively returns the system to an undermoderated state. Second, loose fuel is considered above and below the active fuel region of this most reactive missing rod array. This analysis is performed within a finite cask model. The

results of this study, provided in Table 6.6.1-1-10, show that any possible mixture combination of fuel and water above and below the active fuel region and, hence, above and below the BORAL sheet coverage, will not significantly increase the reactivity of the system beyond that of the missing rod array. Loose fuel is also considered to replace all contents of the Maine Yankee fuel can in each four corner fuel tube location. As shown in Table 6.6.1-1-11, the results of this study, which include modeling of the Maine Yankee fuel can, show that any mixture of fuel and water within this cavity will not significantly increase the reactivity of the system beyond that of the missing rod array.

Damaged fuel within the fuel can may also result from a loss of integrity of a consolidated fuel assembly. As described in Section 6.6.1-1-7, the consolidated assembly missing rod study shows that a potentially higher reactivity heterogeneous configuration does not increase the overall reactivity of the system beyond that of loading 24 Westinghouse 17x17 OFA assemblies when this configuration is restricted to the four corner locations. The homogeneous mixture study of loose fuel and water replacing the contents of the Maine Yankee fuel can (in each of the four corner fuel tube locations) considers more fuel than is present in the 289 fuel rod consolidated assembly. This study shows that a homogeneous mixture at an optimal H/U ratio within the fuel can also does not affect the reactivity of the system.

Preferential flooding during the transport cask hypothetical accident flooding could result in different moderator densities existing in the transportable storage canister (canister) cavity and damaged fuel can cavity. To investigate the impact of preferential flooding of the canister and damaged fuel can cavity, various moderator densities were evaluated in the damaged fuel can while retaining a fully flooded canister, and vice versa. As shown in Table 6.6.1-1-12, any reduction in moderator density in either the canister or damaged fuel can will result in reduced system reactivities.

The transport cask loaded with the Westinghouse 17x17 OFA fuel assemblies is subcritical. Therefore, it is inherent that a statistically equivalent, or less reactive, canister loading of four Maine Yankee fuel cans containing assemblies with up to 176 damaged rods, or consolidated assemblies with up to 289 rods and 20 of the most reactive Maine Yankee fuel assemblies is also subcritical. Therefore, assemblies with up to 176 damaged rods and consolidated assemblies with up to 289 rods are allowable contents as long as they are loaded into Maine Yankee damaged fuel cans.

Fuel Debris Evaluation

Prior to loading fuel debris into the screened Maine Yankee fuel can, fuel debris must be placed into a rod type structure. Placing the debris into rods confines the spent nuclear material to a known volume and allows the fuel debris to be treated identically to the damaged fuel for criticality analysis.

Based on the discussion presented in Section 6.6.1.1.1, the maximum k_{∞} of the UMS® canister with fuel debris will be less than 0.95, including associated uncertainty and bias.

6.6.1.1.9 Fuel Assemblies with Start-up Sources or Other Non-Fuel Components Inserted in a Guide Tube

Maine Yankee fuel assemblies are evaluated for criticality safety with components inserted in the center or corner guide tubes of the fuel assembly. These components include start-up sources, Control Element Assembly (CEA) fingertips, and a 24-inch ICI segment. Start-up sources are inserted in the center guide tube. The CEA fingertips and ICI segment must be inserted in a corner guide tube that is closed at the bottom end of the assembly.

Assemblies with Start-up Sources

Maine Yankee has three Pu-Be sources and two Sb-Be sources that will be installed in the center guide tubes of 14x14 assemblies that subsequently must be loaded in one of the four corner fuel positions of the basket. Each source is designed to fit in the center guide tube of an assembly. All five of these start-up sources contain Sb-Be pellets, which are 50% Be by volume. The moderation potential of the beryllium is evaluated to ensure that this material will not increase the reactivity of the system beyond that reported for the accident condition. The antimony (Sb) content is insignificant and is not considered. The start-up source is assumed to remain within the center guide tube for all conditions. The base case infinite height model used for comparison is the bounding Maine Yankee fuel assembly with 24 empty rod positions as reported in Table 6.6.1.1-6. The center guide tube of this model is filled with 50% water and 50% beryllium. The analysis assumes that assemblies with start-up sources are loaded in all four corner fuel positions of the basket. This configuration, resulting in a system reactivity, $k_{\infty} \pm \sigma$ of 0.91085 ± 0.00087 , shows that loading Sb-Be sources or the used Pu-Be sources into the center guide tubes of the assemblies in the four corner locations of the basket does not significantly change the reactivity of the system.

One of the three Pu-Be sources was never irradiated. Analysis of this source is equivalent to assuming that the spent Pu-Be sources are fresh. The unused source consists of two capsules that have a total of 1.4 grams of plutonium. All of this material is conservatively assumed to be in one capsule and is modeled as ^{239}Pu . The diameter of this capsule is 0.270 inch and its length is 9.75 inches. This corresponds to a capsule volume of approximately 9.148 cubic centimeters. Thus, the 1.4 grams of ^{239}Pu occupies ~0.77% of the volume at a density of 19.84 g/cc. This material composition is then conservatively assumed to fill the entire center guide tube, which models considerably more ^{239}Pu than is actually present within the Pu-Be source. The remaining volume of the guide tube is analyzed at various fractions of Be, water and/or void to ensure that any combination of these materials is considered. The results of these analyses, provided in Table 6.6.1.1-13, show that loading a fresh Pu-Be start-up source into the center guide tube of each of the four corner assemblies does not significantly change the reactivity of the system.

Fuel Assemblies with Inserted CEA Fingertips or ICI Segment

Maine Yankee fuel assemblies may have CEA fingertips or an ICI segment inserted in one of the four corner guide tubes of a 14x14 assembly. The ICI segment is approximately 24 inches long. These components do not contain any fissile material or moderating material. Therefore, it is conservative to ignore these components, as they displace moderator when the basket is flooded, reducing reactivity.

6.6.1.1.10 Transport Cask Top End Drop Event

The exposed fuel evaluation performed for the design basis WE 17x17 OFA fuel in Section 6.4.5 bounds that of the less reactive Maine Yankee fuel.

6.6.1.1.11 Maine Yankee Criticality Results and Fuel Loading Restrictions

The criticality analyses for the Maine Yankee site specific fuel demonstrates that the UMS® basket loaded with these fuel assemblies results in a system that is less reactive than loading the basket with the Westinghouse 17 x 17 OFA fuel assemblies, provided that loading is restricted to the four corner fuel tube positions in the basket for

- All 14 x 14 fuel assemblies with less than 176 fuel rods or solid filler rods
- All 14 x 14 fuel assemblies with hollow rods
- All 17 x 17 consolidated fuel lattices
- All 14 x 14 fuel assemblies with fuel rods in the guide tubes and a maximum of 176 fuel rods or solid rods and fuel rods

The following Maine Yankee fuels are not restricted as to loading position within the basket:

- All 14x14 fuel assemblies with 176 fuel rods or solid filler rods at a maximum enrichment of 4.2 wt % ^{235}U
- Variably enriched fuel with a maximum fuel rod enrichment of 4.21 wt % ^{235}U with a maximum planar average enrichment of 3.99 wt % ^{235}U
- Fuel with solid stainless steel filler rods, solid Zircaloy filler rods or solid poison shim rods in any location
- Fuel with annular axial end blankets of up to 4.2 wt % ^{235}U
- Fuel with a maximum of 2 intact fuel rods in each guide tube for a total of 186 fuel rods

Assemblies defined as unrestricted may be loaded into the basket in any basket location and may be mixed in the same basket. While not analyzed in detail, CEAs and ICI thimble assemblies may be loaded into any intact assemblies. The CEA fingertips and ICI segment may be loaded in the corner guide posts of any intact fuel assembly provided that a CEA flow plug is also installed in the fuel assembly to close the top of the guide tubes. The basket loading position of these assemblies is not restricted. These components displace a significant amount of water in the fuel lattice while adding parasitic absorber, thereby reducing system reactivity.

Based on the evaluation of Maine Yankee fuel assemblies with start-up sources, the following loading restrictions for criticality control apply:

- Any Maine Yankee fuel assembly having a component evaluated in this section inserted in a guide tube must be loaded in one of the four corner fuel loading positions of the basket. Corner positions are also peripheral positions and are marked "P" in the figure in Section 1.3.1.1.1
- Start-up sources containing plutonium or beryllium shall be restricted to loading in fuel assemblies classified as intact and must be loaded in a center guide tube
- Only one start-up source may be loaded into any intact fuel assembly
- Up to four intact fuel assemblies with inserted start-up sources may be loaded in any canister using the corner positions of the basket

When loaded in accordance with these restrictions, the evaluated components do not significantly increase the reactivity of the system

Figure 6.6.1.1-1

24 Removed Fuel Rods - Diamond Shaped Geometry, Maine Yankee Site
Specific Fuel

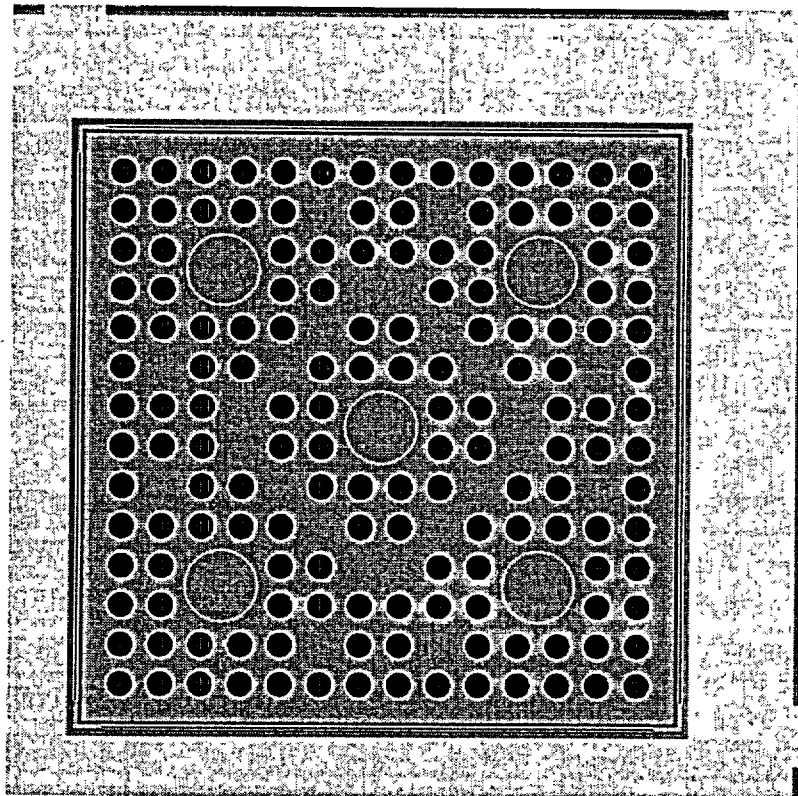


Figure 6.6.1.1-2 Consolidated Fuel Geometry, 113 Empty Fuel Rod Positions, Maine Yankee Site Specific Fuel

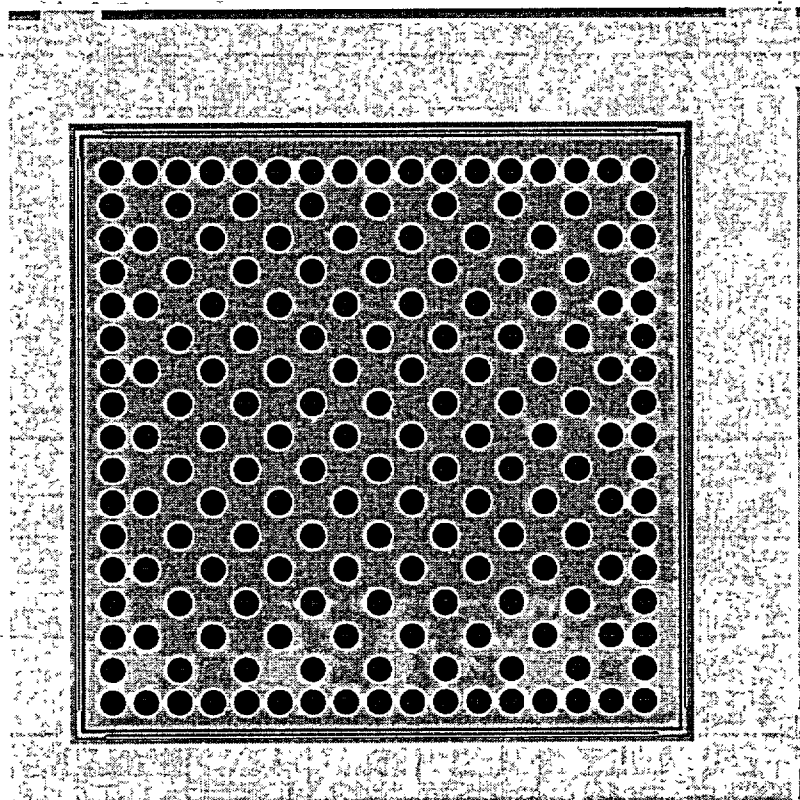


Table 6.6.1.1-1 Maine Yankee Standard Fuel Characteristics

Fuel Class	Vendor	Array	Version	Number of Fuel Rods	Pitch (in.)	Rod Diameter (in.)	Clad ID (in.)	Clad Thickness (in.)	Pellet Diameter (in.)	GT Thickness (in.)
1	CE	14x14	Std	160-176	0.570-0.590	0.438-0.442	0.3825-0.3895	0.024-0.028	0.376-0.380	0.036-0.040
1	EX/ANF	14x14	CE	164-176	0.580	0.438-0.442	0.3715-0.3795	0.0294-0.031	0.3695-0.3705	0.036-0.040
1	WE	14x14	CE	176	0.575-0.585	0.438-0.442	0.3825-0.3855	0.0262-0.028	0.376-0.377	0.034-0.038

1. All fuel rods are Zircaloy clad

2. Guide Tube thickness

3. Up to 16 fuel rod positions may have solid filler rods or burnable poison rods

4. Up to 12 fuel rod positions may have solid filler rods or burnable poison rods

Table 6.6.1.1-2 Maine Yankee Most Reactive Fuel Dimensions

Parameter	Bounding Dimensional Value
Maximum Rod Enrichment	4.2 wt % ²³⁵ U
Maximum Number of Fuel Rods	176
Maximum Pitch (in.)	0.590
Maximum Active Length (in.)	N/A - Infinite Mode
Minimum Clad OD (in.)	0.4375
Maximum Clad ID (in.)	0.3895
Minimum Clad Thickness (in.)	0.024
Maximum Pellet Diameter (in.)	0.3800 - Study
Minimum Guide Tube OD (in.)	1.108
Maximum Guide Tube ID (in.)	1.040
Minimum Guide Tube Thickness (in.)	0.034

1. Variably enriched fuel assemblies may have a maximum fuel rod enrichment of 4.2 wt % ²³⁵U with a maximum planar average enrichment of 3.99 wt % ²³⁵U
2. Assemblies with less than 176 fuel rods or solid dummy rods are addressed after the determination of the most reactive dimensions

Table 6.6.1-3

Maine Yankee Pellet Diameter Study

Diameter (inches)	k-eff	σ	k-eff + 2 σ
0.3800	0.95585	0.00085	0.95755
0.3779	0.95784	0.00080	0.95944
0.3758	0.95714	0.00085	0.95884
0.3737	0.95863	0.00082	0.96027
0.3716	0.95862	0.00084	0.96030
0.3695	0.95855	0.00083	0.96021
0.3674	0.95863	0.00085	0.96033
0.3653	0.95982	0.00084	0.96150
0.3632	0.95854	0.00088	0.96030
0.3611	0.95966	0.00083	0.96132
0.3590	0.95990	0.00084	0.96158
0.3569	0.96082	0.00082	0.96246
0.3548	0.96053	0.00083	0.96219
0.3527	0.96104	0.00082	0.96268
0.3506	0.95964	0.00087	0.96138
0.3485	0.95993	0.00086	0.96165
0.3464	0.95916	0.00084	0.96084
0.3443	0.95847	0.00083	0.96013
0.3422	0.95876	0.00083	0.96042
0.3401	0.95865	0.00081	0.96027
0.3380	0.95734	0.00084	0.95902

Table 6.6.1-4

Maine Yankee Annular Fuel Results

Case Description	k-eff	σ	k-eff + 2 σ
All pellets with a diameter of 0.3527 inches	0.90896	0.00083	0.91061
Annular pellet diameter changed to 0.3800 inches	0.91013	0.00087	0.91187

Table 6.6.1-1-5 Maine Yankee Removed Rod Results with Small Pellet Diameter

Number of Removed Rods	Number of Fuel Rods	k_{eff}	Δk_{eff}	$k_{eff} + 2\sigma$
4	172	0.91171	0.00088	0.91347
4	172	0.91292	0.00086	0.91464
4	172	0.91479	0.00081	0.91640
4	172	0.91125	0.00087	0.91299
6	170	0.91418	0.00087	0.91592
6	170	0.91264	0.00085	0.91435
6	170	0.91314	0.00086	0.91487
6	170	0.90322	0.00086	0.90493
8	168	0.91555	0.00087	0.91729
8	168	0.91490	0.00093	0.91676
8	168	0.91457	0.00088	0.91633
8	168	0.91590	0.00087	0.91764
8	168	0.89729	0.00088	0.89905
12	164	0.91654	0.00086	0.91827
12	164	0.91469	0.00085	0.91639
12	164	0.91149	0.00083	0.91315
16	160	0.91725	0.00084	0.91893
16	160	0.91567	0.00084	0.91735
16	160	0.90986	0.00088	0.91162
16	160	0.90849	0.00083	0.91015
16	160	0.90704	0.00086	0.90876
24	152	0.91572	0.00083	0.91739
32	144	0.91037	0.00088	0.91213
48	128	0.89385	0.00085	0.89554
48	128	0.84727	0.00079	0.84886
64	112	0.79602	0.00083	0.79768
96	80	0.69249	0.00077	0.69402
Westinghouse 17x17 OFA		0.9192	0.0009	0.9210

Table 6.6.1.1-6
 Maine Yankee Removed Fuel Rod Results with Maximum Pellet Diameter

Number of Removed Rods	Number of Fuel Rods	Count	Count	Count
1	172	0.91078	0.00086	0.91250
1	172	0.90916	0.00085	0.91085
1	172	0.91164	0.00087	0.91338
1	172	0.90809	0.00085	0.90979
1	170	0.91223	0.00085	0.91393
1	170	0.91223	0.00080	0.91384
1	170	0.91270	0.00086	0.91442
1	170	0.90245	0.00086	0.90416
1	170	0.89801	0.00086	0.89972
1	168	0.91567	0.00085	0.91736
1	168	0.91448	0.00085	0.91618
1	168	0.91355	0.00086	0.91526
1	168	0.91293	0.00085	0.91463
1	164	0.91639	0.00090	0.91818
1	164	0.91803	0.00086	0.91974
1	164	0.91235	0.00083	0.91401
1	160	0.91663	0.00091	0.91847
1	160	0.92136	0.00087	0.92310
1	160	0.91231	0.00084	0.91400
1	160	0.90883	0.00087	0.91057
1	152	0.92227	0.00087	0.92400
1	144	0.92164	0.00088	0.92340
1	128	0.91212	0.00081	0.91373
1	128	0.86308	0.00082	0.86472
1	112	0.81978	0.00080	0.82138
1	88	0.72087	0.00083	0.72247
24 (Four Corners)	152	0.91153	0.00085	0.91323
Westinghouse 17x17 OFA	0.9192	0.0009	0.9210	

Table 6.6.1-1-7 Maine Yankee Fuel Rods in Guide Tubes Results

Number of Guide Tubes with Rods	Number of Rods in Each	k_{eff}	β	$k_{eff} + 2\sigma$
1	1	0.91102	0.00089	0.91280
2	1	0.91059	0.00088	0.91234
3	1	0.91172	0.00087	0.91346
5	1	0.91411	0.00086	0.91583
1	2	0.91169	0.00090	0.91349
2	2	0.91201	0.00087	0.91375
3	2	0.91173	0.00086	0.91344
5	2	0.91357	0.00086	0.91529
Design Basis Westinghouse 17x17 OFA		0.9192	0.0009	0.9210

Table 6.6.1-1-8 Maine Yankee Consolidated Fuel Empty Fuel Rod Position Results

Number of Empty Positions	Number of Fuel Rods	k _{eff}	k _{eff}	k _{eff} ± 2σ
4	285	0.79684	0.00082	0.79848
9	280	0.80455	0.00081	0.80616
9	280	0.80812	0.00079	0.80970
13	276	0.81573	0.00083	0.81739
24	265	0.84187	0.00080	0.84347
25	264	0.84017	0.00083	0.84182
25	264	0.84634	0.00081	0.84795
25	264	0.84583	0.00083	0.84750
25	264	0.85524	0.00083	0.85690
25	264	0.83396	0.00081	0.83558
25	264	0.84625	0.00083	0.84790
27	262	0.85438	0.00083	0.85604
29	260	0.85179	0.00081	0.85340
31	258	0.85930	0.00084	0.86098
33	256	0.86407	0.00082	0.86571
35	254	0.86740	0.00082	0.86904
37	252	0.87372	0.00084	0.87541
45	244	0.88630	0.00081	0.88793
45	244	0.87687	0.00079	0.87844
52	237	0.90062	0.00083	0.90228
57	232	0.87975	0.00087	0.88149
61	258	0.89055	0.00083	0.89221
73	216	0.90967	0.00082	0.91131
84	205	0.93261	0.00091	0.93443
85	204	0.94326	0.00086	0.94499
113	176	0.95626	0.00084	0.95794
117	172	0.95373	0.00088	0.95549
119	170	0.95315	0.00085	0.95485
125	164	0.95020	0.00086	0.95192
141	148	0.94348	0.00086	0.94521
145	144	0.93868	0.00089	0.94047
113 (Four Corners)	176	0.91292	0.00087	0.91466
Design Basis Westinghouse 17x17 OFA		0.9192	0.0009	0.9210

Table 6.6.1.1-9 Fuel Can Infinite Height Model Results of Fuel - Water Mixture

Between Rods

Volume Fraction of UO_2 in Water	K _{eff}	Alt. to 2 ₄ (Hour Count)
0.000	0.91090	0.00063
0.001	0.91138	0.00015
0.002	0.91120	0.00033
0.003	0.91177	0.00024
0.004	0.91283	0.00132
0.005	0.90908	0.00245
0.006	0.91001	0.00152
0.007	0.90893	0.00258
0.008	0.91003	0.00148
0.009	0.90986	0.00167
0.010	0.90864	0.00289
0.020	0.91003	0.00150
0.030	0.90963	0.00190
0.040	0.91063	0.00090
0.050	0.90931	0.00222
0.060	0.90763	0.00388
0.070	0.90753	0.00400
0.080	0.91088	0.00065
0.090	0.91122	0.00031
0.100	0.90879	0.00274
0.150	0.90968	0.00185
0.200	0.90952	0.00201
0.250	0.90813	0.00338
0.300	0.90748	0.00403
0.350	0.90581	0.00572
0.400	0.90963	0.00190
0.450	0.90547	0.00606
0.500	0.90603	0.00550
0.550	0.90753	0.00400
0.600	0.90674	0.00479
0.650	0.90589	0.00564
0.700	0.90594	0.00559
0.750	0.90568	0.00583
0.800	0.90532	0.00621
0.850	0.90693	0.00460
0.900	0.90639	0.00514
0.950	0.90684	0.00469
1.000	0.90677	0.00476

See Table 6.6.1.1-6

6.6.1-20

Table 6.6.1.1-10 Fuel Can Finite Model Results of Fuel - Water Mixture Outside BORAL Coverage

Volume Fraction of UO₂ in Water	k_{eff}	Δk_{eff} to 0.00 UO₂ in Water	Δk_{eff} to 24 (Four Corners)
0.00	0.910452	NA	0.00108
0.05	0.90781	0.00264	0.00372
0.10	0.90978	0.00067	0.00175
0.15	0.91048	0.00003	0.00105
0.20	0.90916	0.00129	0.00237
0.25	0.90834	0.00211	0.00319
0.30	0.90935	0.00110	0.00218
0.35	0.90786	0.00259	0.00367
0.40	0.90892	0.00153	0.00261
0.45	0.91015	0.00030	0.00138
0.50	0.91011	0.00034	0.00142
0.55	0.91003	0.00042	0.00150
0.60	0.90874	0.00171	0.00279
0.65	0.91165	0.00120	0.00012
0.70	0.90977	0.00068	0.00176
0.75	0.90813	0.00232	0.00340
0.80	0.90909	0.00136	0.00244
0.85	0.91028	0.00017	0.00125
0.90	0.91061	0.00016	0.00092
0.95	0.91129	0.00084	0.00024
1.00	0.91076	0.00031	0.00077

1 See Table 6.6.1.1-6

2 $\sigma = 0.00084$

Table 6.6.1-1-1 Fuel Can Finite Model Results of Replacing All Rods with Fuel - Water Mixture

Volume Fraction of UO ₂ in Water	k_{eff}	Δk_{eff} to 24 (Four Corners) Finite Height Model	Δk_{eff} to 24 (Four Corners) Infinite Height Model
0	0.90071	-0.00974	-0.01082
5	0.90194	-0.00851	-0.00959
10	0.90584	-0.00461	-0.00569
15	0.90837	-0.00208	-0.00316
20	0.91008	-0.00037	-0.00145
25	0.91086	0.00041	-0.00067
30	0.90964	-0.00081	-0.00189
35	0.90828	-0.00217	-0.00325
40	0.90805	-0.00240	-0.00348
45	0.90730	-0.00315	-0.00423
50	0.90637	-0.00408	-0.00516
55	0.90672	-0.00373	-0.00481
60	0.90649	-0.00396	-0.00504
65	0.90632	-0.00413	-0.00521
70	0.90435	-0.00610	-0.00718
75	0.90792	-0.00253	-0.00361
80	0.90376	-0.00669	-0.00777
85	0.90528	-0.00517	-0.00625
90	0.90454	-0.00591	-0.00699
95	0.90360	-0.00685	-0.00793
100	0.90416	-0.00629	-0.00737

1. The k_{eff} comparison basis for this column is the finite height model with the four corner locations of the basket loaded with Maine Yankee assemblies in the most reactive missing rod geometry. This case is the first case presented in Table 6.6.1-1-10 with 0% UO₂ in the water above and below the active fuel of the missing rod array.

2. The k_{eff} comparison basis for this column is the infinite height model with the four corner locations of the basket loaded with Maine Yankee assemblies in the most reactive missing rod geometry, the first case presented in Table 6.6.1-1-6 labeled "24 (Four Corners)," $k_{eff} = 0.91153$.

Table 6.6-11-12

Maine Damaged Fuel Can Preferential Flooding Evaluation

Canister H ₂ O Density (g/cm ³)	Can H ₂ O Density (g/cm ³)	K _{eff}	ΔK _{eff}
1.0	1.0	0.910864	NA
1.0	0.0	0.90257	-0.00829
1.0	0.1	0.90193	-0.00893
1.0	0.2	0.90413	-0.00673
1.0	0.3	0.90335	-0.00751
1.0	0.4	0.90355	-0.00731
1.0	0.5	0.90323	-0.00763
1.0	0.6	0.90638	-0.00448
1.0	0.7	0.90500	-0.00586
1.0	0.8	0.90881	-0.00205
1.0	0.9	0.90668	-0.00418
1.0	1.0	0.87518	-0.03568
0.1	1.0	0.85137	-0.05949
0.2	1.0	0.84234	-0.06852
0.3	1.0	0.84145	-0.06941
0.4	1.0	0.84220	-0.06866
0.5	1.0	0.84550	-0.06536
0.6	1.0	0.84947	-0.06139
0.7	1.0	0.85834	-0.05252
0.8	1.0	0.87003	-0.04083
0.9	1.0	0.88926	-0.02160

1) Base case for comparison is the maximum reactivity case for the damaged fuel can documented in Table 6.6-11-11 (25% UO₂)

Table 6.6.1-1-13

Infinite Height Analysis of Maine Yankee Start-up Sources

Pu Vf	Be Vf	H2O Vf	Void Vf	k _{eff}	sd	k _{eff} 2sd	Δk _{eff}
0	0.9	0.9	0	0.91085	0.00087	0.91259	0.00068
0.00771371	0.99228629	0	0	0.91034	0.00089	0.91212	0.00119
0.00771371	0.9	0.09228629	0	0.91151	0.00087	0.91325	0.00002
0.00771371	0.8	0.19228629	0	0.91138	0.00087	0.91312	0.00015
0.00771371	0.7	0.29228629	0	0.91042	0.00085	0.91212	0.00111
0.00771371	0.6	0.39228629	0	0.91231	0.00086	0.91403	0.00078
0.00771371	0.5	0.49228629	0	0.90922	0.00083	0.91088	0.00231
0.00771371	0.4	0.59228629	0	0.91192	0.00087	0.91371	0.00044
0.00771371	0.3	0.69228629	0	0.91203	0.00086	0.91375	0.00050
0.00771371	0.2	0.79228629	0	0.90922	0.00084	0.91090	0.00231
0.00771371	0.1	0.89228629	0	0.91140	0.00085	0.91310	0.00013
0.00771371	0	0.99228629	0	0.91149	0.00086	0.91321	0.00004
0.00771371	0.9	0	0.09228629	0.91075	0.00087	0.91249	0.00078
0.00771371	0.8	0	0.19228629	0.91143	0.00091	0.91325	0.00010
0.00771371	0.7	0	0.29228629	0.91182	0.00086	0.91354	0.00029
0.00771371	0.6	0	0.39228629	0.91072	0.00082	0.91236	0.00081
0.00771371	0.5	0	0.49228629	0.90984	0.00085	0.91154	0.00169
0.00771371	0.4	0	0.59228629	0.90982	0.00091	0.91164	0.00171
0.00771371	0.3	0	0.69228629	0.91053	0.00087	0.91229	0.00098
0.00771371	0.2	0	0.79228629	0.91054	0.00085	0.91224	0.00099
0.00771371	0.1	0	0.89228629	0.91006	0.00088	0.91182	0.00147
0.00771371	0	0	0.99228629	0.90957	0.00086	0.91129	0.00196

* Change in reactivity from case "24 (Four Corners)" in Table 6.6.1-1-6

Chapter 7

2. Detorque and remove the vent coverplate bolts.

3. Remove the vent port coverplate from the lid.

Note: The drain port coverplate need not be removed for dry loading or unloading.

4. Visually inspect the port coverplate o-rings for damage or defects and replace if necessary. Store the coverplate so that the o-rings and o-ring grooves are protected from incidental damage.

5. Detorque the cask lid bolts using the reverse torquing sequence.

6. Remove the bolts and store them in a temporary storage area.

7. Clean and visually inspect bolts for damage. Replace any damaged bolts.

8. Install the two cask lid alignment pins.

9. Install lifting hoist rings in the lid-lifting holes.

10. Attach the lid-lifting device to the lid and an overhead crane.

Caution: Ensure that the o-rings and o-ring grooves in the lid are protected from any incidental damage to the seal area in its temporary storage position.

11. Remove the lid and store in a temporary storage area.

12. Decontaminate the lid and visually inspect the lid o-rings for damage and wear and replace as necessary.

Note: Visually inspecting and cleaning of bolts can be performed in parallel to other operations performed in this procedure.

13. Clean and visually inspect the threaded connections in the top forging.

14. Remove the two cask lid alignment pins.

15. Visually examine the internal cavity to ensure that no damage has occurred during transit and that no foreign materials are present.

16. Record all inspection results.

17. Install the cask adapter ring to protect the cask sealing surfaces.

18. If a canister spacer is to be installed:

a) Attach the spacer lift fixture to the spacer.

b) Using an appropriate crane, lower the spacer into the cask cavity and remove the lift fixture.

19. Install the transfer cask adapter plate guide pins.



20. Install the adapter plate on top of the cask.


21. Remove the adapter plate guide pins.

22. Install the transfer cask on the adapter plate.




7.1.3 Loading Transportable Storage Canister into Universal Transport Cask

A transfer cask is used to load the Transportable Storage Canister  into the Universal Transport Cask at the spent fuel building or at the ISFSI loading area. The assumptions underlying this procedure are .

- The canister is already loaded with fuel that meets the cool times shown in Tables 1.2-6 and 1.2-7 for PWR and BWR fuel, respectively, or GTCC waste that has a minimum five-year cool time from March 1998. Contents must be in accordance with the transport Certificate of Compliance (71-9270).
- The canister is seal welded, vacuum dried, and helium backfilled.
- The canister is located in a transfer cask. (The procedures for closing the canister following fuel loading, and for draining, sealing, drying, inerting, and leak testing the canister and installing hoist rings are provided in Section 7.5 of the UMS® Storage System FSAR.)
- All of the required steps of Section 7.1.2 are complete, including adapter plate and bottom spacer installation (if necessary).
- 
- The Universal Transport Cask is positioned in the designated area in the spent fuel building or at the ISFSI with the cask lid off.

The movement and operation of the transfer cask with a loaded canister prior to inserting the canister into the Universal Transport Cask are part of in-plant operations and preparation for storage. Steps for these operations are therefore not included in the following procedures.



1. Verify that the retaining ring is installed on the transfer cask.
2. Lift the transfer cask and lower it on top of the adapter plate on the transport cask and engage the hydraulic cylinders with the doors.
3. Engage the transportable storage canister lifting sling's master ring with the crane hook and engage the individual sling hooks with their respective hoist rings located on the structural lid of the transportable storage canister. 
4. Raise the canister enough to remove the load on the Transfer Cask doors and then open the doors.

CAUTION: While lowering the canister in Step 5, be careful to avoid contact with the interior cavity wall of the Universal Transport Cask.

5. Lower the canister into the Universal Transport Cask.
6. Disengage the lift sling hooks from the hoist rings and close the Transfer Cask doors.
7. Remove the Transfer Cask and store it in the designated location.
8. Remove the hoist rings from the top of the canister structural lid and install threaded plugs.
9. Attach the adapter plate lifting sling to the adapter plate.
10. Remove the four bolts attaching the adapter plate to the Universal Transport Cask.
11. Remove the adapter plate and store it in the designated location.
12. Remove the cask adapter ring and clean the sealing surface.
- 13.
14. Install the cask lid alignment pins.
15. Attach the lid-lifting device to the lid and to the overhead crane.
16. Install the lid, using the alignment pins to assist in proper seating.
17. Install 10 cask lid bolts equally spaced and torque hand-tight.
18. Remove the lid alignment pins.
19. Install the remaining cask lid bolts and torque all of the bolts to the value specified in Table 7-1.
20. If previously removed, re-install the drain port coverplate.
21. Connect a pressure test fixture to the drain port coverplate o-ring test port and pressurize to 15 (+2, -0) psig and hold for a minimum of 10 minutes. There must be no pressure drop in the test period.
Note: If the test condition is not met, remove the drain port coverplate and inspect and clean the o-rings and o-ring sealing surfaces and re-perform the test. If the test condition is not met on the second attempt, replace the o-rings, cleaning the o-ring grooves and sealing surface. A small amount of vacuum grease may be used to lubricate new o-rings.
Caution: If the drain port o-rings are replaced as a result of the inspection, then a helium leak test of the new o-rings must be performed at Step 29. Using a helium leak detector with a sensitivity of 3.25×10^{-9} cm³/sec, establish a vacuum in the o-ring annulus and test for helium leakage. The leak rate must be less than 6.5×10^{-6} cm³/sec (helium) in accordance with Table 7-2.
22. Connect the Vacuum Drying System vacuum pump to the cask vent port and evacuate the cask cavity to a stable vacuum pressure of 3 mm Hg for 10 minutes.
23. Backfill the cask with high purity helium (99.9% minimum) to 1 atm (absolute) pressure.
24. Operate the vacuum system to obtain a vacuum pressure of 3 mm Hg. When the vacuum pressure is obtained, backfill the cask with high purity helium (99.9% minimum) to 1 atm (absolute) pressure.
25. Disconnect the vacuum system and helium supply.

26. Install the vent port coverplate and torque the bolts as specified in Table 7-1
27. Connect a pressure test fixture to the lid o-ring test port (marked "Seal Test" on cask lid) and pressurize to 15 (+2, -0) psig and hold for a minimum of 15 minutes. There must be no pressure drop in the test period
Note: If the test condition is not met, replace the o-rings, cleaning the o-ring grooves and sealing surface. A small amount of vacuum grease may be used to lubricate new o-rings
Caution: If the lid o-rings are replaced as a result of the inspection in Step 12 of Section 7.1.2, then a helium leak test of the new o-rings must be performed. Using a helium leak detector with a sensitivity of 3.25×10^{-9} cm³/sec, establish a vacuum in the o-ring annulus and test for helium leakage. The leak rate must be less than 6.5×10^{-9} cm³/sec in accordance with Table 7-2
28. Install the plug in the lid Seal Test port, verifying that the test plug o-ring is in place, and torque the plug to the value specified in Table 7-1
29. Connect a pressure test fixture to the vent coverplate o-ring test port and pressurize to 15 (+2, -0) psig and hold for a minimum of 10 minutes. There must be no pressure drop in the test period
Note: If the test condition is not met, remove the vent port coverplate and inspect and clean the o-rings and o-ring sealing surfaces and re-perform the test. If the test condition is not met on the second attempt, replace the o-rings, cleaning the o-ring grooves and sealing surface. A small amount of vacuum grease may be used to lubricate new o-rings
Caution: If the vent and/or drain port o-rings are replaced as a result of the inspection, then a helium leak test of the new o-rings must be performed. Using a helium leak detector with a sensitivity of 3.25×10^{-9} cm³/sec, establish a vacuum in the o-ring annulus and test for helium leakage. The leak rate must be less than 6.5×10^{-9} cm³/sec in accordance with Table 7-2
30. Install the vent port o-ring test plug, verifying that the test plug o-ring is in place and torque the test plug to the value specified in Table 7-1
31. Perform external decontamination activities and radiation surveys to verify that contamination is within acceptable levels (2,200 dpm/100 cm² B, γ, and 220 dpm/100 cm² α) as identified in 10 CFR 71.87 [2]

7.2 Preparing Universal Transport Cask for Transport Following Loading

The assumptions underlying this procedure are as follows:

- The Universal Transport Cask has been loaded and decontaminated.
- The containment boundary has been leak tested.
- The cask is in the vertical position ready for loading on the transport vehicle.

The cask is not intended to remain in the vertical orientation for an extended period. The cask should be rotated to the transport orientation within 25 days of closing the cask.

If redundant lifting must be used to move the cask prior to cask placement on the transport vehicle, the redundant lifting yoke system must be installed on the crane, and the bolt torque of the secondary trunnions must be verified to meet the requirement in Table 7-1. The cask cannot be installed on the transport vehicle using the redundant lifting system.

The procedures for preparing the cask for transport following loading are as follows:

1. Attach the cask lifting yoke to a crane hook with the appropriate load rating.
2. Engage the yoke with the primary (welded) lifting trunnions on the cask.
Note: Verify engagement with primary trunnions ☒ prior to lifting.
3. Lift and move the cask over the transport vehicle so that the rotation pockets are aligned with the rear supports on the transport vehicle.
4. Load the cask onto the transport vehicle by gently lowering the cask until the rear support is fully engaged in the cask rotation pockets.
5. Rotate the cask to the horizontal position by moving the overhead crane in the direction of the front support while keeping the crane cables vertically aligned over the lifting yoke.
6. Using a lifting sling, place the tiedown assembly over the cask upper forging between the neutron shield top plate and the lifting trunnions.
7. Install the front tiedown pins and retaining pins to each side of the front support.
8. Install the lower impact limiter positioner.
9. Perform a contamination survey of the cask and document the results to ensure compliance with 49 CFR 173.443 [3].
10. Using the designated lifting slings and a crane of appropriate capacity, install the upper impact limiter.
11. Install and torque the impact limiter retaining rods ☒.


12. Install and torque the impact limiter attachment nuts and the impact limiter jam nuts to the torque values specified in Table 7-1.
13. Install the impact limiter lock wires.
14. Repeat Steps 10 through 13 for the lower impact limiter.
15. Install tamper indicating seals through holes provided in the upper impact limiter and one of the lifting trunnions.
16. Install tamper indicating seals through holes provided in the lower impact limiter and on the shipping frame assembly.
17. Record the serial number of the seals in the cask-loading checklist.
18. Apply labels to the cask in accordance with 49 CFR 172.200 [6].
19. Install the personnel protection barrier and torque all attachment bolts to the torque values specified in Table 7-1.
20. Install padlocks on any personnel barrier access portal.
21. Perform a radiation survey of the cask and document the results to ensure compliance with 49 CFR 173.441 [3].
22. Perform a contamination survey of the transport vehicle and document results to ensure compliance with 49 CFR 173.443 [3].
23. Complete all shipping documentation in accordance with 49 CFR 172 Subchapter C [6].
24. Apply placards to the transport vehicle in accordance with 49 CFR 172.500 [6].
25. Provide special instruction for Exclusive Use Shipment to the carrier.

8. Remove the threaded plugs and attach the lifting eyes in the cask lid.
9. Attach the lid-lifting device to the cask lid and to the overhead crane.
10. Remove the cask lid and place the lid in a designated area.
11. Ensure that the O-ring grooves in the lid are protected so that they will not be damaged during handling.
12. Decontaminate the lid as necessary.
13. Remove the two alignment pins.
14. Install the cask adapter ring to protect the sealing surfaces of the cask.
15. Install the adapter plate guide pins.
16. Install the transfer cask adapter plate to protect the sealing surfaces of the transport cask and to provide a seating surface for the Transfer Cask.
17. Install **the four** adapter plate bolts.
18. Install the transfer cask alignment pins in the adapter plate.

7.3.3 Unloading Transportable Storage Canister from Universal Transport Cask

A transfer cask is used to unload the Transportable Storage Canister. The transfer cask could be used to transfer the loaded canister to the spent fuel building for subsequent storage in the spent fuel pool or to transfer it to another storage or disposal overpack. Prior to beginning operation of the transfer cask doors and the hydraulic system should be checked. The transfer cask retaining ring should be installed.

1. Remove threaded plugs from structural lid.
2. Install the swivel hoist rings in the canister structural lid.
CAUTION: The structural lid may be thermally hot.
3. Install the transport cask adapter ring to protect the sealing surfaces of the transport cask.
4. Install the transfer cask adapter plate on the transport cask.
5. Attach the canister lifting sling to the hoist rings in the structural lid. Position the sling so that the free end of the sling can be engaged by the cask-handling crane hook.
6. Attach the transfer cask lifting yoke to the cask-handling crane hook.
7. Engage the yoke to the lifting trunnions of the transfer cask.
8. Lift the transfer cask and move it above the Universal Transport Cask.
9. Lower the transfer cask to engage the alignment pins of the transfer cask adapter plate.
10. Once the transfer cask is fully seated, remove the transfer cask lifting yoke and store it in the designated location.

11. Install the transfer cask bottom door hydraulic operating system.
12. Open the transfer cask bottom doors.
13. Lower the cask-handling crane hook through the transfer cask and engage the canister lifting sling.
CAUTION: When raising the canister in Step 14, be careful to minimize any contact between the canister and the cavity wall of the Universal Transport Cask and between the canister and the cavity wall of the transfer cask.
14. Raise the canister into the transfer cask just far enough to allow the transfer cask bottom doors to close.
15. Close the transfer cask bottom doors and install the door locking pins.
16. Carefully lower the canister until it rests on the transfer cask bottom doors.
17. Disengage the canister lifting sling from the crane hook.
18. Retrieve the transfer cask lifting yoke and engage it with the transfer cask trunnions.
19. Lift the transfer cask from the transport cask and move it to the designated location.
20.  Attach the adapter plate lifting fixture.
21. Remove the four bolts securing the adapter plate to the Universal Transport Cask.
22. Using the auxiliary crane, lift the adapter plate from the top of the cask and move the adapter plate to the designated storage location.
23. Remove cask adapter ring.
24. Install the vent port coverplate over the vent port in the cask lid.
25. Install/torque the coverplate bolts to the values specified in Table 7-1.
26. Install the cask lid alignment pins.
27. With the lid-lifting device, install the cask lid by using the alignment pins to assist in proper seating.
28. Remove the lid-lifting device, lid lift hoist rings, and the lid alignment pins.
29. Install the lid bolts and torque them to the value specified in Table 7-1.
30. Using a pressure test fixture, pressurize the o-ring annulus of the cask lid to 15 psig and hold for 15 minutes. There should be no loss of pressure during the test period.
31. Install the plug in the Seal Test port, verifying that the test plug o-ring is in place, and torque the plug to the value specified in Table 7-1.
32. Using a pressure test fixture, pressurize the vent coverplate o-ring annulus to 15 psig and hold for 10 minutes. There should be no loss of pressure during the test period.
33. Install the plug in the seal test port, verifying that the test plug o-ring is in place, and torque the plug to the value specified in Table 7-1.
34. Repeat Steps 32 and 33 for the drain port, if the drain port was used.

Chapter 8

8.1.2.2 Rotation Pocket Load Testing

There are two rotation pockets, located on opposite sides of the bottom of the cask, which are simultaneously load tested prior to cask acceptance. The rotation pockets are designed and analyzed to satisfy the more restrictive of 10 CFR 71.45(b) [1] or AAR Field Manual [8] load conditions for nuclear waste transport. The rotation pockets are not used to lift the cask at any time. During intermodal transport, the loaded cask with the top and bottom impact limiters attached, the cask is horizontally mounted on a tiedown structure/personnel barrier. The tiedown structure is designed with four pick-up points specifically for moving the loaded cask. The rotation pocket recesses at the lower end of the cask shall be load tested. The load test shall be performed in accordance with approved written procedures.

The load test for recesses shall consist of applying a vertical load of 390,000 lb, $\pm 5/-0$ percent, to the rotation pocket pair. The load will be applied in a vertical direction and equally distributed between the two rotation trunnion recesses by the use of hydraulic rams combined with a load spreading beam.

Following completion of the rotation pocket load test, all trunnion recess welds and load bearing surfaces shall be visually inspected for permanent deformation, galling or cracking. Inspections utilizing liquid penetrant examination shall be performed in accordance with the "ASME Boiler and Pressure Vessel Code," Section V, Article 6 [3]. Liquid penetrant acceptance standards shall be as indicated in paragraph NF-5350 of the "ASME Boiler and Pressure Vessel Code," Section III, Division 1 [9].

Any evidence of permanent deformation, cracking, galling of the load bearing surfaces or unacceptable dye penetrant results shall be cause for rejection of the rotation pocket recesses or related welds.

8.1.2.3 Hydrostatic Pressure Testing of the Containment Boundary

The Universal Transport Cask primary containment boundary components, described in detail in Section 4.1, include the bottom forging, inner shell, top forging, and cask lid. The cask containment boundary is hydrostatically pressure tested to 125% of the design pressure in

accordance with ASME Boiler and pressure Vessel Code Section III, Paragraph NB-6220 [6]. This test is in lieu of the 10 CFR 71.85(b) requirement that the cask containment be tested at an internal pressure at least 50% higher than the maximum normal operating pressure. The transport cask containment is hydrostatic tested to 85 psig for a minimum of 30 minutes during which time a visual inspection is conducted to detect any evidence of leakage. The containment maximum normal operating pressure (MNOP) is calculated to be 73 psig Table 6.4-4.

Following the hydrostatic pressure test, all containment boundary components weld joints, connections and regions of high stress are visually examined to verify that no permanent deformation or breach of the containment boundary resulted from the hydrostatic test. All accessible containment boundary welds shall be liquid penetrant inspected for ASME Code Section V, Article 6 [3], with acceptance per ASME Code Section III, NB-5350 [6].

8.1.2.4 Pneumatic Bubble Testing of the Neutron Shield Shell

A pneumatic bubble test of the neutron shield annulus will be performed in accordance with Section V, Article 10, Appendix I, of the ASME Code following final closure welding of the bottom closure plates. The bubble test pressure shall be 51(+1/-0) psig. The test shall be performed in accordance with approved written procedures.

During the test, the two relief valves on the neutron shield annulus will be removed. One of the relief valve threaded connections will be used for connection of the air pressure line and test pressure gauge. The other relief valve connection will be plugged with a threaded plug.

Following introduction of pressurized air into the neutron shield, a 15 minute minimum soak time will be required. Following completion of the soak time, approved soap bubble solution will be applied to all heat transfer fins to neutron shield shell, and neutron shield shell to end plate welds. The acceptance criteria for the bubble test will be no air leakage from any tested weld as indicated by continuous bubbling of the solution. If air leakage is indicated, the weld shall be repaired in accordance with approved weld repair procedures and the pneumatic bubble test shall be repeated until no unacceptable air leakage is observed.